NTNU
Norwegian University of
Science and Technology

Mechanical temperature control of oil based heat storage

Oskar Stadaas Sjøgren
Alexander Bjåen Steen

Master of Science in Mechanical Engineering
Submission date: June 2018
Supervisor: Ole Jørgen Nydal, EPT
Co-supervisor: Erling Næss, EPT

Norwegian University of Science and Technology
Department of Energy and Process Engineering

NTNU
Norwegian University
of Science and Technology

Department of Energy
and Process Engineering

EPT-M-2018-80
EPT-M-2018-88

MASTER THESIS

for

Oskar Stadaas Sjøgren and Alexander Steen

Spring 2018

English title
Mechanical temperature control of oil based heat storage

Norwegian title
Mekanisk temperaturkontroll av oljebasert varmelager

Background and objective

Oil can be used as heat transfer fluid, as well as heat storage medium for solar heat storage systems. Energy storage units are useful devices in solar energy systems. The intermittent solar energy can then be stored for continuous use either as electrical power (electrical batteries) or as heat. We are in particular interested in heat storage for cooking applications, which requires temperatures typically in the range 150-250 degrees C. This is an acceptable temperature range for thermal oils, as well as for many edible oils.
A thermal control system is needed in order to obtain a heat storage at a desired temperature. A new design for a frying and a cooking pan which can be operated using hot storage oil is also needed.
Temperature control can be achieved with a thermostat valve, in which a thermostat provides a switch for an actuator which drives a valve. For implementation in a rural African setting, a simple and robust solution is desired. For this purpose a fully mechanical thermostat valve will be developed and tested. The valve will be an important element in solar systems which are developed in a collaboration with several African universities. An oil powered solar frying pan is one type of application which is needed in such solar systems.

The following tasks are to be considered:

1 A short literature review of solar cooking methods with heat storage
2 Design and testing of a mechanical thermostat valve and a cooking application
3 Design of a full solar system
4 Reporting

-- " --

Within 14 days of receiving the written text on the master thesis, the candidate shall submit a research plan for his project to the department.

When the thesis is evaluated, emphasis is put on processing of the results, and that they are presented in tabular and/or graphic form in a clear manner, and that they are analyzed carefully.

The thesis should be formulated as a research report with summary both in English and Norwegian, conclusion, literature references, table of contents etc. During the preparation of the text, the candidate should make an effort to produce a well-structured and easily readable report. In order to ease the evaluation of the thesis, it is important that the cross-references are correct. In the making of the report, strong emphasis should be placed on both a thorough discussion of the results and an orderly presentation.

The candidate is requested to initiate and keep close contact with his/her academic supervisor(s) throughout the working period. The candidate must follow the rules and regulations of NTNU as well as passive directions given by the Department of Energy and Process Engineering.

Risk assessment of the candidate's work shall be carried out according to the department's procedures. The risk assessment must be documented and included as part of the final report. Events related to the candidate's work adversely affecting the health, safety or security, must be documented and included as part of the final report. If the documentation on risk assessment represents a large number of pages, the full version is to be submitted electronically to the supervisor and an excerpt is included in the report.

Pursuant to "Regulations concerning the supplementary provisions to the technology study program/Master of Science" at NTNU §20, the Department reserves the permission to utilize all the results and data for teaching and research purposes as well as in future publications.

The final report is to be submitted digitally in DAIM. An executive summary of the thesis including title, student's name, supervisor's name, year, department name, and NTNU's logo and name, shall be submitted to the department as a separate pdf file. Based on an agreement with the supervisor, the final report and other material and documents may be given to the supervisor in digital format.

☒ Work to be done in lab (Water power lab, Fluids engineering lab, Thermal engineering lab)
☐ Field work

Department of Energy and Process Engineering, 15. January 2018

Ole Jorgen Nydal

NN
Academic Supervisor Ole Jorgen Nydal

Co-Supervisor: Erling Næss

Acknowledgment

We would like to express a sincere gratitude to our supervisor, Ole Jørgen Nydal, and co-supervisor, Erling Næss, for the continuous support, enthusiasm and guidance they have provided throughout the work with this project. Besides our supervisor, we would like to thank Paul Svendsen and Benjamin Foss Hansen for their immense assistance in the laboratory, and for always having a solution to the challenges faced during the experimental work. A sincere thanks also goes to Karidewa Nyeinga. The field study at Makerere University would not have been possible without his tremendous support.

As this work is an extension of our previous work in the report *Solar heat storage in oil based rock bed*, some of the material is based on the results from this report. For additional insight we encourage the reader to study this report.

Abstract

A cooking application and a mechanical temperature controller based on the thermal expansion of sunflower oil were constructed and tested. Both components are parts of a solar cooking system, storing energy in an oil-based rock bed, made in the project work *Solar Heat Storage In Oil Based Rock Bed*. This thesis is a part of a network project with universities in Mozambique, Uganda, Ethiopia and Tanzania, and focuses on energy supply to rural and off-grid communities in Africa. The motivation is to store energy from renewable energy sources, for later to be used in food preparations after sunset. Moreover, a simple system is desired, to make the operation and maintenance as easy as possible. This functional mechanical temperature controller will provide more flexibility to the solar cooking system, making it feasible for more settings than the system constructed in the project work.

A mechanical temperature controller was made from two components; a piston actuator and a sliding valve. Three piston actuator designs were constructed and tested, all of which were connected to a closed pipe system with a copper coil filled with sunflower oil. The copper coil was submerged in a container holding sunflower oil and a heating element. During heating, the sunflower oil inside the copper coil expands due to the temperature change, giving a displacement of the piston actuator. The displacement is the motion which controls the sliding valve.

Three sliding valve designs were constructed and tested, all utilising the linear motion from the piston actuator. The valve determines the flow direction, either towards the heat storage or for further heating, depending on the flow temperature. The valve can be used with and without circulation of the oil.

Leaks caused problems throughout the production and tests of the components. A functional sliding valve was successfully constructed, whereas the first piston actuators were faulty due to leaks. The accuracy of the piston actuators made in the workshop at NTNU was not satisfying. Therefore, prefabricated pneumatic pistons were acquired. Preliminary tests gave promising results. Nevertheless, tests of the full system were not conducted due to the limited time.

Two designs for a cooking application were made using a practical and a theoretical approach. The practical approach design was constructed and tested. The cooking effect was promising compared to other solar cookers, but it needs to be upscaled and further improved in order to deliver energy in the same order of magnitude as already established solar cookers.

A test setup of the solar cooking system was made at Makerere University, Kampala, Uganda. The fill valve from the co-project was used as the temperature controller. Demonstrations proved the system made at NTNU is capable of being reproduced locally and is a concept suited for further development.

Sammendrag

En kokeapplikasjon og en mekanisk temperaturregulator basert på termisk ekspansjon av solsikkeolje er laget og testet. Begge komponentene er deler av et matlagingssystem basert på solenergi lagret i form av varm olje i et steinlager. Varmelageret ble produsert i prosjektarbeidet *Solar Heat Storage In Oil Based Rock Bed*. Denne oppgaven er en del av et nettverksprosjekt med universiteter i Mosambik, Uganda, Etiopia og Tanzania, og fokuserer på å utvikle energiløsninger til avsidesliggende områder i Afrika, uten tilknytning til strømnettet. Motivasjonen er å lagre energi fra fornybare energikilder, for senere å bli brukt til matlaging etter solnedgang. Videre er et enkelt system ønskelig for å gjøre drift og vedlikehold ukomplisert og brukervennlig. En mekanisk temperaturregulator vil gi mer fleksibilitet enn systemet laget i det tidligere prosjektarbeidet, som gjør det attraktivt for fler brukssituasjoner.

En mekanisk temperaturregulator ble laget av to komponenter; en stempelaktuator og en glideventil. Tre stempelaktuatordesign ble produsert og testet hvor alle var koblet til et lukket rørsystem med en kobberspole fylt med solsikkeolje. Kobberspolen var nedsunket i en beholder med solsikkeolje og et varmeelement. Under oppvarming utvides solsikkeoljen inne i kobberspolen grunnet temperaturøkningen, som medfører en stempelbevegelse. Dette styrer glideventilen.

Tre glideventildesign ble produsert og testet, alle basert på den lineære bevegelsen fra stempelaktuatoren. Ventilen bestemmer strømningsretningen til oljen, enten mot varmelageret eller for videre oppvarming, avhengig av oljetemperaturen. Ventilen kan brukes med og uten sirkulasjon av oljen.

Lekkasjer ga problemer under produksjon og testing av komponentene. En velfungerende glideventil ble laget, men de første stempelaktuatorene var mislykkede grunnet lekkasjer. Presisjonen som kreves for å lage en fungerende stempelaktuator ble ikke oppnådd på verkstedet ved NTNU. Derfor ble prefabrikkerte pneumatiske stempler kjøpt inn. Initielle tester har gitt lovende resultater, men fullstendige tester av pneumatikken har ikke blitt gjennomført, da det ikke var tilstrekkelig med tid.

To ulike design for en kokeapplikasjon ble laget. Et med en praktisk, og et annet med en teoretisk tilnærming. Det praktisk utformede designet ble produsert og testet. Varmeeffekten var lovende sammenlignet med andre solkokere. Likefult må den oppskaleres og forbedres ytterligere for å levere energi i samme størrelsesorden som allerede etablerte solkokere.

Et testoppsett for matlagingssystemet ble laget ved Makerere University, Kampala, Uganda. Flottøren fra et samarbeidsprosjekt ble brukt som temperaturregulatoren under testene. Demonstrasjonene viste at systemet laget ved NTNU er i stand til å reproduseres lokalt, og er et konsept egnet for videre arbeid og utvikling.

Contents

List of Figures

List of Tables

Nomenclature

α_V	Volumetric thermal expansion rate $[K^{-1}]$
$\bar{h}$	Average heat transfer coefficient $[\frac{W}{m^2 \cdot K}]$
$\bar{N}u_D$	Nusselt number $[-]$
$\bigvee$	Velocity $[\frac{m}{s}]$
ΔH_r	Reaction entalphy $\left[\frac{J}{mol}\right]$
ΔL	Displacement length $[m]$
ΔP	Pressure difference $[Pa]$
ΔT	Temperature change $[K]$
Δt	Time change $[s]$
ΔT_A	Temperature difference in/out side A $[K]$
ΔT_B	Temperature difference in/out side B $[K]$
ΔV	Volume change $[m^3]$
$\dot{Q}$	Heat transfer $[W]$
$\dot{q}$	Heat transfer per area $\left[\frac{W}{m^2}\right]$
μ	Dynamic viscosity $[Pa \cdot s]$
π	Constant $[-]$
ρ	Density $\left[\frac{kg}{m^3}\right]$
ζ	Dimensionless position $[-]$
A_c	Cross section area $[m^2]$
a_m	Fraction of melted material $[-]$
c	Dimensionless coefficient E.1 $[-]$
c_p	Specific heat capacity at constant pressure $\left[\frac{J}{kg \cdot K}\right]$
$c_{f,app}$	Length-averaged friction coefficient $[-]$

D_h Hydraulic diameter $[m]$

Gz_D Dimensionless position $[-]$

h_m Heat of fusion per unit mass $\left[\frac{J}{kg}\right]$

k Thermal conductivity $[\frac{W}{m \cdot K}]$

K_∞ Dimensionless coefficient E.1 $[-]$

m Mass $[kg]$

n_a Mol number $[mol]$

$Nu_{duct,fd}$ Nusselt number for fully developed flow in duct $[-]$

$Nu_{pipe,fd}$ Nusselt number for fully developed flow in pipe $[-]$

P_{HS} Hydrostatic pressure $[Pa]$

Pr Prandtl number $[-]$

Q Energy $[J]$

Re Reynolds number $[-]$

T_1 Initial temperature $[K]$

T_2 Final temperature $[K]$

T_m Melting temperature $[K]$

T_o Ambient temperature $[K]$

T_w Wall temperature $[K]$

U Overall heat transfer coefficient $\left[\frac{W}{m^2 \cdot K}\right]$

V Volume $[m^3]$

x Position $[m]$

A Area $[m^2]$

D Diameter $[m]$

L Length $[m]$

Pe Wetted perimiter $[m]$

Chapter 1

Introduction

1.1 Background

In Uganda, biomass accounts for 89,9% of the energy generated in the country, mostly used for cooking purposes [1]. More than 90% of the country's population depends on non-sustainable use of firewood or charcoal as their primary energy source for cooking fuel. This is neither an environmental-friendly or sustainable energy resource for an increasing population [2]. Consequently, the excessive use of these energy sources will lead to a vast increase in deforesting of the rural areas [3].

According to P. T. Heteu [4], almost 30% of the households in Uganda are under the poverty line, most of them located in rural areas where the access to a power grid may not exist. Providing a low-cost energy storing system can improve the life standard for householders in these areas and reduce the non-sustainable firewood consumption. Thus, providing an alternative primary energy source has a huge potential regarding environmental and social benefits.

Biomass as an energy source is predominantly used for cooking, which requires low quality energy [5]. Therefore, low quality energy storage systems, such as a thermal energy storage (TES), should be addressed as a possible solution for storing necessary energy. In addition, the Sub-Saharan parts of Africa are exposed to large amounts of sun at relatively stable conditions [6]. Combining TES and solar energy could provide a sustainable and environmental-friendly energy source. This would reduce the negative impact humans have on the environment regarding deforestation, in addition to introducing a renewable and sustainable energy source.

The aid provided by non-governmental organisations (NGOs) can make a huge impact, improving life standard in local communities throughout the world. However, a challenge for the NGOs is the adaption to local societies. Differences in knowledge, culture and resources are some factors which may negatively influence the impact of the aid provided. It is important that the technology provided is well adapted to its working environment so it may be well taken care of and further developed. Due to educational difficulties in rural parts of the Sub-Saharan Africa, maintenance and operation of a heat storage system can be challenging [7]. To ensure safe operation of such systems, it should be as simple as possible, thus being suited for people with various level of education. In addition, the system should contain as few mechanical components as possible, making it easy to repair, maintain and operate.

This work is part of a network project, including Norwegian University of Science and Technology (NTNU) and universities located in Mozambique, Uganda, Ethiopia and Tanzania. During this collaboration, there have been done several studies on small scale concentrating solar energy systems with heat storage, with a greater focus on solar collectors and air as a heat storage medium [8]. This work is an extension of the project work *Solar heat storage in oil based rock bed*, which focused on a TES using oil and pebbles [9]. The supply rate and temperature of hot oil into the TES turned out to be challenging using mechanical mechanisms. A fill valve, made in the co-project *Passive Temperature Control of Heat Based Storage*, gave steady temperature supply but reduces the options of heating the oil [10]. As the full solar cooking system should be applicable in various settings, a temperature controller which is independent of the heating mechanism gives a broader potential user group.

1.2 Objective

- Design and testing of a mechanical temperature controller
- Design and testing of a cooking application
- Design of a full solar cooking system

Chapter 2

Theory

This chapter will give the reader insight in different types of solar cookers, the principal of heat storage, and important aspects when optimising the amount of energy stored. Some of the theory presented is not entirely in focus further on in this thesis, but is necessary to understand the principles of the full solar cooking system designed, which is based on the previous work *Solar Heat Storage in Oil Based Rock Bed* [9]. Further, a brief review of different heat storage solutions, as well as combined systems of TES and solar cookers, will be presented. Finally, a short presentation of mechanical valves with the purpose of controlling temperatures is included.

2.1 Solar cooker

A solar cooker is a device utilising the sun's energy for food preparation, often classified as direct or indirect. The simplest method is direct. Indirect systems require some sort of energy storage, which can be done in multiple manners [11].

2.1.1 Direct solar cookers

Direct methods can be separated into three categories; panel cookers, solar box cookers and solar parabolic cookers, as represented in figure 2.1.

Solar panel cookers may be considered the most common due to their ease of construction and low-cost material [13]. Their simple design makes them easy to use and requires little expertise from the operator. In its simplest form, it can be constructed only using cardboard and a reflective foil. Despite its simplicity, it is often not desirable due to limited cooking power. Hence, this system is often used for small scale cooking [14].

Solar box cookers consist of an insulated box with a transparent glass cover and reflective surfaces to direct sunlight into the box. The inside of the box is painted black in order to maximise the sunlight absorption [15]. M. Telkes investigated solar box cookers and discovered they work well even if there is conduction heat loss due to wind, diffuse radiation, cloudy weather and low ambient temperature [16]. A drawback is that they are slow to heat up.

Solar parabolic cookers concentrate reflected sunlight to a focus point, creating a high-energy area. Hence, they can achieve extremely high temperatures in very short time. Unlike the panel cookers and box cookers there is no need for a special cooking vessel. Regular frying pans and

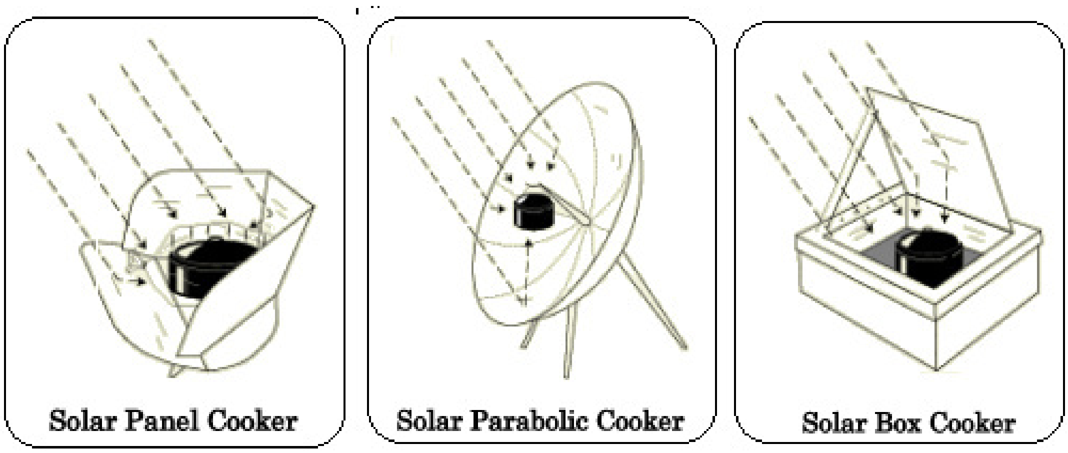

Figure 2.1: Different types of solar cookers [12].

boilers can be used. However, due to the potential high temperature at the focus point there is a risk of burning the food if left unattended. Yet, for commercial purposes the advantages of parabolic cookers regarding technical and behavioural matters should be improved [17].

2.1.2 Indirect solar cookers

Indirect solar cookers are in some extent similar to direct cookers. Their purpose is to utilise the collected energy in a different location, by using a heat transfer medium. The medium can be gas, liquid or solid [18]. There are many considerations which should be recognised when choosing the right heat transfer medium. Properties as heat capacity, conduction/convection rate, density, viscosity, and more, will be deciding factors and should be addressed carefully as most are temperature-dependant. To design a robust and long lasting system the operational pressure is of significance, as well as the corrosiveness of the heat transfer medium [19].

2.2 Heat storage

Indirect systems may use the thermal energy directly or store it for later use. The principal for storing is often divided into sensible heat storage, latent heat storage or thermochemical heat storage. This is used when there is a difference in energy supply and energy consumption.

2.2.1 Sensible heat storage

Sensible heat storage is achieved by changing the temperature of the storage medium, either during charging or discharging. The temperature of the heat storage medium increases when charged and decrease when discharged, as represented in equation 2.1.

$$Q = \int_{T_1}^{T_2} mC_p dT = \rho V C_p (T_2 - T_1) \tag{2.1}$$

Q is the energy, C_p is the specific heat, T_1 is the initial temperature, T_2 is the final temperature, m is the mass of the material, ρ is the density and V is the volume. Thus, the heat storage

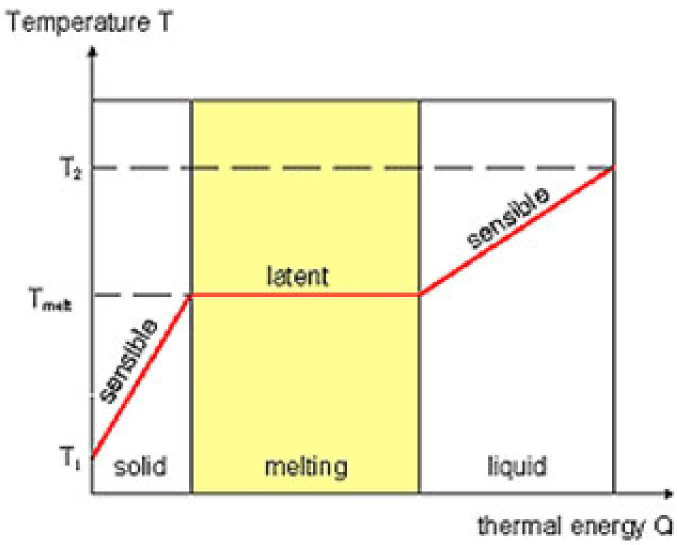

Figure 2.2: Temperature vs thermal energy; sensible and latent heat storage [22].

medium should have high specific heat capacity, long term stability under thermal cycling and preferably low cost [18]. Sensible heat storage may be divided into liquid media storage (water, oil based fluids, molten salts etc.) or solid media storage (rocks, metals etc.). Liquids are often economical competitive, and for low temperatures water is considered one of the best storage media. However, due to its high vapour pressure, it requires costly insulation and pressure withstanding applications. These problems can be avoided by storing thermal energy as sensible heat in solids. In addition, solids do not leak from their container. To reduce costs, a hybrid solution may be relevant, combining properties for the heat storage media. By reducing the required volume of the solid/liquid, expenses can be vastly reduced. The drawback is the reduced quality of the heat storage, which is connected to the introduction of a second medium with different heat storing qualities [20].

2.2.2 Latent heat storage

Latent heat storage is achieved by absorbing heat in a material which undergoes a phase transformation. Both absorbing and releasing energy occur at constant temperatures, being the phase transition temperature of the material [21]. The energy stored during charging is represented by equation 2.2.

$$Q = \int_{T_1}^{T_m} mC_p dT + ma_m \Delta h_m + \int_{T_m}^{T_2} mC_p dT \tag{2.2}$$

a_m is the fraction melted and h_m is the heat of fusion per unit mass. Phase changing provides high energy storage density compared to sensible heat storage. Due to increasing system requirements for gases it is most common to utilise solid-liquid phase changing rather than liquid-gas phase changing, despite this phase transition often being able to store more energy. A visual representation of the temperature behaviour for sensible and latent heat storage is given in figure 2.2.

2.2.3 Thermochemical heat storage

Thermochemical heat storage utilises the energy release in chemical reactions [23]. A chemical compound is involved in an endothermic chemical reaction when storing heat, splitting the compound into new substances. When releasing heat the chemical reaction is reversed, now being exothermic, according to equation 2.3. The chemical compounds undergo a chemical reaction and heat is released. The amount of heat released is linked to the reaction enthalpy, as seen in equation 2.4. This type of heat storage is becoming progressively more popular as the heat losses related to the chemical reaction are small [24].

$$A + heat \rightleftharpoons B + C \tag{2.3}$$

$$Q = n_a \Delta H_r \tag{2.4}$$

2.3 Insulation

Insulation is a key factor to maintain a high temperature over time, independent of the heat storage method [19]. This is to prevent excessive heat losses. By applying insulation, the overall heat transfer coefficient decreases, and so the heat loss rate is consequently decreased. This can be seen from the heat loss relation:

$$\dot{q} = U(T_w - T_o) \tag{2.5}$$

Therefore it is of high importance that the system is well insulated with a material which provides the lowest possible U-value. Due to economical aspects the insulation should also be low cost and accessible. Rock wool is the most common used insulation material for thermal storage systems, while several other alternatives also exist [25].

2.4 Stratification

A common method to optimise the amount of energy stored in a container of hot fluid, is to apply the principal of stratification. This occurs due to the fact that hot fluid enters at the top of the storage, while cold fluid is discharged at the bottom, resulting in a larger thermal gradient because of the natural buoyancy in the heated fluid. This larger thermal gradient will further result in a greater potential of thermal energy to be stored. It can be as much as up to 32% more efficient than the commonly and commercially available heat storage, at least regarding hot-water TES [26]. By obtaining thermal stratification, more high-temperature fluid can be extracted, which is essential for cooking.

Regarding what influences the amount of stratification, several studies have shown that geometry of the storage tank, geometry of the inlet flow pipe, and flow rate will have an impact. For instance, one study concluded that a height/diameter aspect ratio of 4 would maximise the obtainable thermal stratification for hot water storage tanks [27]. Another recent paper claims that an optimisation between cubical and cylindrical containers has not yet been sufficiently studied, and is therefore not determinable, but will however also affect the stratification [28]. Among several parameters which measure the degree of stratification (DOS), Richardson number (Ri) is one of the most prominent. This compares buoyancy forces to mixing forces. A small Ri indicates a greater mixed fluid, and hence a lower DOS, while a high Ri implies the opposite.

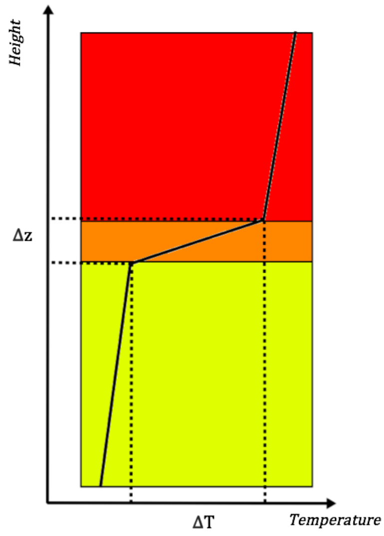

Figure 2.3: Temperature distribution in a TES with high temperature at the top (red), low temperature at the bottom (yellow) and a stratification layer in between (orange). The black line represents the temperature profile.

Y. H. Zurigat et. al. have argued with their study that inlet geometry started influencing the stratification in a thermocline TES for Ri below 3,6 [29], while another study showed that the effect of inlet geometry for TES systems is negligible for Ri above 10 [30]. Numerical simulations of a three dimensional flow in a hot water tank also conclude that a better DOS is obtained by increasing the aspect ratio, decreasing charging and discharging flow rates and having the inlet and outlet positioned on the outer most points of the storage unit [31]. A paper by A. Castell et. al. shows, by comparing different dimensionless numbers for measuring thermal stratification in water tanks, that Ri gives the most accurate description of thermal stratification [32]. They also pointed out that other parameters do not give a clear description by themselves, but can be useful in combination with the Ri. It is worth mentioning that this experiment was conducted with constant flow rates, while charging at a variable flow rate results in better thermal stratification and thermal efficiency [33]. In a study on thermal analysis of stratified storage tanks, the effects of the thickness of the tank wall and thermal insulation were discussed. Experimental results showed that the outside insulation can enhance tank wall axial conduction, which tends to degrade the stratification. However, the reduction of heat loss outweighs the enhancement of axial conduction, and better stratification is still maintained for insulated tanks compared to bare walls [34].

With a simulation comparing energy and exergy levels in the TES with different charging methods, results showed that charging flow with constant temperature gave a better DOS along the height of the storage unit [33]. In addition, another study indicates that a controlled power discharging is more effective than constant flow rate discharging [35]. A TES system with oil has an advantage over TES systems with water, in the sense that they can hold a much higher temperature without vaporisation, given the same pressure. Hence, different parameters and characteristics may be of importance. From the experiments conducted by A. Mawire and S. H. Taole, they concluded that the temperature distribution along the height and the stratification number are the best parameters when evaluating thermal stratification in an oil/pebble tank [35].

In the study prior to this thesis, temperature distribution of the storage tank was chosen as the only parameter that would be evaluated. This is the parameter which best describes the DOS by giving an explicit view of how the heat is distributed throughout the tank, graphically represented in figure 2.3. The goal of the former study was not to review how to achieve the most efficient thermal stratification, but to obtain a DOS good enough for the deliverance of heat for cooking purposes. However, it is of importance to understand which factors that influence the stratification, as this can have a huge impact of the obtainable amount of heat from the rock bed.

2.5 Previous studies of applied TES

The application of stratification in TES has been used for some time, especially in water tanks [36]. In addition, many earlier studies have considered air as heat transfer fluid in the TES, with promising results [37], [38]. However, air lacks the potential of various sources of heating. Oil, on the other hand, can be heated in many ways due to good thermodynamic properties regarding heat transfer. Therefore, an oil based heat storage system can be applied to a broader range of heating sources, compared with air, such as solar collectors, PV-panels and wind turbines.

Studies on stratification in oil based heat storage, on the other hand, is of much less extent, and few studies have been conducted compared to studies with other heat transfer fluids. However, one earlier study has reviewed different oils used as heat transfer fluid in a TES packed with quartzite rocks, to investigate the storage properties of the oils. By comparing palm oil with two other synthetic oils, results showed that palm oil could ensure the same performance with lower inlet fluid temperature or reduced charging time, regarding the achievement of the same temperature distribution in the TES for working temperature below 300°C [39]. Although few earlier studies have been reviewing an oil based rock bed TES, one other experimental study on forced stratification has been carried out at NTNU and tested in full scale in Ethiopia as a part of the network project [40], [8]. The system performed well, but due to high accuracy requirements during construction, its range of application is somewhat limited for rural areas as access to parts and construction expertise may be limited.

2.6 Combined systems of solar cookers and energy storage

A full solar cooking system consisting of solar collectors with reflectors and a cooking unit, presented by Schwarzer and da Silva in their paper [41], has been developed and been installed in several different countries around the world. The system serves the purpose of replacing firewood as fuel in developing regions. The system is made as an indirect cooker, with vegetable oil as the heat transfer fluid, transferring the heat from the solar collectors to the cooking pots. If night cooking is desired, a heat storage may also be installed. In that case, a tank filled with pebbles is added to the system. A flat plate collector cooker has been favoured as the most promising type of cookers, after several thermal and technical requirements were regarded. The vegetable oil is heated at this part, and moves by natural flow to either the heat storage or the cooking units where it transfers sensible energy to the cooking goods in double-walled pots. Since the system is developed both for families and for larger institutions, different sizes have been made, whereas the collectors ranges from 1 m^2 to 12 m^2 and the cooking pots from 5 to 100 litres. The standard size consists of a 2 m^2 collector and two pots in the range of 12-15 litres, and may

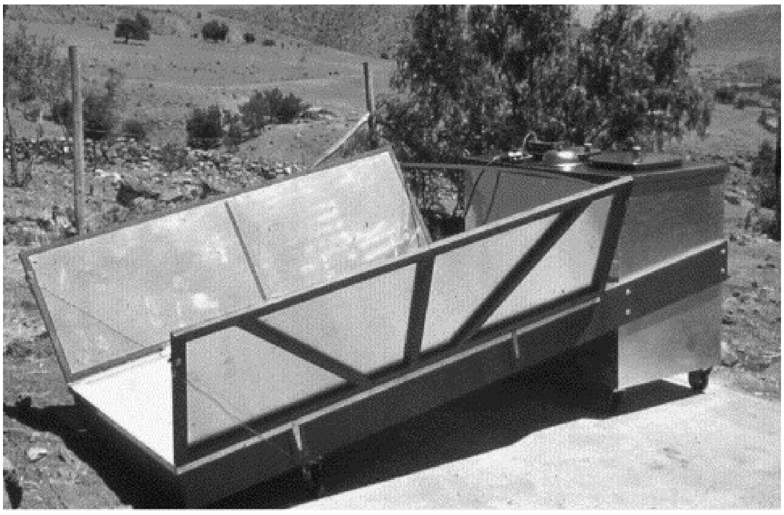

Figure 2.4: Outdoor cooker with 2 m^2 collector area and two pots [41].

during good conditions boil 5 litres of water in 10-12 minutes, when the heated oil flows directly to the cooking pots without being stored. Figure 2.4 shows a standard sized system installed in an elementary school in northern Chile, South America

This solution exhibits promising potential, and larger systems have already been installed in schools with over 250 students. In addition, at the time the paper was published, another system with a capacity for 450 persons was being planned. However, drawbacks such as the high investment cost as the most prominent, makes this system less attractive as it mus be affordable for the communities to acquire. It should also be easy to produce locally, and the access of materials and competence may be an issue.

Another and more recent solar cooker, is the Small Scale Box type Hybrid (SSBH) solar cooker made by S. B. Joshi and A. R. Jani [42]. This solution uses both thermal and photovoltaic effects at the same time by having solar panels attached to the SSBH, as can be seen in figure 2.5. The design consist of a small and classic solar box cooker (SSB), which has 5 foldable solar panels attached to it, each of 15 W, connected with hinges to each other. The PV-panels are further connected to a battery with a capacity of 45 Ah, which, by experimental tests, can endure for 3 hours of cooking when fully charged. In addition to provide the user the opportunity to cook both during day and night, results show that combining the photovoltaic effect along with the thermal effect will reduce the cooking time considerably. It can cook as much as 4-5 meals on a sunny day, and is with a total weight of 6,5 kg, a far lighter version than other solar cooker designs. Other benefits are the low cost and easy implementation due to its size. The developers estimate the price to be roughly 120 USD with the promise of further reduction in price if the solution will be commercialised. However, excessive energy goes to spill when the battery is full and when the cooker is not being used.

The aim with this thesis is therefore to make a system, which may be seen as a combination of the two solutions presented, able to store the excessive energy from energy converters such as PV-panels, when a battery has been fully charged. It is also desired to add the dump load energy into a TES for the purpose of preparing food in an indirect solar cooker at any given time of the

(a) (b) (c)

Figure 2.5: (a) SSB solar cooker, (b) SSBH solar cooker with folded solar panels, and (c) SSBH solar cooker with open solar panels [42].

day.

2.7 Mechanical thermostat valve

Maintaining a constant temperature supply into the TES is a key factor to achieve stratification. Hence, the need of a thermostat. Previously, a fill valve has been used to control the temperature [10]. Nevertheless, to make the system more flexible for various heating sources, a new design is desired. The biggest drawback with a mechanical thermostat is a high machining accuracy required during production. Leaks cause a substantial problem and may occur both during expansion and contraction of the temperature sensitive fluid. The biggest advantage is its simplicity, with few moving parts and potential robust design. All mechanical thermostats function to execute some kind of movement by converting a motion, such as a rotary motion into a linear motion. The operation is based on combinations of structural components and/or material properties, such as thermal expansion. An example of a mechanical self regulated thermostat utilising fluid expansion and bellows is given in figure 2.6.

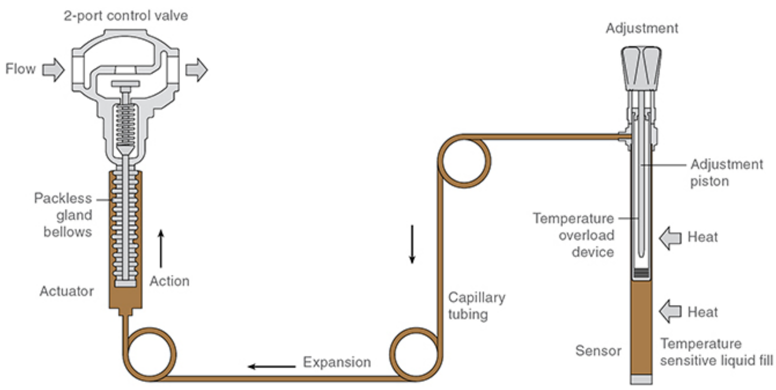

Figure 2.6: Mechanical thermostat valve with adjustment piston and bellows [43].

2.7.1 Thermal expansion valve

The driving force for the thermostat is caused by the expansion of a temperature sensitive fluid. A closed circuit, containing only this fluid, is exposed to a temperature change resulting in a volume change, according to equation 2.6. The fluid is a part of the actuator, giving the motion which controls the valve position, resulting in a change of the output. For incompressible fluids, the rate of change in volume expansion to actuator displacement can be linearly expressed as shown in equation 2.7, if the pressure is held constant.

$$\frac{\Delta V}{V} = \alpha_V \Delta T \tag{2.6}$$

$$\Delta V = A_c \Delta L \tag{2.7}$$

A high volumetric thermal expansion rate, α_V, is preferred as a small change in temperature results in a large volume change. Hence, a more precise thermostat can be achieved. A large volume change can also be achieved by a large initial volume, but is less desirable as the size of the thermostat increases, which is unpractical.

Chapter 3

Design

This project is based on previous work involving several students, where the tasks and responsibilities have been divided, and thus been described in different reports. To give the reader an insight of the ideas and designs of the components that are produced, it is therefore necessary to include a short review of the complete system, as it has been made and described in the previous reports *Passive Temperature Control of Heat Based Storage* and *Solar Heat Storage in Oil Based Rock Bed* [10], [9]. Moreover, the design of the new solar cooking system, including the mechanical temperature controller and the cooking application, will be presented in this chapter.

3.1 System setup

The following description is the basis for the system setup and depicts how it was made in the previous project. A full overview of the components, with its dimensions and materials may be found in the report for the previous project [9].

The total system is divided into the Heating side and the Storage side where the aim is to add the dump load from a PV-panel into a container of oil. The dump load is, in this project, simulated by a heating element connected to a variac. Further, the heated oil in the heating container will, when reaching the desired temperature, expand just enough to reach a height where a pipe, the hot pipe, is connected to the rock bed for the storage of the hot oil. When the heated oil starts to flow over to the rock bed, the idea is that another storage tank with cold oil, the cold container, will balance the outlet flow by supplying just enough oil to the heating container, ensuring that the oil flowing over to the rock bed maintains at a constant temperature. This is done by having a fill valve in the cold container, which at all times maintains a given and constant level of oil by being connected to another reservoir of oil, reservoir 1. With this solution, a fully mechanical and self-regulated system is obtained, in compliance with the goal of making a system made as simple as possible. The full system is described in figure 3.1, where the Heating side contains all the components on the right side, starting from the hot pipe.

The hot oil from the heating container is charged at the top of the rock bed, through the hot pipe, which is immersed down into the thermal storage. At the bottom of the rock bed, another pipe is connected, the cold pipe, going up and along the rock bed. On this pipe there are assembled two valves. One of which, valve 1, is placed directly under the rock bed so that the system can be drained of oil, if desired. The second, valve 2, is put at the other end of the cold pipe; with the intention of controlling mass flow rate for cooking applications. From the second valve, the

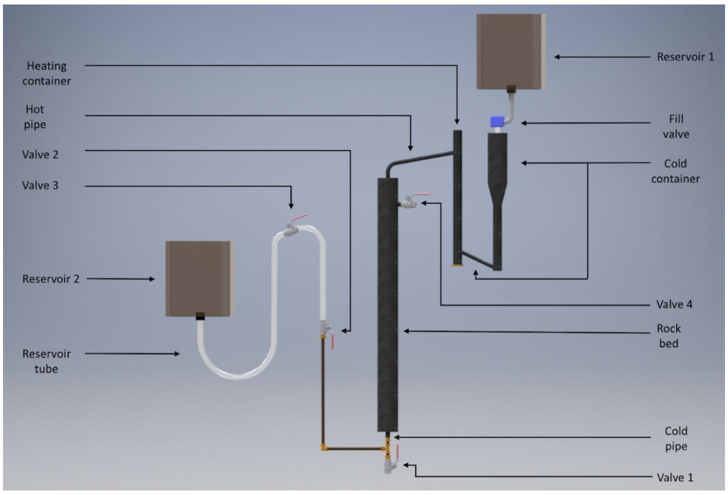

Figure 3.1: CAD model of the full system, with name tags. The Heating side starts at reservoir 1 and ends after hot pipe.

reservoir tube connects the cold pipe to another reservoir of oil, reservoir 2. Along the reservoir tube, there is a third valve assembled, valve 3, for the purpose of balancing the desired level of oil in the rock bed by ensuring atmospheric pressure at the reference level. Reservoir 2 may alter in height, depending on whether the rock bed is being charged with hot oil, or discharged of hot oil for cooking purposes.

The components that will be in contact with hot oil are mainly made by stainless steel and copper pipes, and are insulated with FyreWrap. Other parts, not in contact with hot oil, such as the reservoirs and tubes connected to these, are made of plastic. The rock bed is filled with rocks to store heat and to reduce the amount of oil needed. Sunflower oil is used as heat transfer fluid as this exhibits sufficient thermal properties, and is cheap and easily accessible compared to other synthetic thermal oils.

The major difference between the existing system and the system intended for this thesis, is the replacement of the fill valve as the temperature controller. Consequently, other parts, such as the heating container, needs to be modified. In addition, a cooking application shall be designed and attached to the rock bed at valve 4 for the purpose of boiling water. Two proposals for a new design of the solar cooking system are presented in figure 3.2. Each with a mechanical temperature control based on fluid expansion, but with different schemes. One of which has a pump and a circulating flow, while the other has a gravitational driven flow. From the sketches, it can be noticed a different layout compared to the existing system.

3.2 Mechanical temperature controller

The temperature controller consist of two parts; an actuator and a valve. By making two separate parts, both production and testing can be done independent of each other resulting in a more flexible design.

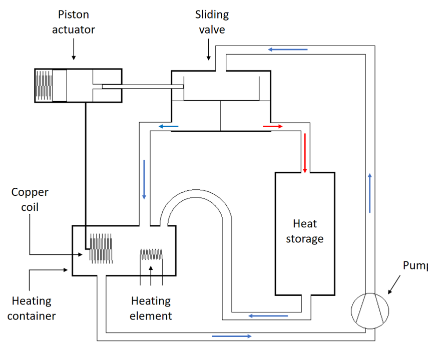

(a) Sketch of a TES system with circulation and a mechanical thermostat controller based on fluid expansion. Blue arrows indicate oil with temperature bellow set point. Red arrows indicate oil with temperature above set point.

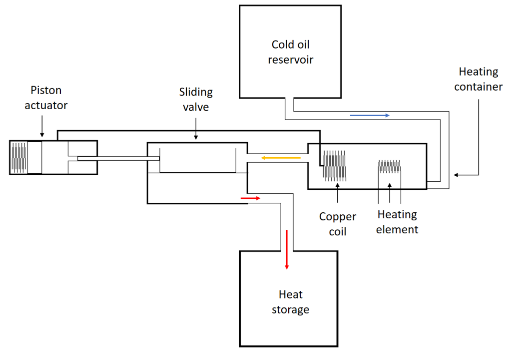

(b) Sketch of a TES system with a mechanical temperature controller based on fluid expansion. Blue arrows indicate oil with temperature below set point. Red arrows indicate oil with temperature above set point. The yellow arrow indicates oil with changing temperature.

Figure 3.2: Sketches of two possible TES systems for the mechanical temperature controller.

3.2.1 Piston actuator

The actuator is based on a concept of two pistons of different sizes moving independent of each other inside a cylinder, frame 1 figure 3.4. The motion of the actuator, i.e. the piston, is caused by an expansion of a temperature sensitive fluid inside a copper coil submerged in a heating container. The copper coil is connected to the piston cylinder, which only contains the temperature sensitive fluid, and no air. As the temperature in the heating container increases, so does the temperature of the fluid inside the copper coil. The temperature change causes the heated volume, i.e. the fluid inside the submerged copper coil, to expand according to equation 2.6. Since sunflower oil, used as the temperature sensitive fluid in this project, is incompressible, the pressure inside the coil, and therefore piston cylinder, increases. This results in a pressure difference on the inside versus the outside of the pistons, which are exposed to the ambient. Moreover, the small piston is connected to a small spring preventing its motion. Therefore, the big piston will start moving, balancing the pressure difference. At a certain temperature, the big piston has moved a given length were a large spring is placed to prevent further motion, frame 2 in figure 3.4. Now, the small spring force is no longer sufficient to hold the small piston at rest, as the large piston is held in a fixed position by a much stiffer spring. Consequently, the small piston starts to move due to the pressure difference, frame 3 in figure 3.4.

As the small piston has a smaller cross section, the displacement distance is greater compared to the big piston, given the same temperature change in the heating container, according to equation 2.7. For sunflower oil, the thermal expansion factor is approximately linear and equal to $0,07\frac{\%}{K}$ [44]. With an initial expansion volume in a 3 m copper coil having an inner diameter of 4,65 mm, the piston displacement versus piston diameter is shown in figure 3.3. As seen from the figure, a small piston, compared to a big, results in a greater displacement response, which is preferred.

As cold oil enters the heating container, its temperature will drop. This temperature reduc-

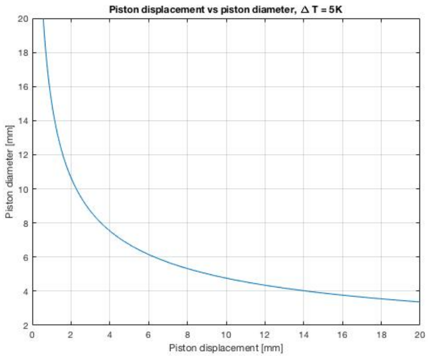

(a) $\Delta T = 5\ K$.

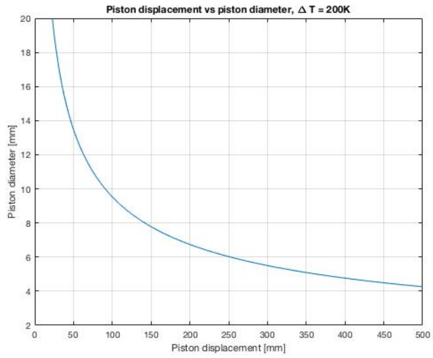

(b) $\Delta T = 200\ K$.

Figure 3.3: Piston displacement versus piston diameter due to thermal expansion of sunflower oil in a submerged copper coil with inner diameter of 4,65 mm and length 3 m, according to equation 2.6 and 2.7.

tion results in a contraction of the volume inside the submerged copper coil. Combined with a decreasing pressure force inside piston cylinder, the spring force initiates motion on the small piston, towards its initial position. When the small piston is at its initial position, i.e. the small spring is fully extended, the big piston starts to move. This can be viewed in figure 3.4, going from frame 3 to 1.

Controlling the temperature response of the actuator is achieved by mounting a threaded rod to the big spring. By adjusting the rod in/out, the distance from the big spring to the big piston is altered, and hence the temperature response. A greater displacement length of the big piston results in a larger volume expansion. Consequently, the motion of the small piston is initiated at a higher temperature.

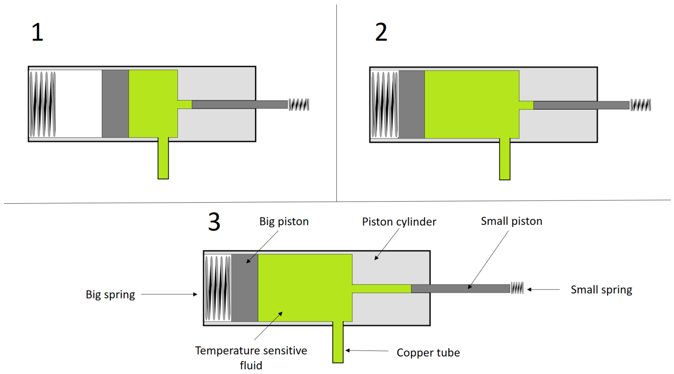

Figure 3.4: Schematic representation of the piston actuator principle. Frame 1: the pistons are at rest. Frame 2: a pressure difference over the big piston has caused it to move towards the big spring. The small piston is held at rest by the small spring. Frame 3: The big piston is held still by a stiff spring. The small piston has moved due to a force from the pressure difference being greater than the small spring force trying to prevent the movement.

3.2.2 Sliding valve

This component controls the flow direction of the oil. The idea is that the sliding valve is connected between the heating container and the heat storage. After the oil has left the heating container, it will flow through the valve, which will decide whether the oil will flow to the rock bed or back to the heating container. This way, the oil will keep circulating until it has reached a given temperature. Then the valve will close the opening towards the heating section, and the oil will flow into the rock bed instead, as proposed in figure 3.2a.

The valve is made with three chambers, one for the inlet flow, and one for each outlet flow. The inlet flow chamber, which is placed above the other two chambers, will have openings down to the other two chambers below. Inside the inlet chamber there is another plate, referred to as the slider. This slider is also made with holes, but these holes only match one of the chambers below at any given time, as illustrated in figure 3.5. However, during transition, both of the chambers will be partially opened as a safety feature, providing constant flow through the valve. This is both to prevent issues regarding the pump, and to avoid undesirable high temperatures of the oil inside the heating container. The slider is controlled by the motion of the small piston in the piston actuator, entering through an opening at the left side of the top chamber.

If no circulation of the oil is intended, the outlet for the heat container can be blocked. This way, oil will only flow through the valve when the slider is in position 2, as proposed in figure 3.2b.

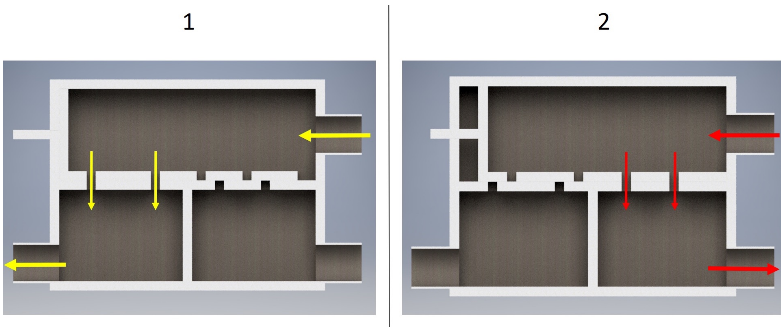

Figure 3.5: The small piston from the actuator pushes the slider through a hole at the left side of the top chamber, while the oil from the heating container enters from the right. The figure to the left shows the slider in position 1, having the chamber towards the heating container open for the oil to flow through. The figure to the right shows the slider in position 2, where the chamber of the heating container is closed, while the chamber to the rock bed is open.

3.3 Cooking application

The intention of the cooking application is to use the stored hot oil from the rock bed as heat transfer fluid in a heat exchanger containing a cooking pot, for the purpose of boiling water or other goods. First of all, a design should be made to withdraw as mush heat as possible from the oil, and direct it towards the cooking pot. Secondly, it should be safe to operate, avoiding the possibility of hazardous situations, such as oil spilling. And finally, made simple as it should be regarded as easy to produce locally.

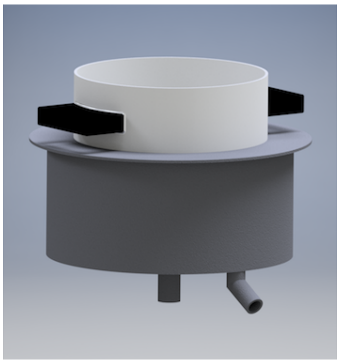

(a) Design 1: The small pot inside the cooking application. The inlet pipe at the bottom and the exit pipe on the side.

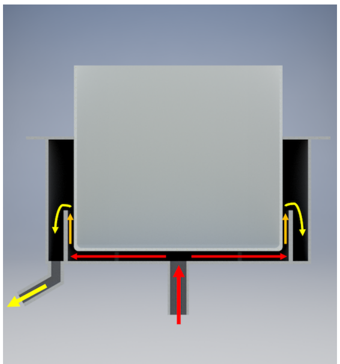

(b) Design 1: Hot oil enters at the bottom (red arrow), transferring heat to the small pot (red and orange arrow), before it exits through the large pot (yellow arrow).

(c) Design 2: Bottom half of the proposed cooking application. The hot oil will enter form the centre, moving outwards and will exit at the side of the plate.

Figure 3.6: Proposed designs of two cooking applications intended for the solar cooking system.

From previous work, one design had been made and been intended for production and testing in this project [9]. It consists of 3 pots put together inside each other, where the smallest pot contains the cooking goods, the medium pot contains the hot oil, and the largest pot contains the oil after heat has been extracted. A pipe connected to valve 4 at the rock bed goes down along the storage tank and to the bottom of the large pot. The large and the medium pot both contain a hole in the centre of the bottom, and are assembled together so that there are no voids between the pots. In addition, the medium pot should have low side walls, and the large pot having an outlet pipe attached on the side wall, near its bottom. At the end, the smallest pot is put inside the medium pot, resting in a position where a small gap exist between the two pots. This way, the oil may flow out from the inlet hole of the medium pot. Now, the hot oil can flow from the rock bed, going up through the large and medium pot, covering the bottom and the outer sides of the submerged small pot, flow over the edges of the medium pot, and then exit the outlet pipe of the large pot to a collecting tank. This is illustrated in figure 3.6b. To control the temperature coming in and out of the cooking application, and hence the heating effect, the mass flow of the oil leaving the rock bed can be adjusted by valve 2, figure 3.1.

In addition to the cooking application above, an alternative solution is designed to see if a larger heat transfer may be obtained. To make it even more safe to operate, a solution needs to be formed where the pot containing the cooking goods are not in direct contact with the hot oil. A possible design is therefore to have a thin plate with an internal channel for the oil to flow through. This has a resemblance of a normal stove, where the cooking pot is put on top of a heated plate. The channel will be formed as a spiral, where the hot oil enters at the centre and moves outwards toward the side where it exits, see figure 3.6c.

Chapter 4

Production and tests

Finding a solution to a practical problem is an iterative process of testing and failure. The goal of this thesis is to test a concept to see whether it is feasible for further development and adaption in rural areas of Africa, or not. Accordingly, the main part of this project was to test different approaches to a problem and improving the solution along the way. This section will present how the mechanical temperature controller and cooking application evolved from simple ideas to functional products, and how challenges were approached during this process. A brief discussion will be introduced for each component, presenting the key challenges and the potential they offer. For more pictures than the ones listed in this chapter, see Appendix C.

4.1 Piston actuator

Three different piston actuator designs were produced and tested. The first was based on a combination of two pistons with different sizes, the second was based on one piston and the third was based on pneumatic pistons. The tests were conducted to observe the pistons' displacement response, as well as leaks in the piston actuator systems.

4.1.1 Double piston actuator

Production

The first piston actuator was made in compliance with the concept design, as in figure 3.4. A metal rod of stainless steel was lathed to an outer diameter of 25 mm and a length of 150 mm. The centre of the rod was drilled from each sides, to make the space for the two pistons. Both holes were first drilled and later broached to create a smoother surface, minimising the surface tension, and hence the friction forces. This way, the pistons would move more easily, while reducing the possibility of leaks over one of the piston heads. The hole for the big piston was made with an inner diameter of 20 mm and a total length of 100 mm, while the hole for the small piston was made to have an inner diameter of 6 mm and a length of 50 mm. The piston cylinder, and how it looks like inside, may be viewed in figure 4.1. Two additional holes were drilled through the piston cylinder giving an inlet for the copper tube and an outlet to release excessive air when filling the piston cylinder with oil. These were positioned 90 mm from the big piston opening side. Both holes were made with a diameter of 8 mm and later threaded. The large piston was lathed out of a rod, so that the piston head had a diameter of 20 mm and a length of 30 mm, while the rest of the piston had a diameter of 10 mm and a length of 120

(a) The piston cylinder, made out of stainless steel.

(b) The inlet side for the big piston.

(c) The inlet side for the small piston.

Figure 4.1: Pictures of the inside and outside of the piston cylinder. The copper coil inlet is connected at the right side. The air outlet is connected at the left side.

mm. In addition, two grooves were made at the piston head where rubber seals were attached, to further prevent leaks. The small piston was first made out of a rod with a length of 100 *mm*, with three grooves and rubber seals attached near one of the sides. However, during a preliminary test when submerging the whole piston cylinder under water while checking for air bubbles, it was discovered that the small piston was leaking, and a new had to be made. It was later discovered that the piston rod was 5,95 *mm* in diameter, not 6,0 *mm*, which induced the leaks. The new piston was made out of a rod of 6,0 *mm* where the grooves for the rubber seals were not as deep as for the prior piston. Further, the mechanism for stopping and adjusting the big piston was made. The same preliminary test was conducted and no air bubbles were observed, indicating a leak-proof piston. The outer side of the piston cylinder was threaded, so that the lid could be attached. In this lid, a hole with a diameter of 16 *mm* was made so that a rod could be screwed in and out, altered to a given length. The threaded rod was drilled inside out to a cylinder so that the piston rod could move freely within. At the end of the adjustable rod, a flat washer was attached to meet the piston head and to stop further movement. Between the flat washer and the piston head, a large and stiff spring of 35 *mm* was installed as a safety mechanism. This way, the large piston can move even further if the oil is still expanding and the slider has reached its full length. The piston actuator with all its parts may be seen in figure 4.2.

Testing

When testing the piston actuator, the movement of the two pistons was the main focus. However, if these were to move back and forth at the same distance each time, no leaks could be present. Otherwise, the amount of oil inside the actuator would decrease, resulting in smaller piston displacements given the same temperature difference. Prior to testing, a temporarily copper coil had to be made and attached to the piston cylinder, which was filled with the temperature sensitive fluid. The idea was, that by using this copper coil submerged in a pot containing oil, it would serve the purpose as the heating container, while this was being produced. By having a thermocouple in the pot with the heated liquid, the temperature inside the copper coil could be

(a) The piston cylinder with a brass lid, threaded adjustable cylinder, big spring, big piston and small piston.

(b) All parts of the piston actuator aligned, ready to be assembled.

Figure 4.2: Pictures of all parts included in the piston actuator.

monitored, and the displacement distance for the two pistons inside the piston cylinder could be measured and compared to the theoretical displacement. A copper coil with an outer diameter of 3/8" was used, and made in a way so that a total length of 3 meters of this coil would be submerged in the pot, figure 4.3a. The inside diameter of this copper coil was 7,82 mm, which gave a total volume of $1,441 \cdot 10^{-4} m^3$ according to equation 4.1.

$$V = \frac{\pi \cdot D^2}{4} \cdot L \tag{4.1}$$

By applying the known fact that sunflower oil expands linear with temperature by a factor of approximately 0,07 $\frac{\%}{K}$ and by using equation 2.6, the volume of the inside of the submerged coil will be expanded by a factor of $1,0086 \cdot 10^{-7} \frac{m^3}{K}$.

To put this in perspective, the displacement length of the two pistons for several temperature differences are presented in table 4.1.

Table 4.1: Theoretical displacement lengths of the big and small piston due to expansion of the oil in the copper coil made for testing. Different temperature ranges are presented.

Displacement length			
Temperature difference $\Delta T[K]$	**Volume difference** $\Delta V[m^3]$	**Big piston displacement length** $[mm]$	**Small piston displacement length** $[mm]$
5	$5,043 \cdot 10^{-7}$	1,6	17,8
20	$2,017 \cdot 10^{-6}$	6,4	71,3
100	$1,009 \cdot 10^{-5}$	32,1	356,7
200	$2,017 \cdot 10^{-5}$	64,2	713,4

Further, the copper coil was connected to a thinner copper pipe, with an outer diameter of 1/4", which again was attached to the piston cylinder. This was to avoid that any of the hot oil from the coil would enter the piston cylinder, and by that, avoiding the fact that some of the parts in the piston cylinder had to be made to withstand temperatures above $200°C$. Also, by having a thinner copper pipe connected to the piston cylinder, it would make the piston actuator more agile for movements. In fact, the first copper pipe made for this purpose, had an outer diameter

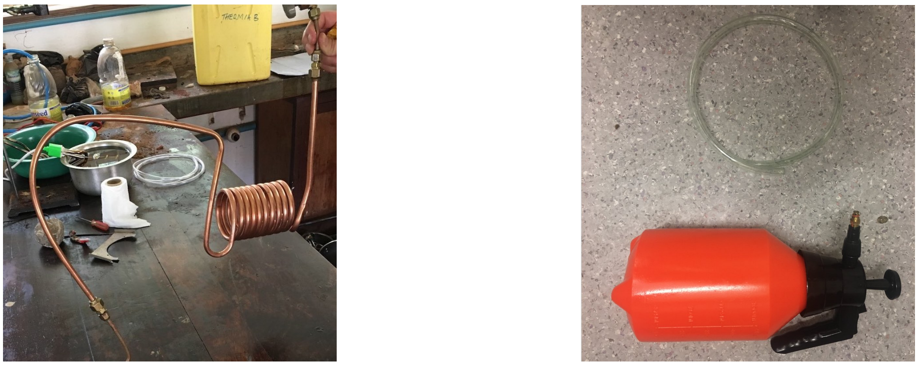

(a) The copper coil made for testing the movements of the pistons in the actuator.

(b) The pressurised filler with a hose that connects it to the closing valve of the copper coil.

Figure 4.3: Pictures of the equipment used for testing the piston actuator.

of 1/8", but the inner diameter, measuring 1,58 mm, was so small that it was impossible to fill this with oil due to great viscous forces relative to the inertial forces. The next step was to fill the copper coil and the piston cylinder with oil, and to extract all the air inside. Having air within the system would cause an issue. During heating, the expanding oil would start to compress the air instead of pushing the pistons. However, removing air turned out to be more difficult than what was anticipated, because the copper pipes were both thin and long. This resulted in a slow movement of the oil being pushed through, and thus air being trapped inside. A pressurised filler had to be acquired so that the oil would be sent through the pipes and the piston cylinder by a greater force, filling all the voids, figure 4.3b. After several attempts of filling the system, one solution for removing excessive air was favourable. This was done by connecting the pressurised filler to the valve attached to the copper coil at the other side than the piston cylinder, pushing the oil through the system from this end. Then, having the piston cylinder in a vertical position, with the big piston pointing down and pushed all the way towards the spring, and the ventilation hole on the side of the piston cylinder closed, the small piston could be detached so that the oil would flow out of this opening. When a greater volume of oil had been sent through, approximately 1 litre, and no more air bubbles were observed, the valve connected to the pressurised filler was closed. Then, the big piston was pushed fully in, to further fill voids, resulting in more oil flowing out from the small piston opening. Next, the small piston was pushed in towards its opening. The piston cylinder was tilted back to its horizontal position, before the ventilation hole, now being the highest point of the piston cylinder, was opened, and the small piston was gently pushed in to its starting position. If any more air would be inside of the piston cylinder at this time, the residual air would be pushed through the ventilation hole, before it finally would be closed.

Results and modifications

Test 1

Prior to the test, the piston cylinder was mounted to a rack, securing a sturdy and horizontal position, so that both of the piston displacement lengths could be observed. It was also mounted in a way that the small piston would not exceed its maximum displacement length, causing the piston to fall out of the cylinder. In addition, the big piston was positioned 22,5 mm from the large spring, meaning that in theory the big piston should move 22,5 mm before the small piston should start its motion.

The results from the measured temperature of the oil in the pot where the copper coil was submerged, with the corresponding piston displacement lengths are listen in table 4.2.

Table 4.2: Displacement lengths of the big and small piston due to expansion of the oil in the copper coil, test 1.

Test 1										
Temperature [°C]	32	50	70	90	110	130	140	145	150	155
Big piston displacement length [mm]	0	2,9	9,6	15,2	22,6	28,2	32,2	34,0	35,2	35,7
Displacement length difference [mm]	0	2,9	6,7	5,6	7,4	5,6	4	1,8	1,2	0,5
Small piston displacement length [mm]	0	0	0	0	0	0	0	0	0	17,4
Displacement length difference [mm]	0	0	0	0	0	0	0	0	0	17,4

The measured temperature of the oil inside the pot was not necessarily the mean temperature. Since the thermocouple was placed at a fixed position, and there was no mixing of the oil, natural convection may create considerable temperature differences. It can be observed that the big piston moved with a mean displacement length of 5,8 mm for a measured temperature difference of 20°C. This deviated from the theory in table 4.1, with roughly 10%. The reason for the deviation may be due to several factors, such as leaks or inaccurate temperature and displacement length readings. However, the interesting part was to observe whether the displacement length would be consistent with other tests. Moreover, the piston did not stop after 22,5 mm, as it should have, but kept moving more than 13 mm further, over a temperature range of roughly 45°C. Then, the small piston suddenly moved a long distance in just a few degrees Celsius. This implied that either the large spring was not stiff enough to stop the big piston, the friction forces on the small piston were too great to be overcome by the pressure on the small piston head, or a combination of these two. Either way, improvements had to be done.

Test 2

For the second test, both the piston cylinder and sliding valve 2 were mounted on the same rack, aligned together. The small piston reached all the way from the piston cylinder and through the inlet hole of the sliding valve, pushing the slider. In addition, the grooves for the rubber seals on the small piston were lathed some tenths of a millimetre deeper, and the big spring was replaced with a new, stronger spring, so that the small piston would start to move sooner.

Table 4.3: Displacement lengths of the big and small piston due to expansion of the oil in the copper coil, test 2.

Test 2									
Temperature [°C]	21,6	40	60	80	90	100	110	115	120
Big piston displacement length [mm]	0	3,5	10,0	15,4	18,4	22,6	24,5	26,7	30,0
Displacement length difference [mm]	0	3,5	6,5	5,4	3,0	4,2	1,9	2,2	3,3
Small piston displacement length [mm]	0	0	0	0	0	0	0	0	0
Displacement length difference [mm]	0	0	0	0	0	0	0	0	0

This time, the mean displacement length for a measured temperature difference of 20°C was 6,1 *mm*. The small piston did not move at all. It was observed that a leak was present between the piston cylinder and the 1/4" copper pipe connector, which may have been the cause. As the pressure inside the piston cylinder increased, the small piston should have started moving at one point. However, it seems that the forces holding the small piston back was not overcome, and the over pressure created a leak at a seemingly weak part of the construction instead. The tension between the small piston and the piston cylinder wall prior to the test had been reduced due to deeper grooves, but another issue had occurred as it was difficult aligning the piston cylinder and the sliding valve at the same height. If the two components were not at the same height, the long piston rod would have problems sliding smoothly through the hole into the sliding valve. Again, the small piston seemed to be the issue.

Test 3

Prior to this test, the small piston rod was cut in half so that the piston would not be in tension due to alignment problems between the piston cylinder and the sliding valve. Instead of having one long rod, the small piston was now half its original length, pushing the other half that was placed at rest through the opening of the sliding valve. By doing this, it was no longer necessary to align the two components at a perfect height relative to each other. In addition, the copper pipe connector, where the leak occurred, was sealed using plumber tape.

Table 4.4: Displacement lengths of the big and small piston due to expansion of the oil in the copper coil, test 3.

Test 3.										
Temperature [$°C$]	22	40	60	80	100	120	130	135	143	128
Big piston displacement length [mm]	0	5,4	11,1	17,7	24,0	30,5	33	33,2	33,8	31,5
Displacement length difference [mm]	0	5,4	5,7	6,6	6,3	6,5	2,5	0,2	0,6	-2,3
Small piston displacement length [mm]	0	0	0	0	0	0	5,2	8,5	8,5	8,5
Displacement length difference [mm]	0	0	0	0	0	0	5,2	3,3	0	0

The mean displacement length for a measured temperature difference of $20°C$ was 6,1 mm. This time, the small piston moved and pushed the slider all the way in. After the small piston had reached its full length, the power was shut off and the temperature of the oil inside the copper coil started to drop, which can be seen in table 4.4. As intended, the big piston stopped its movement at the same time as the small piston started to move, but kept going a bit further after the small piston stopped, since the temperature still increased somewhat. However, what also happened, was that the new, big spring, which was supposed to stop the big piston after 15 mm of displacement, was exceeded by almost 19 mm. This indicated that the small piston still had issues overcoming the forces preventing its motion. And the consequences of this, which can also be seen in table 4.4, was that the big piston started to retract before the small piston, when the temperature inside the copper coil dropped. In fact, the small piston was stuck in its full extent even when the temperature in the copper coil reached the ambient temperature of $22°C$. Yet, if an extra force was applied, the small piston could be pushed all the way back to its initial position. This resulted in a concept that does not work. One possibility was that the large spring was too weak, resulting in a greater displacement than desired for the big piston. Other explanations might be that a leak over the small piston had occurred due to the surface treatment, or even a leak in one of the other parts of the piston actuator due to the increased pressure inside the piston cylinder and copper coil. Although the idea of having one big piston handling the large temperature range and then one small piston acting as an actuator for a valve, works in theory, it seemed difficult to make this in reality. The idea was therefore discarded. However, as the big piston seemed to move smoothly, and with an almost constant mean displacement length throughout the tests, the idea of only using one piston in the actuator was decided to be tested in future designs.

Test 4

The piston cylinder and the sliding valve was still mounted on the same rack. The piston cylinder was, on the other hand, mounted in the opposite direction so that the big piston would be pushing the rod going through the sliding valve. By means of this, the big piston would hopefully extend and retract according to a predicted temperature range. The small piston was still inside the piston cylinder, and was locked in a fixed position, with the only purpose of sealing the opening.

Table 4.5: Displacement lengths of the big piston due to expansion of the oil in the copper coil, test 4.

Test 4												
	Heating					Cooling						
Temperature [$^{\circ}C$]	22	40	60	80	82	**Time [min]**	2	4	6	8	10	12
Big piston displacement length [mm]	0	3,4	9,1	14,9	17,9		15,1	14,2	13,5	13,2	12,4	12,4
Displacement length difference [mm]	0	3,4	5,7	5,8	3		-2,8	-0,9	-0,7	-0,3	-0,8	0
Slider displacement length [mm]	0	0	0	5,2	8,2		5,4	4,5	3,8	3,5	2,7	2,7
Displacement length difference [mm]	0	0	0	5,2	3		-2,8	-0,9	-0,7	-0,3	-0,8	0

In table 4.5, it can be seen that the big piston was extracted in a smooth motion, pushing the slider all the way to position 2. However, the mean displacement length for a measured temperature range of $20^{\circ}C$ was only 5,6 mm. The piston retracted when the coil was removed from the pot with the hot oil and exposed to ambient air temperature. It did not retract all the way back to its initial state, but stopped at the displacement length of 12,4 mm, where it was stuck a long time after the test ended. Without pushing it back to its initial state, the copper coil was heated once more to observe the movement of the big piston and the slider again. The temperature response was not measured during reheating, only the final displacement. The big piston was extended the same length as last time, pushing the slider all the way to position 2. However, this happened at a higher temperature than in the prior test. During cooling the piston retracted back to a similar position of a displacement length of 12,5 mm. As in the prior test, if an extra force was applied to the piston, it could be pushed back to its initial position.

With the last test in mind, it was decided that the idea of having only one piston in the piston actuator was a concept worth investigating further. Nonetheless, the design should be improved, making the component less complex so it would be easier removing all the excessive air inside the system. That way, it would be more likely for the piston to move the same length during extraction and retraction. However, having only one piston would imply that the actuator would either be temperature sensitive but having a long displacement length, or being less temperature sensitive but with a shorter displacement length.

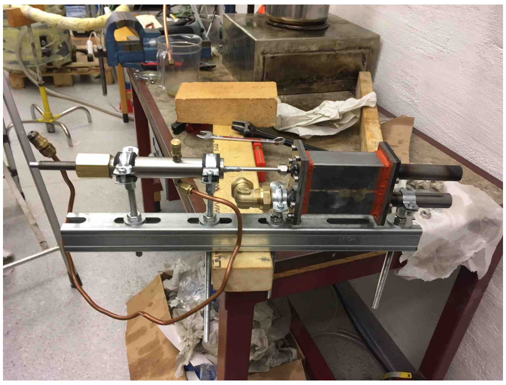

(a) The small piston facing the sliding valve, as it was during test 2 and 3.

(b) The piston cylinder has been turned around so that the big piston faces the sliding valve. During test 4.

Figure 4.4: The piston actuator and the sliding valve assembled on the same rack during testing. The copper coil can be seen submerged in the pot in the background.

4.1.2 Single piston actuator

Production

To make this design less complex, resulting in easier production and less parts, and hence less room for errors, the piston cylinder was made with only two openings. The cooper coil was attached at one end, while the piston was entering the other end. This way, it was no longer need for the two openings on the side of the cylinder. The trouble with the small piston in the prior design seemed to be that it had a cross sectional area too small for the pressure force to overcome the friction force. According to figure 3.3a, an inner diameter of 10 mm yields a displacement response almost a third of the 6 mm diameter piston, but also four times the displacement response of a 20 mm diameter piston. Although the response of a 10 mm piston is far from as good as the 6 mm piston, a cross sectional area that is 2,8 times the size would more likely enhance movement of the piston. The inner diameter was therefore chosen to be somewhere around 10 mm. By alternating the diameter, the length of the piston cylinder also needed to be adjusted to provide for the volume expansion of the oil, according to figure 3.3b. Thin and long drill bits are expensive tools and the assortment in the lab was thus the limiting factor when choosing the piston cylinder dimensions. The best alternative resulted in an inner diameter of 14 mm and a length of 120 mm. The piston was made the same way as for the big piston in the Double piston actuator. The total length was 144 mm with a piston head of 14 mm in diameter, having a length of 24 mm. The inside of the cylinder was broached, and rubber seals were attached to the piston head to prevent leaks. The copper coil was connected to the piston cylinder by a pipe reduction muff made of brass, attached to the one end in a similar manner as for the lid in the prior design. The completed piston actuator can be seen in figure 4.5.

Testing

Instead of being connected to the copper coil submerged in a pot of oil, this piston actuator was now connected to the heating container during testing. This was to test both the piston actuator

(a) All parts aligned.

(b) All parts assembled together.

Figure 4.5: The Single piston actuator. The piston will move back and forth on the right side, while the copper coil will be attached on the left side.

and the heating container at the same time. The heating container will be further discussed later in this chapter. The piston actuator was filled with oil the same way as for the prior solution, only with other difficulties. The pressure filler was pushing oil through the valve at the other end of the copper coil, the same way as last time, with the piston cylinder in vertical position. This way, oil was flowing out of the end of the piston cylinder, which was not connected to the copper coil. After approximately 1 litre of oil had been pushed through the system, and no air bubbles were observed, the filling was stopped. Then, the piston was pushed down the cylinder as far as it would go, resulting in oil flowing out on the other side of the copper coil, through the valve. After the piston was carefully pushed all the way down, the valve was closed, and the piston actuator was ready for testing. Although the filling was less complex, it has its drawbacks. Since the copper coil was built inside the heating container, without the possibility of removing it, the heating container had to be disassembled from the rack in order to fill the coil. It was difficult to manage the container at the same time as filling the coil, since the piston cylinder had to be in a certain position during filling, preventing air bubbles in the system, as well as oil spill. Regardless, given some time, the copper coil was filled and the heating container and piston cylinder was installed in the rack once more.

Results and modifications

Two tests were conducted. The first was a concept test to check for movement of the piston. It reacted to temperature rise by extracting in a smooth motion, but during cooling, it got stuck while retracting. As before, with some extra force applied, the piston could be pushed back to its initial position prior to the first heating. The concept was proven, but the same issues regarding retraction during cooling, as for the earlier design, were still present and improvements had to be made.

Test 2

Before initiating test 2, the surface inside the piston cylinder and the surface of the piston head were polished to reduce tension. This was done carefully to avoid leaks between the two components.

The test was conducted with a reheating, to see if the piston would move the same distance both times during heating and cooling. Prior to the test, a quick calculation was made to review the displacement length of the piston due to temperature difference in the copper coil. However, since the theoretical and practical displacement length had already been analysed in the first design, the only data of interest was the final position after heating and cooling. The heating ended when the measured temperature was 150°C. The temperature still increased while the heating container was flooded with cold oil, reaching a maximum temperature of 162°C. The copper coil was then cooled to 60°C before it was reheated once more to 150°C.

Table 4.6: Displacement length of the Single piston actuator during heating and cooling.

Test 2										
	Heating			Cooling		Reheating			Cooling	
Temperature [°C]	22	150	162	160	60	60	150	162	160	60
Piston displacement length [mm]	0	14,2	16,3	14,3	13,2	13,2	13,2	15,2	14,9	12,9
Displacement length difference [mm]	0	14,2	2,1	-2,0	-1,1	0	0	2,0	-0,3	-2,0

From the test results seen in table 4.6, it can be observed that the piston actuator did not work as desired. The piston extended during heating as intended. However, during cooling, it first retracted with a greater length per temperature change than during heating, before it stopped at a temperature of approximately 140°C. When reheating, it did not reach the same extension as during the first heating, and when cooled once more, it stopped at the same point. From the results, it can be concluded that this design was far to unpredictable to handle the accuracy required by the piston actuator in this project. In addition, with all the problems related to the production and surface treatment, it was hard to imagine the success of manufacturing this component in certain parts of Africa where the production facilities may be limited. Thus, the idea of making a piston actuator in the workshop was discarded as it seemed impossible to produce this component without a great effort.

4.1.3 Pneumatic double piston actuator

Production

The third and final solution was to acquire prefabricated pistons and to assemble them together with the copper coil. This assured leak-proof pistons, and thus the concept of using two pistons of different sizes was decided to be tested once more. Ideally, hydraulic parts should have been acquired. However, due to the easy accessibility of pneumatic parts and limited time, this was chosen. Two pneumatic pistons were acquired, one with a cylinder diameter of 25 mm and one with 10 mm. Both had a displacement length of 50 mm, see figure 4.6. The inlet hole for each of the pistons were of different sizes, and custom connections had to be made to attach them to the 1/4" copper pipe. Further, the pistons were connected with the copper pipe in a tee, while a ventilation opening was attached close-by, to be used during filling.

Testing

Two tests were conducted with the Pneumatic double piston actuator. The first was with only the big piston attached to the copper coil, while the second was with both the big and small piston attached. The piston actuator was connected to the heating container, same way as the Single piston actuator.

A greater effort had to be made when filling this actuator, especially when both of the pistons were attached to the copper coil. First, each of the two pistons were filled with oil on their own.

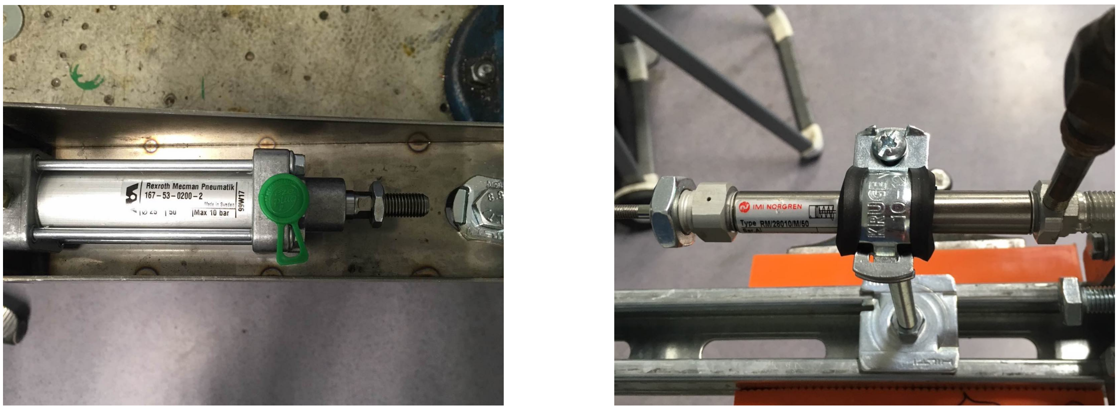

(a) The big piston, inside a container. The piston displacement movement is to the right.

(b) The small piston, fitted in a rack. The piston displacement movement is to the left.

Figure 4.6: The pistons acquired for the Pneumatic piston actuator.

By holding the big piston submerged in a tank of oil, the piston was extracted all the way out, filling the internal volume with oil. By extracting and retracting several times, no air bubbles would be left inside. The small piston tried being filled in the same manner, but this did not work due to a thin inlet pipe and a small displacement volume. Instead, a thin metal pipe was filled with oil using suction pressure while one end was submerged in oil. The pipe was inserted into the inlet of the small piston while the oil was forced out, filling the piston cylinder from the inside. This way, the air was pushed out. After both piston actuators were filled, they were connected to the tee. Then, the copper coil was attached to the last inlet of the tee before the pressurised filling tank was connected to the other end of the copper coil. Further, oil was filled through the system and out of the ventilation opening. While still having this open, both of the pistons were pushed all the way in. Consequently, more oil, in addition to the residual air that might have been inside the system, was pushed out of the ventilation opening. Finally, a piece of wood was attached near the big piston to stop its extraction during heating, instigating motion of the small piston. The full system setup can be see in figure 4.7.

Results and modifications

Test 1

The displacement length of the big piston versus temperature was tested. The test results are presented in table 4.7.
The piston moved with a relatively constant and smooth motion during heating, and retracted all the way back to its initial position during cooling. This implied no leaks and no air inside the system. On the other hand, it seemed that the piston retracted faster during cooling than how it extracted during heating. There may have been several reasons for this. The readings might have been inaccurate and/or the temperature measured inside the heating container was not representative for the temperature inside the copper coil. The thermocouple was placed at the outlet of the heating container. Therefore, the copper coil was exposed to the cold oil coming from the inlet, earlier than the thermocouple. In addition, natural convection transferred hot oil towards the top of the heating container, making the temperature readings higher than the mean temperature. Therefore, the retraction of the piston might have been in compliance with

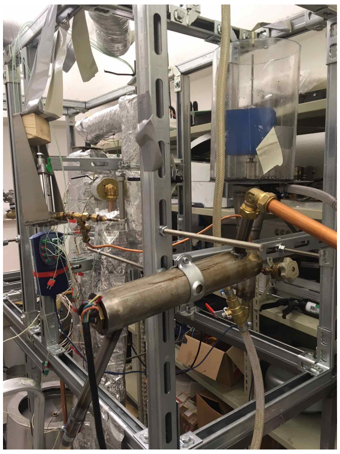

(a) The two pistons can be seen to the left, while the copper coil and the heating container can be seen in front and to the right in the picture.

(b) A closer look at the two pistons. The big piston is to the left, with the piece of wood attached above the piston extraction direction. The the small piston is to the right.

Figure 4.7: The full setup during testing of the Pneumatic double piston actuator, as it was temporarily assembled within the rack along the rock bed and the other components.

Table 4.7: Displacement length of the big pneumatic piston during heating and cooling.

Test 1										
Heating										
Temperature [$°C$]	27	50	70	90	110	130	150	170	190	210
Displacement length [mm]	0	0,7	1,7	3,3	5,0	7,0	8,7	10,4	12,3	14,5
Displacement length difference [mm]	0	0,7	1,0	1,6	1,7	2,0	1,7	1,7	1,9	2,2
Cooling										
Temperature [$°C$]	210	190	170	150	130	110	90	70	50	27
Displacement length [mm]	14,5	7,8	4,5	3,1	2,3	1,3	1	0,6	0,3	0,2
Displacement length difference [mm]	0	-6,7	-3,3	-1,4	-0,8	-1,0	-0,3	-0,4	-0,3	-0,1

the theoretical displacement response, but was indecisive.

The second test was conducted with both pneumatic pistons attached to the copper coil. As some earlier tests, this was a concept test to see whether it would yield the desired outcome or not. Hence, no results of the displacement length versus temperature are presented. However, a test with heating, cooling, reheating and cooling once more was conducted. First, the big piston moved the distance up to the piece of wood, approximately 10 mm. As it hit the wood, some time went by as the big piston went a bit into the soft wood. After some seconds, the small piston started to move, at a greater rate than the big piston. When the small piston had been extracted for almost 30 mm, the power was shut off and a valve was opened, allowing cold oil to flow through the heating container at a steady rate. The small piston still moved 2-3 mm further, before retracting to its initial position, without the big piston moving at all. When the small piston stopped, the big piston started to retract in a smooth motion, seemingly at the same rate as during extraction. At a point, the supply of cold oil was stopped and the power was turned on. After a short while, the same procedure started once more, having the big piston move all the way into the wood, followed by the movement of the small piston. Again, the power was shut off, cold oil was supplied into the heating container, and the pistons started to retract in the same manner as before. It was observed that the big piston did not retract all the way back to its initial position, although the oil inside the copper coil reached ambient temperature.

The reason why the big piston did not retract all the way back was due to leaks observed during the test. It was noticed that the piston actuator was leaking from the connection between the copper coil and the tee. Consequently, air might be drawn in due to the under pressure created inside the piston actuator during cooling. The air will occupy space resulting in less retraction. Further, this will also result in a higher temperature needed to achieve the same displacement of the pistons, and thus the oil in the heating container will have a higher temperature when the sliding valve is opened. If the system is reheated many times without refilling the piston actuator, the deviation of delivered temperature to the set point temperature will increase with time. Nevertheless, this was by far the most prominent of the designs tested, and leaks in the connections should manageable. At the time this report was written, the piston actuator was currently being assembled together with the sliding valve and the heating container, and mounted in the test rig with the rock bed. Therefore the system setup was not completed and further testing could not be conducted.

4.2 Sliding valves

Three different sliding valves were made, all based on the concept described in chapter 3. To make the design simple, the valves were made from rectangular steel profiles measuring 40x40 *mm* and 35x35 *mm*, both with a wall thickness of 2 *mm*. This saved both time and money as prefabricated profiles are cheap and accessible. Machine drawings of each sliding valve are presented in Appendix A.

4.2.1 Sliding valve 1

Production

The first sliding valve was made with rectangular holes in the inlet chamber and slider. Three holes were made for each outlet chamber, giving a total of six holes in the slider. The holes in the chambers measured 30x8 *mm* while the ones in the slider were cut slightly smaller, 28x5 *mm*. This was to ensure a smooth flow through the outlet chamber avoiding disturbances due to imprecise machining. The inlet and outlet chambers were made from two pieces of the big steel profile, both measuring 200 *mm* in length. These were welded carefully together to avoid deformation, which could lead to an uneven sealing surface for the slider. If too much heat had been applied during welding, the steel profile may have been deformed, ruining the smooth surface where the slider would slide between position 1 and 2. To separate the outlet chambers, a thin plate was spot welded in the middle of the bottom chamber. Sliding valve 1 can be seen in figure 4.8.
If the oil in the heating container for some reason would extend the set point temperature, the slider would travel a further distance than its design displacement. Hence, one of the openings in the inlet and outlet chambers were cut bigger than the others, 30x16 *mm*. This was added as a safety mechanism to maintain a flow of cold oil into the heating container. The design difference can be seen from the machine drawings in Appendix A.

Figure 4.8: Sliding valve 1. The slider has six rectangular holes. On the left hand side is the lid with the piston rod penetration unit for the small piston and the outlet for the cold oil. On the right hand side is the inlet of oil and outlet for the hot oil. The profiles are welded together and the flanges are spot welded. Holes for the mounting bolts can be seen in the detached lid to the right.

The inlet, outlets and piston rod penetration unit were connected to the sides of valve, as they were already open. Therefore, no additional holes had to be cut in the steel profiles. In addition, insulating would be easier. Square flanges were milled from steel plates and fitted around the outside of the valve, as seen in figure 4.8. The inlet and outlets were made from steel pipes of 22 mm outer diameter, which were welded onto the lids. The piston rod penetration unit was made from a Swagelok fitting with a set of PTFE gaskets, welded onto the lid. This provided a sealed penetration where the piston rod could slide smooth back and fourth. Bolts were used to tighten the lids to to the flanges In addition, gaskets were made for both flanges to prevent leaks, as seen in figure 4.10c.

To provide a force, which would push the slider back to its initial position during contraction of the oil in the piston actuator, a spring needed to be mounted inside the sliding valve. This was accomplished by welding a threaded rod to the inlet pipe, as can be seen in figure 4.9a. The rod size was chosen to be smaller than the inner diameter of the spring so the spring could be fitted around the rod. A nut was placed on the rod, providing an adjustable foundation for the spring. To provide a foundation on the slider, a plate was welded on one of the slider openings, as seen in figure 4.9b.

Testing

Tests were conducted to inspect leaks, both from the flanges and between the chambers, and to test the flow response when changing the slider position. Gaskets were placed between the flanges and lids, as they were tighten together using eight bolts on each side. The piston rod was placed in the penetration unit to prevent leaks and giving the possibility to change the slider position. A plastic hose was connected to the inlet pipe, providing a fluid flow into the sliding valve, as shown in figure 4.10a. Sunflower oil at $220^{\circ}C$ has similar fluid properties as water at room temperature. Thus, tap water was used during the tests as this was more convenient.

With the slider placed in position 1 (figure 3.5), opening the holes to the cold outlet chamber, the

(a) Threaded rod with a nut to provide an adjustable foundation for the small spring. The rod was spot welded to the inlet pipe.

(b) A sealed end providing the spring foundation.

Figure 4.9: Pictures of how the small spring is mounted and where it was in contact with the slider.

sliding valve was filled with water. After the flow settled, the piston rod was pushed further in, moving the slider to position 2 (figure 3.5). Consequently, the holes to the cold outlet chamber were closed and the holes to the hot chamber were opened. After the flow had settled, the piston rod was released, allowing the spring to push the slider back to position 1.

A paper towel was prepared to form a temporarily seal for the wall separating the outlet chambers. This was used to determine whether potential leaks were located between the outlet chambers or the inlet chamber an outlet chambers.

The smoothness and sealing of the piston rod penetration unit was tested as follows. The sliding valve was tilted so the piston rod was pointing towards the floor. Water was added to the inlet chamber, creating a water basin. The piston rod penetration unit was tightened to a point where no leaks occurred, yet the motion of the piston rod was smooth through the penetration unit.

Results

With the slider in position 1, a successful sliding valve should direct the water flow through the cold chamber only. As water was flowing out of both outlets, the valve was dysfunctional. The leaks between the inlet and outlet chambers were easily detected, as the surface inside the inlet chamber was not sufficiently levelled. Deformations, possibly from the welding, generated gaps between the slider an the underlying surface. In addition, as the separation plate between the outlet chambers was spot welded, it did not provide a sufficiently good seal. Thus, there were leaks between them as well. Nevertheless, the spring response was satisfying, pushing the slider back into position 1 when the piston rod was released.

(a) Test setup for the sliding valves. The valves were filled with water using a plastic hose.

(b) Lid with the piston rod penetration unit made out of a Swagelok fitting. The PTFE gaskets and tightening bolt are placed on the right hand side.

(c) Rubber gaskets to seal the flanges during tests with water.

Figure 4.10: The sliding valve test setup, a lid with the piston rod penetration unit and a pair of rubber gaskets for the flanges.

4.2.2 Sliding valve 2

Production

Based on the results from sliding valve 1, a second valve was made. Hence, circular holes were used to increase the sealing surface between the slider and the inlet chamber to prevent leaks. As the flow capacity through the valve was not an issue, the number of openings to each outlet chamber was reduced from three to two holes. Consequently, the length of the sliding valve was reduced, now measuring 120 mm. The safety aspect of the sliding valve was neglected to make the design simpler. Hence, all holes were the same size, as seen in figure 4.12a. The holes in the slider and chambers had a diameter of 5 mm and 8 mm respectively. To reduce the risk of deformation due to heat, the inlet and outlet chambers were soldered together, not welded. An overview on the sliding valve is given in figure 4.12.

To seal the separation wall between the outlet chambers, they were made out of three parts. Two steel profiles of 40x40 mm, measuring half the length of the inlet chamber, were welded onto each side of a thin metal plate. This plate ensured a completely sealed separation wall, as it was welded at the outer perimeter of the outlet chambers. The outer surface was grinded to even the surface, and later sanded to make it smooth. Hence, the brushed surface finish seen in figure 4.12a.

From preliminary tests, some leaks occurred between the inlet and outlet chambers. Therefore, the inside of the inlet chamber and outside of the slider were sanded to give a smoother surface. This provided a better seal between the slider and the inlet chamber surface due to a more even and planar sealing surface. The sandpaper used had a grit size of 400. In addition, to keep the slider in contact with the sliding surface in the inlet chamber, a thin metal plate of thickness 0,5

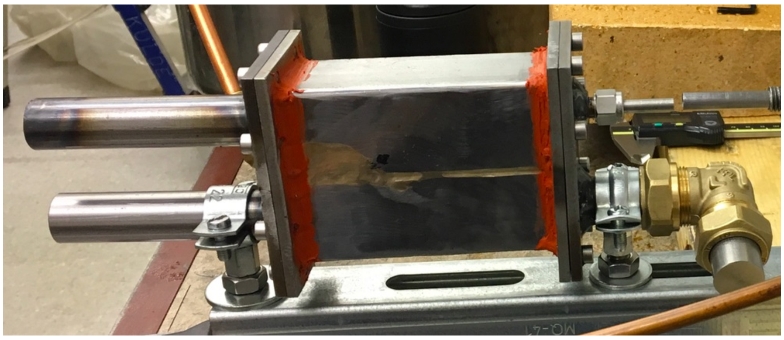

Figure 4.11: Side view of sliding valve 2 in a test rig with the right outlet blocked. The flanges were glued using Loctite SI 5399, providing extra sealing.

mm was placed at the top of the slider. This provided a tighter fit of the slider inside the inlet chamber, pushing the slider surface down in the inlet chamber, providing a better seal, as seen in figure 4.12b.

The flanges and lids from sliding valve 1 were reused in sliding valve 2 to save time and materials. Instead of spot welding the flanges to the slider, a silicon based glue, which tolerates temperatures up to $350°C$, Loctite SI 5399, was used. This provided an extra seal around the flanges, as seen in figure 4.11.

The spring foundation was made out of a small metal plate welded onto one of the slider openings. As the valve would be full of oil during operation, the spring base size was reduced so the slider would move easier through the oil. A small bolt was welded to the spring foundation, preventing the spring from being dislocated. The spring foundation and slider are shown in detail in figure 4.12c.

Testing

Tests were conducted in the same manner as for sliding valve 1. In addition, to test for leaks between the outlet chambers, some water was filled in one of the outlet chambers at a tilted angle, without the lids mounted. The tilted angle allowed the water to rest at one side of the outlet separation wall. By inspecting the opposite outlet chamber, leaks through the separation wall would be detected.

Results

No leaks were found in the opposite outlet chamber while the separation wall was inspected. During the preliminary tests, small leaks were present through the slider and some of the flow exited through the wrong outlet pipe. Hence, the sealing surfaces were sanded and the thin metal plate was introduced. A tighter fit between the slider and chamber surface made a better seal, stopping the leaks from the inlet to the outlet chambers. Consequently, as the slider was positioned in either position 1 or 2, water flowed only through one outlet, proving there were no leaks. There were also no leaks from the flanges. The piston rod penetration unit and spring response system were not changed from sliding valve 1. Thus, they were still functioning satisfying.

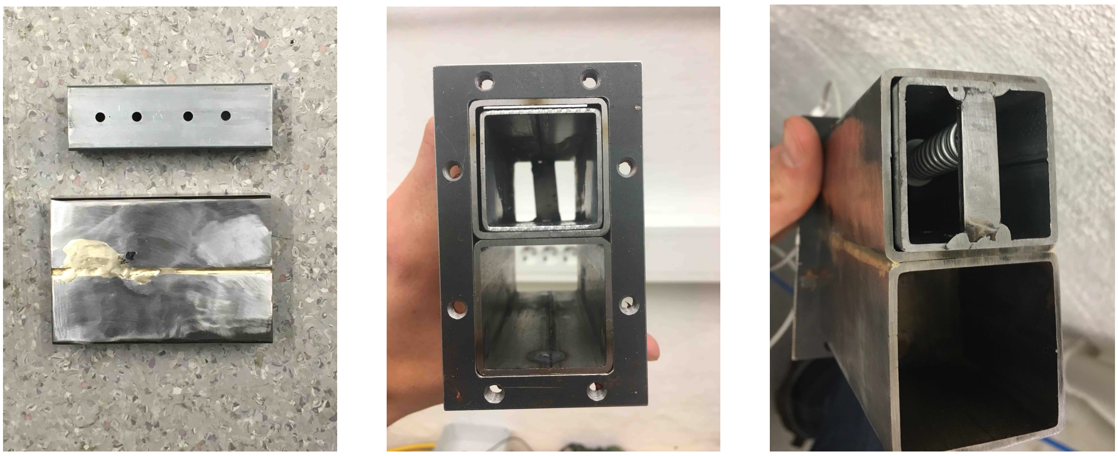

(a) The inlet and outlet chambers were soldered. The holes in the slider and chambers were circular.

(b) A thin metal plate between the top surface of the slider and the inlet chamber provided a tighter fit of the slider.

(c) The spring foundation in contact with the spring. The slider was pushed out by the small spring.

Figure 4.12: An overview of sliding valve 2.

4.2.3 Sliding valve 3

Production

Despite already having made a functional sliding valve, an improved version was desired. The goal for sliding valve 3 was to improve the response of the valve, i.e. faster valve opening/closing for a given temperature difference. To achieve this, the holes in the slider and between the chambers were made rectangular. To avoid the same leak problems as for sliding valve 1, the holes were made smaller, measuring 20x10 mm Hence, the sealing surface was larger. To ensure a free flow from the inlet to the outlet chamber, the slider holes were slightly smaller than the holes between the chambers, as seen in figure 4.14b. As the lids used for sliding valve 1 and 2 were left at Makerere University, new ones had to be made.

Considering the sliding valve was meant for a test rig without circulation, sliding valve 3 was made with only one outlet chamber. When the slider rests at position 1, there is no flow through the valve. This only occurs when the slider is at position 2. A principle sketch of the slider design is found in figure 4.14a

To reduce the risk of deformation due to heat, the inlet and outlet chambers, as well as the flanges, were glued together using Loctite SI 5399. Even though it was only one outlet chamber, there were two outlet pipes, as seen in figure 4.13. This was a mistake made during production due to miscommunication. It was intended to be one outlet pipe as there was only one outlet chamber. However, this had no influence on the functionality of the valve. During operation, one of the outlet pipes was blocked using a pipe fitting.
A thin metal plate was used to make a tight fit for the slider, in the same manner as for sliding valve 2. To make the sealing surface between the slider and the inlet chamber as smooth as possible, both surfaces were sanded using sandpaper of grit size 400.

Figure 4.13: Sliding valve 3. Both the flanges and the profiles were glued using Loctite SI 5399.

After preliminary tests, small leaks were discovered. Therefore, the slider surface was improved using a milling machine. The milling procedure provided an accurate and planar surface. As the sealing surface in the inlet chamber was on the inside of the steel profile, the same procedure could not be done on this surface. To even this surface further, a file was used to make the corners inside the steel profile sharper, reducing their radius.

Testing

The test setup and test procedure for sliding valve 3 was the same as for sliding valve 2.

Results

Initially, the slider had small leaks between the inlet and outlet chambers, measuring approximately 1 drop every second. The flanges and piston rod penetration unit were completely sealed. After the slider was milled, the leaks to the outlet chamber were greater. Even though this result was surprising, the reason was concluded to be the difference in the accuracy of the slider surface and the inlet chamber sealing surface. The profile of the inlet chamber sealing surface had a concave shape, giving a low point in centre. Consequently, when the slider was planar, a gap formed between the profiles, providing leaks. By filing the sides of the inlet sealing surface, the corners were reduced, giving a better fit and seal. Despite the surface treatments, some leaks were still present. The leaks had a drop rate of approximately 1 drop every 2 seconds.

Discussion

Making a sliding valve from prefabricated steel profiles proved to be challenging. The simple design had the drawback of leaks between the inlet and outlet chambers. Despite this, a successful sliding valve was made using circular holes. Rectangular holes yielded a better response, yet due to the leaks, this solution was not successful. During production, applying heat should be done with care and at best avoided. Hence, silicon based glue was used to join parts. A key to success was having a smooth slider and inlet chamber surface to make the sealing as good as possible. The fitting of the profiles should also be tight. The concept of making an affordable slider from prefabricated material was successfully produced. Nevertheless, it should be further developed to improve the slider response.

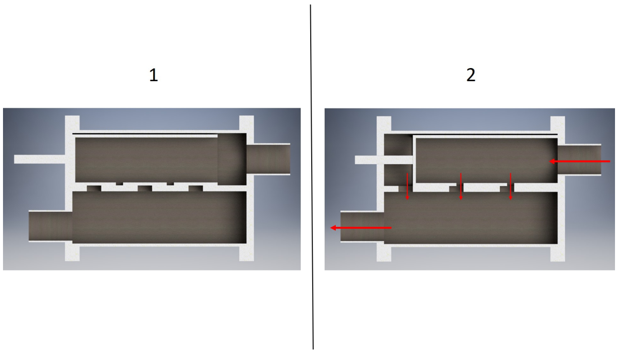

(a) In position 1 the inlet chamber is filled with oil, but there is no flow going through. In position 2 the holes are aligned and hot oil flows through the sliding valve.

(b) The holes in sliding valve 3 were rectangular to achieve a better response.

Figure 4.14: A sketch of the principle for sliding valve 3 and a rectangular holes.

4.3 Heating container

The heating container is an essential part of the mechanical temperature controller. However, this was neither addressed as a crucial component in the project nor assumed to be difficult to produce. The other components, i.e. the piston actuator, the sliding valve and the cooking application, were anticipated to need more time, as several prototypes had to be made and tested. Thus, less attention was granted to the heating container, and a design with corresponding machine drawings was not made prior to the production. Instead, a standard heating element was acquired, and the heating container was made to fit this.

Production

A heating container was designed in order to achieve a good response for the mechanical temperature controller. The new design should be made so the container could be fit into the test rig in compliance with the system sketches in figure 3.2. A heating element of 2000 W was mounted inside a cylinder made out of stainless steel. The steel cylinder dimensions were chosen to be a bit longer than the heating element and having a diameter such that a copper coil could fit around the heating element without touching either the element or the cylinder walls. The diameter was 60 mm and the height was 325 mm. Two steel pipes of 20 mm inner diameter were welded to the cylinder walls. These provided an inlet at the bottom and an outlet at the top. The inlet and outlet were placed at the opposite sides of each other to reduce the risk of a shortcut flow of oil through the heating container. In addition, the inlet pipe was long and attached at an angel, reducing the risk of a backflow of hot oil. The copper coil was made out of a 1/4" outer diameter copper pipe, with an inner diameter of 4,65 mm. The submerged copper coil measured a total of 3,4 m. The copper coil was made by bending the copper pipe around a cylinder mounted in a slow rotary machine. The copper coil was fitted around the heating element, as seen in figure 4.15a. This way, when subtracting the volume occupied by the heating element and the copper coil, the heating container holds 0,76 litres of oil when full. After the coil was submerged, a lid was welded on the top, sealing the heating container. The lid had two holes for each end of the copper coil, which was soldered to make a seal. A small hole was drilled to fit a thin sealed pipe for a thermocouple, near the outlet of the container. This was also soldered, as seen in figure 4.15b. One end of the coil extended 100 mm from the top lid. At this end, a valve was

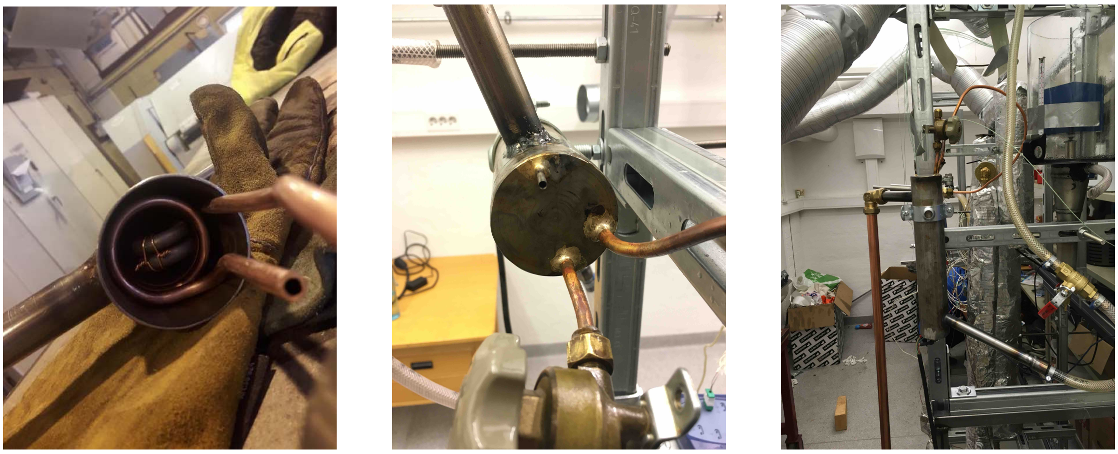

(a) Heating element with the copper coil fitted around, inside the heating container.

(b) The top lid of the heating container with the copper coil and thermocouple pipe soldered to seal the penetration.

(c) The heating container mounted in the test rig. The oil supply tube can be seen on the right side, while the outlet of the heating container is to the left.

Figure 4.15: Heating container.

mounted for filling the copper coil with oil. The other end measured approximately 1,5 m, and was connected to the piston actuator. As the copper pipe was annealed, it was flexible. Thus, the 1,5 m copper pipe gave flexibility to alter the position of the piston actuator.

The heating container was designed to have a constant supply of cold oil. This was achieved by connecting the inlet pipe to a plastic tank filled with oil, via a plastic hose. A valve was mounted on the hose, making it easier to connect/disconnect the hose to the heating container when needed. An overview of the heating container can be seen in figure 4.15.

Testing

During tests of the Single piston actuator and the Pneumatic double piston actuator the heating container was used, and thus tested. A variac was used to control the power of the heating element, which was set to 500 W at first, and later 250 W. The temperature was measured using the thermocouple at the outlet. In addition, a temperature response could be seen from the piston movement during heating and cooling. At the first tests, the heating container was mounted vertically. Later, it was mounted horizontally.

Results

Even though a temperature distribution was not measured using more than one thermocouple, it could be felt by touching the outside of the heating container. With a vertical mounting, there was a large temperature difference, whereas the top was hot and the bottom was closer to room temperature. After changing the position to an horizontal setup, the temperature felt even along the whole cylinder. When lowering the power of the heating element the temperature distribution felt more even than for a higher power.

Discussion

The volume of the heating container should be grater than what was designed. A greater volume gives a better temperature distribution in the oil. Hence, a better correlation between the temperature of the copper coil and surrounding oil would be achieved. The geometry of the container should have a large diameter to height ratio reducing temperature difference caused by natural convection. By placing the copper coil close to the inlet of cold oil, a faster cooling of the coil would be obtained, hence a faster response of the piston actuator. During testing, more thermocouples should have been used to get more accurate readings of the temperature which the copper coil was exposed to. As the displacement response of the pistons were compared to the temperature measured at only one point, this may have given wrong indications when analysing the data. The temperature of the oil exposed to the copper coil may have been lower than what was measured at the top in the heating container. Therefore, during retraction of the pistons, the actual retraction rate may have been different as the measured displacement was compared to a temperature which did not reflect the actual temperature inside the heating container.

4.4 Cooking application

The two concepts for the cooking application had somewhat different approaches during the design phase. Since a solution that could quickly be tested was needed, one cooking application was made with a practical approach, while the other was theoretical. This way, one cooking application would be yielding fast results, while the other could be designed more thoroughly, with respect to optimising the heat transfer.

4.4.1 Three-pot cooker

Production

This solution was assumed to be the fastest and easiest to make of the two designs. 3 pots of different sizes, made of stainless steal were acquired. The smallest pot had a volume of 1,5 litres, the medium had a volume of 1,7 litres, and the largest pot had a volume of 2,8 litres. To have them fit inside each other, the handles of the small and medium pot had to be removed, while the handles of the large pot were removed to easier attach the insulation. Further, the first idea of cutting down the edges of the medium pot was discarded. Instead, holes in the side walls with a diameter of 5 mm were drilled at a height of 56 mm from the bottom, giving the same effect, as seen in figure 4.16a.

The next step was to attach the medium and the large pot together with an opening at the bottom for the oil to flow through them both. This opening had to be made in a way that no leaks would appear during operation. In addition, the two pots had to be attached firmly together, so that there would not be any voids between their bottoms where residual oil could be left and absorb heat. To make this attachment, a hole of 22 mm were made in the bottom centre of the medium and large pot. Further, the first idea was to weld these together to the pipe going through both. However, when the holes were made, it was discovered that the bottom of the pots were not only made out of stainless steel, but had a core of aluminium. As this was difficult to weld, due to the fact that aluminium has a far lower melting temperature than steel,

(a) Medium and large pot. Exit holes at the side walls of the medium pot and a hole in the centre for the inlet pipe.

(b) The soldered pipe with its nut, before cutting, for attaching the medium and large pot together.

(c) The inlet pipe connected at the lower side and the outlet pipe connected at the upper side.

Figure 4.16: Pictures of the Three-pot cooker during production and before testing.

another solution had to be made. Instead, a brass fitting was soldered to the end of a pipe, which was fitted through the two pots and tightened with a brass nut at the other end, seen in figure 4.16b. The edges of the brass nut was cut at several points to ensure that the small pot would not block the inlet flow. In addition, a gasket was made to avoid leaks in the pipe penetration, made from a material which can withstand high temperatures. At the outside walls of the large pot, another hole was made in the same dimensions as the inlet hole, and another pipe with the same diameter and material was welded to the opening, for oil to flow out. Finally, the cooking application was insulated with Pyrogel XT-E and covered in a casing. This was to avoid the possibility of spilling oil on the insulation and to close the gap along the side walls between the pots, reducing heat loss. The completed cooking application can be seen in figure 4.16c. Technical specifications for the insulation is listed in Appendix B.

Testing

Three tests were carried out, to observe whether the cooking application could be used for boiling water, and if so, to which extent. Each time, the rock bed was charged and then drained through the cooking application, connected at valve 4. The pipes between the rock bed and the cooking application were insulated, as well as a lid had been put on top of the pot where the water was being boiled, to reduce heat loss. Three thermocouples were used; one installed at the exit of the rock bed, one at the outlet of the cooking application, and one inside the pot containing the water. A plot will be presented for each of the tests, showing the temperature versus time for the listed positions.

Results

Test 1

The first test was a concept test, to see if the cooking application would work at all. The small pot was filled with 0,1 litre of water and the lid was put on top. The rock bed was not fully charged, but from the plot in figure 4.18, it can be seen that the initial temperature of the oil leaving the rock bed was roughly 180°C. After 600 seconds, the temperature at the outlet of the rock bed started to drop at a higher rate as the mass flow was large and the rock bed was almost empty of hot oil. At this point, the temperature at the outlet of the cooking application peaked. 400 seconds later, the outlet of the rock bed and the outlet of the cooking application

(a) The cooking application implemented in the full system, with the connecting pipes on the left coming down from the rock bed.

(b) A lid was covering the small pot containing water. Oil exited from the pipe coming out of the upper part of the cooking application.

Figure 4.17: The cooking application test setup.

reached the same temperature, and maintained the same temperature profiles throughout the test. This may imply that the mass flow of oil was too high, meaning it did not have time to transfer as much heat as it could have done, along the way through the cooking application. At the same time, t = 1000 seconds, the water reached the boiling temperature of $100°C$. It maintained a temperature above $90°C$ for 2000 seconds more, even though the supply of oil was stopped when the temperature out of the rock bed was below the water temperature. With this test, the concept of boiling water was proven.

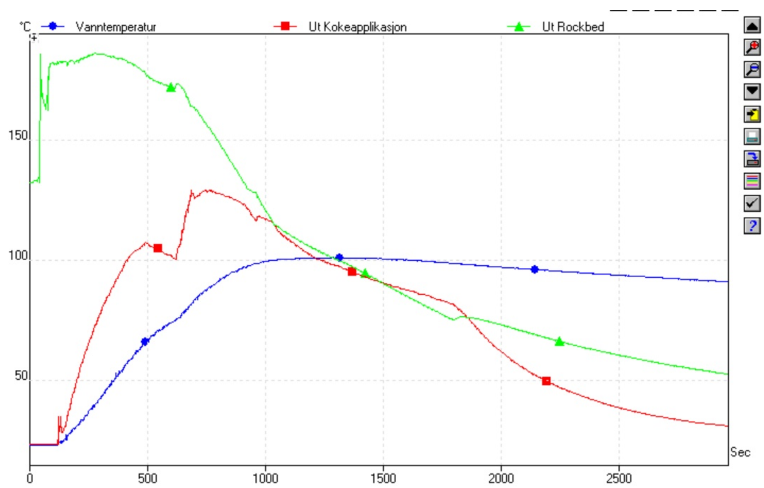

Figure 4.18: Plot of the temperature profile versus time, at the exit of the rock bed (green line), at the outlet of the cooking application (red line), and of the water (blue line), for test 1.

Test 2

The second test was conducted with 1 litre of water in the small cooking pot. The initial mass flow of oil flowing through the application was set to be 0,0041 $\frac{kg}{s}$ while the water temperature was increasing. When the water started to boil, the mass flow of oil was lowered to be 0,00027 $\frac{kg}{s}$, to maintain the water boiling. From figure 4.19, it can be observed that the water reached 100°C after 1400 seconds. At this point the mass flow was lowered, before it was increased once again at t = 2300 seconds to maintain the water at 100°C. It can also be observed instabilities in the temperature of the outlet of the cooking application between t = 800 and t = 1000. This was caused by the thermocouple falling out of its position, which happened twice. The supply of hot oil was stopped at t = 2700 seconds when it reached 110°C. However, the water still maintained a temperature above 90°C for more than 500 seconds after shutdown. By applying equation 2.1, the amount of energy needed for boiling the water can be calculated, by using mean values for density and specific heat capacity [45]. The result is $Q = 329,2kJ$.

To calculate the energy withdrawn from the oil, the same equation may be applied. However, since the temperature difference between the outlet of the rock bed and the outlet of the cooking application differed in the same period as it took to heat up the water, a step-wise calculation was needed. By a rough estimate, with the given mass flow of 0,0041 $\frac{kg}{s}$, it took the oil 116 seconds to flow through the cooking application. Hence, the temperature difference of the flow had to be registered at $t = t_0$ at the outlet of the rock bed, and $t = t_0 + 116$ at the outlet of the cooking application. In addition, for each of the time intervals, a mean specific heat value and density had to be applied. The oscillations caused by the dislocated thermocouple are regarded as small and thus neglected. From these calculations, the oil supplied a total of 961,0 kJ of energy during the same period it took to boil the water. As observed, a great deal of the available energy from the oil was not transferred to the water. This was partly due to the large thermal mass that absorbed much of the heat in the beginning. In addition, heat loss occurred through non-insulated parts, as well as other parts where the insulation was not sufficiently good.

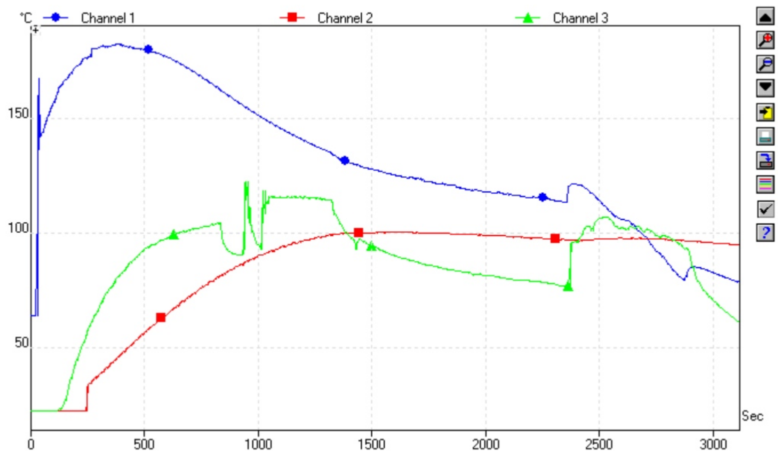

Figure 4.19: Plot of the temperature profile versus time, at the exit of the rock bed (blue line), at the outlet of the cooking application (green line), and of the water (red line), for test 2.

Test 3

The third test was carried out with the same initial conditions as for test 2. 1 litre of water was to be boiled, and the initial outlet temperature of the rock bed was $180°C$. In this test, the mass flow was adjusted several times. At first, it was set to be 0,0021 $\frac{kg}{s}$. At t = 500 seconds, the mass flow was set to be 0,0011 $\frac{kg}{s}$ to observe the effect it would cause. However, it was noticed that with this mass flow, it would take a long time for the water to reach $100°C$. Therefore, at t = 800 seconds, the mass flow was increased to 0,0073 $\frac{kg}{s}$. At the time the water started boiling, roughly at t = 1300 seconds, the mass flow was adjusted back to its initial level of 0,0021 $\frac{kg}{s}$. The supply of oil to the cooking application was stopped at approximately t = 2800 seconds, while the water still maintained a temperature above $90°C$ for 1200 more seconds. The data is presented in figure 4.20.

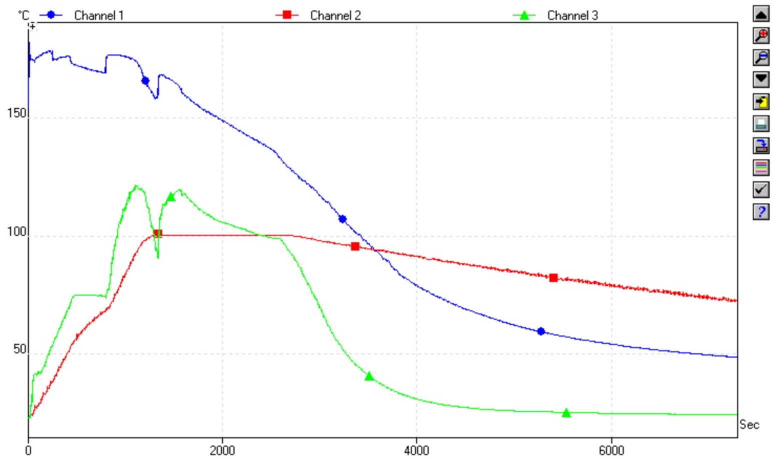

Figure 4.20: Plot of the temperature profile versus time, at the exit of the rock bed (blue line), at the outlet of the cooking application (green line), and of the water (red line), for test 3.

In addition, after the supply of oil ended in the final test, the temperature of the water dropped at a seemingly constant rate from $100°C$ to $80°C$ in 4000 seconds. The heat loss from the water to the ambient was calculated using equation 4.2. The density and the specific heat capacity corresponded to the mean temperature of $90°C$, while the volume was set to be 0,95 litres, as some of the water evaporated during boiling. This resulted in a heat loss of $\dot{Q} = 19,28W$.

$$\dot{Q} = m \cdot C_p \cdot \frac{\Delta T}{\Delta t} \tag{4.2}$$

This was based on an estimate where the heat loss rate was constant, which was not the real case. However, it was the mean heat loss during a given time period, and was used as a prediction. With the calculated mean heat loss rate, the average heat transfer coefficient was calculated using the following equation.

$$\dot{Q} = (UA) \cdot LMTD \tag{4.3}$$

The logarithmic mean temperature difference (LMTD) was calculated by equation 4.4, using temperature differences from $100°C$ to $20°C$ and $80°C$ to $20°C$. The result was a LMTD of

$69,52K$.

$$LMTD = \frac{\Delta T_A - \Delta T_B}{ln(\frac{\Delta T_A}{\Delta T_B})} \tag{4.4}$$

By applying the LMTD with the average heat loss rate of 19,28 W, the overall heat transfer coefficient times area, UA, was calculated by equation 4.3 to be 0,28$\frac{W}{K}$ from the water to the ambient in the temperature range $100°C$ to $80°C$.

Discussion

The goal of boiling water was achieved. With test 2 and 3, it was concluded that the cooking application may boil 1 litre of water in roughly 20 minutes if the mass flow was set to 0,005 $\frac{kg}{s}$. With this mass flow, a total of 6 kg of hot oil was consumed in that period of time, which was a great part of what was available in the rock bed. However, due to the amount of energy required to heat the thermal mass in the beginning, it required less energy to maintain the water boiling, and a lower mass flow was applied. By lowering the mass flow to a tenth of the initial flow rate, the water could maintain a temperature above $90°C$ for a long period of time. As the mass flow was adjusted several times during the tests, it was difficult to determine the exact time the residual oil in the rock bed could maintain a high temperature of the water. However, from the plots it is safe to say that it kept the water boiling for at least 20 minutes.

A previous study investigated the minimum energy required to cook 1 kg of rice in 1,6 litres of water. The cooking time was measured to be 44 minutes on a stove with a power of 626 W, while the total energy transferred to the cooking pot and rice-water mixture was measured to be 1,5 MJ [46]. The heat loss was not calculated, and therefore the amount of energy absorbed by the rice-water mixture was only known to be less than 1,5 MJ. In comparison, the cooking application made in this study consumed a total of 961,0 kJ, while heating 1 litre of water from room temperature to boiling temperature. As can be noticed, the ratio of supplied energy to the amount of cooking goods was lower for this cooking application. Thus, to cook 1 kg of rice in 1,6 litres of water, it seemed the cooking application needs more energy than 1,5 MJ. However, less energy was needed after the thermal mass had been heated and the water had reached the boiling temperature. Therefore, it can be concluded that the cooking application tested in this thesis offered a good potential, but needs to be optimised and up-scaled to be able to compete with established solar cookers.

4.4.2 Plate cooker

A theoretical approach was carried out when designing the Plate cooker. A full analysis with few uncertainties was not necessary, yet some factors needed to be addressed. This included the heat transfer coefficient and the pressure loss through the pipes and cooker. To calculate the average heat transfer coefficient, several other parameters had to be calculated as well. However, accurate calculations would be an in-depth study in heat transfer, which was considered outside the scope of this thesis. Therefore, simplifications have been made. Consequently, some parameters were based on the mean temperature of the flow. This may have resulted in values which are rough estimates, but would either way provide useful information.

The material was chosen to be aluminium, as it conducts heat well and has a low density. To make internal channels, the cooker needed to be made out of two parts and later attached.

In addition, the accessibility of tools was a limitation, and thus was taken into account when optimising the dimensions of the channels.

Calculations

First of, an estimate had to be made as of how much energy the rock bed contained when fully charged. Since water boils at $100°C$ at 1 atm, oil with a temperature below or just above this temperature would have a small or even negative effect in the heat exchanger, withdrawing heat from the cooking goods instead of supplying heat. By reviewing the plot of the drainage of the rock bed, figure 4.21, it was noticed that oil was withdrawn at a temperature of $200°C$ to begin with, and $120°C$ after 3000 seconds. At this time, about 10 litres of oil had been withdrawn. However, the drainage was done step wise, and an approximation of the mean outlet temperature had to be done. By reviewing the plot, and by accounting for heat loss in the connecting pipes, the inlet temperature to the cooking application was assumed to be $150°C$.

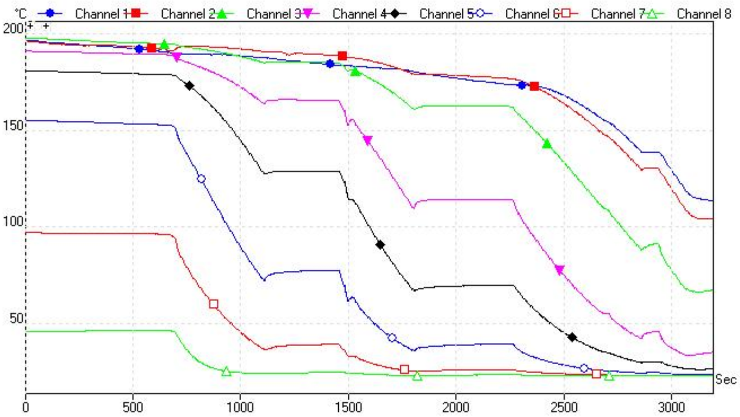

Figure 4.21: Plot of the temperature profile in the rock bed during reversal. The oil was first drained at a temperature of $200°C$, while it had a temperature of $120°C$ after 3000 seconds have passed and approximately 10 litres had been drained.

The outlet temperature of the cooking application was unknown and had to be determined. A temperature above $100°C$ was desired, and a temperature difference of $30°C$ was considered achievable. Therefore, the outlet temperature in this calculation was chosen to be $120°C$. The mean temperature of the oil was thus $135°C$. The characteristics of sunflower oil at this temperature are listed in in table 4.8, [47], [48], [49].

Table 4.8: Characteristics of sunflower oil at $135°C$.

Sunflower oil characteristics		
Specific heat capacity (C_p)	2540,5	$\frac{J}{kg \cdot K}$
Density (ρ)	844,1	$\frac{kg}{m^3}$
Dynamic viscosity (μ)	5,39	m$Pa \cdot s$
Thermal conductivity (k)	0,147	$\frac{W}{m \cdot K}$

The next step was to design the cooking application with the intention of maximising the heat transferred from the oil to the cooking application, represented by equation 4.3. U, often noted as $\bar{h}$, represents the average heat transfer coefficient in ($\frac{W}{m^2 \cdot K}$). To maximise the heat transfer, both $\bar{h}$ and the area should be chosen to be as large as possible. The following calculations, with their equations, were computed in accordance to *Fundamentals of Heat and Mass Transfer,* 7^{th} *edition* [50].

The average heat transfer coefficient was calculated by equation 4.5.

$$\bar{h} = \frac{\bar{N}u_D \cdot k}{D_h} \tag{4.5}$$

If the plate is thin, and the material has good conductivity, one may assume that the temperature of the surface is uniform and constant [51]. In that case, the same $\bar{N}u_D$ may be applied for the whole plate. In addition, to find the $\bar{N}u_D$ in pipes, it is of importance to know whether the flow has fully developed velocity and temperature profiles, or not. For large Prandtl number (Pr) fluids such as oils, the hydrodynamic entry-length is much smaller than the thermal entry-length, and it is reasonable to assume a fully developed velocity profile throughout the thermal entry region. The Pr for the flow through the cooker was calculated using thermodynamic properties for the mean temperature. By using equation 4.6, the Pr was found to be 93,1. Hence, the velocity profile was assumed fully developed throughout the thermal entry region.

$$Pr = \frac{C_p \cdot \mu}{k} \tag{4.6}$$

To find suitable dimensions for the channel in the plate, an iteration process had to be done to maximise the surface area, and hence the heat transfer, without surpassing the limit of maximum pressure loss. Prior to the calculation, some criteria had to be met. As mentioned, the idea was to make two plates, mill a channel in each of them, and then assemble them together to create a channel for the oil to flow through. Doing so, it was far easier to mill a rectangular duct in each plate, than to mill a semicircle in each plate. In addition, with the machines and tools available, a minimum width of 3 mm ducts could be made, and the channels should at least have a spacing of its own width between each other. Also, the final plate diameter was chosen to be 200 mm, with a 20 mm centred hole for the inlet pipe. The mass flow was arbitrarily set to be 0,00468 $\frac{kg}{s}$. This is roughly equivalent to withdrawing 10 litres of oil in 30 minutes. Finally, the hydrostatic pressure creating the flow from the rock bed to the cooking application was calculated from equation 4.7. A 1 m height difference yielded a hydrostatic pressure of 8281 Pa.

$$P_{HS} = \rho \cdot g \cdot h \tag{4.7}$$

With these restrictions, an iteration process was conducted. Different duct geometries and dimensions were tested. A large ratio of depth to width was proved to be the best solution. By using the smallest possible channel width of 3 mm, with 3 mm spacing between each channel, a duct of 5,23 m could be made, and hence a large surface area. By further adjusting the depth of the duct, an optimisation of the surface area, ensuring acceptable pressure loss, was obtained. The pressure loss could not overrule the hydrostatic pressure from the height difference between the rock bed outlet and the cooking application of 1 m. To ensure this, the hydrostatic pressure force should be at least 50% larger than the pressure loss. The result of the iteration process yielded a depth to width ratio close to 5. Hence, the channel geometry was set to be 3x15 mm.

The iteration process was based on the equations below. The results are presented in table 4.9.

First off, the pressure drop was calculated to be 5297 Pa by using equation 4.8.

$$\Delta P = (4 \cdot c_{f,app}) \cdot \frac{x}{D_h} \cdot (\frac{\rho \cdot \forall^2}{2}) \tag{4.8}$$

$c_{f,app}$ was found using equation 4.9.

$$(c_{f,app} \cdot Re) = \frac{3,44}{\sqrt{\zeta}} + \frac{c_{f,p} \cdot Re + \frac{K_\infty}{4 \cdot \zeta} - \frac{3,44}{\sqrt{\zeta}}}{1 + \frac{c}{\zeta^2}} \tag{4.9}$$

ζ and Re were calculated form equation 4.10 and 4.11.

$$\zeta = \frac{\frac{x}{D_h}}{Re} \tag{4.10}$$

$$Re = \frac{\dot{m} \cdot D_h}{\mu \cdot A} \tag{4.11}$$

The coefficients K_∞, c and $(c_{f,p} \cdot Re)$ are listed in Appendix E. The flow was found to be laminar as $Re = 96,6$.

Secondly, $\bar{N}u_D$ needed to be calculated in order to find $\bar{h}$. The $\bar{N}u_D$ for a thermal entry-length problem with $Pr \geq 5$, was calculated by equation 4.12.

$$\bar{N}u_D = 3,66 + \frac{0,0668 \cdot Gz_D}{1 + 0,04 \cdot Gz_D^{\frac{2}{3}}} \tag{4.12}$$

where

$$Gz_D = \frac{D_h}{x} \cdot Re \cdot Pr \tag{4.13}$$

From the calculations, $Gz_D = 8,60$, which further resulted in $\bar{N}u_D = 4,15$.

Since the channel was chosen to be a rectangular duct instead of a pipe, another Nu relation had to be applied. However, the ratio between the Nu_D of a fully developed flow and the $\bar{N}u_D$ for an entry-length problem is the same for both geometries. The $\bar{N}u_D$ for the duct was calculated by equation 4.14 [51]. This resulted in $Nu_{D,duct} = 5,48$.

$$\frac{\bar{N}u_{D,pipe}}{Nu_{D,pipe,fd}} = \frac{\bar{N}u_{D,duct}}{Nu_{D,duct,fd}} \tag{4.14}$$

From equation 4.5, the average heat transfer coefficient was calculated, which yielded $\bar{h} = 161,1 \frac{W}{m^2 \cdot K}$.

The LMTD could be found using a step-wise calculation during heating of the thermal mass in the cooker while later assuming a constant temperature the plate. However, as a first approximation, assuming the plate heats quickly due to large thermal conductivity and modest thermal mass, the LMTD was estimated only using constant temperatures. By using equation 4.4, a plate temperature of 110°C, an inlet and outlet flow to the application of 150°C and 120°C, the

Table 4.9: The results of the final iteration of the plate cooker dimensions.

Final iteration results			
Parameter	**Equation**	**Unit**	**(Value/Result)**
Plate diameter (D)		mm	200
Plate thickness (t)		mm	20
Outlet hole diameter ($D_{outlethole}$)		mm	20
Channel width (w)		mm	3
Channel height (h)		mm	15
Channel length (l)		m	5,227
Cross-sectional area (A)	w · h	m^2	0,000045
Hydraulic diameter (D_h)	$\frac{4 \cdot A}{Pe}$	m	0,005
Reynolds number (Re)	4.11	-	96,6
Prandtl number (Pr)	4.6	-	93,1
Thermal entry-length (x_t^+)	$\frac{Re \cdot Pr}{20} \cdot D_h$	m	2,25
Velocity entry-length (x_h^+)	$\frac{Re}{20} \cdot D_h$	m	0,02
Gzd	4.13	-	8,60
Average Nusselt number,pipe ($\bar{N}u_D$)	4.12	-	4,15
Average Nusselt number, duct ($\bar{N}u_D$)	4.14	-	5,48
Average heat transfer coefficient ($\bar{h}$)	4.5	$\frac{W}{m^2 \cdot K}$	161,1
Logarithmic mean temperature difference (LMTD)	4.4	K	21,6
Heat transfer ($\dot{Q}$)	4.3	W	655,9
Fluid velocity ($\bigvee$)	$\frac{\dot{m}}{\rho \cdot A}$	$\frac{m}{s}$	0,123
ζ	4.10	-	10,83
$C_{f,app} \cdot Re$	4.9	-	19,09
Pressure loss (ΔP)	4.8	Pa	5297

LMTD was calculated to be 21,6 K.

By applying equation 4.3, the heat transfer rate was calculated to be 655,9 W.

Production

This collaboration project both includes the production of a cooking application for the purpose of boiling water and other goods, and the production of an application for frying food, especially injeras, a sourdough-risen flatbread. Thus, a similar design was made for the frying pan-solution, being a part of the co-project *Self-regulating Oil Based Heat Storage*, having a larger diameter [52]. However, since the time consumption and cost of producing the plate cooker were anticipated to be fairly high, a decision had to be made as to which of the two applications that should be produced. As a functional boiler already had been made and tested successfully, and more attention was needed for the piston actuator and sliding valve, it was decided that the plate cooker should be produced as the frying pan-solution. Consequently, the frying pan was built. The calculated dimensions with the theoretical heat transfer rate, as well as the test results, may be reviewed in the co-project report. This means, that no test results were obtainable for the boiler design. Thus, no comparison of the theoretical values and the actual values have been made.

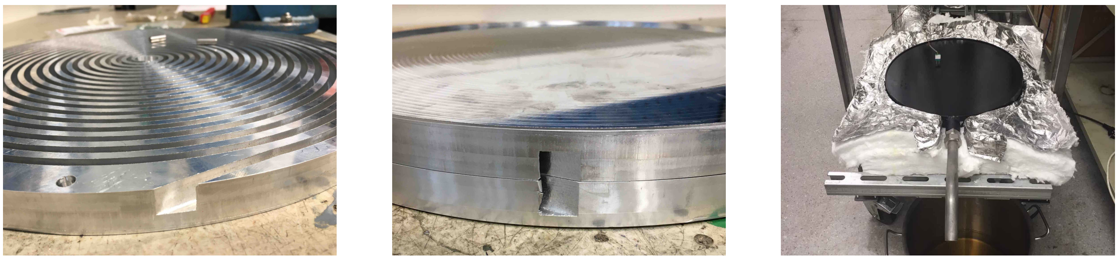

(a) The bottom half of the frying pan, having one channel opening at the side and one channel opening in the middle. The channels dimension on the bottom half are 5 x 12,5 *mm*.

(b) The frying pan with the top half attached to the bottom.

(c) The complete frying pan installed in the test rig. The surface is made black by anodising.

Figure 4.22: Pictures of the manufactured frying pan. Two plates were cut and channels were milled in each of them. Then assembled and surface treated.

When the calculations were done for the frying pan, the channels were milled in a size of 5x25 *mm*, the two plates were assembled together, and the surface anodised to prevent corrosion. The plates, with its channels, as well as the complete frying pan may be seen in figure 4.22.

Although the plate cooker meant for boiling was not manufactured, the design and calculations given in this report yields a proposed solution for further production. In addition to the surface treatment, a thermal pad would have been acquired for the boiling cooker. As cooking pots may be bulky and have uneven bottom surfaces, small gaps between the plate cooker and the pots may occur. This reduces the heat transfer between the two components significantly. Therefore, a soft pad with a certain thickness is desired. This way, the pot may submerge into the pad, eliminating all the voids. It is also of importance that the pad must offer a high thermal conductivity, so as much heat as possible is transferred to the pot.

Chapter 5

Field work at Makerere University, Uganda

This chapter will present the field work done at Makerere University during a one week visit in April 2018. The focus will be the production and testing of a cooking application, however, all parts of the solar cooking system made will be briefly introduced. The reader will be given insight into challenges and possibilities brought forth by the differences in production methods and facilities.

5.1 Motivation

As the overall objective of this study is to make an energy storage system intended for rural areas in Africa, involving local experience and knowledge are important factors for success. Even though the energy storage system made at NTNU provided satisfying results, the main goal is to be able to recreate the same system locally with different production facilities, and a different supply of materials and components. Hence, the motivation for the field trip was to:

- Exchange information and experiences
- Build a solar cooking system based on the principles of the system built at NTNU
- Conduct tests to examine the performance of the system

5.2 Production

The Double piston actuator, a big pneumatic piston, sliding valve 2 and a fill valve was brought to Makerere. As the fill valve from the co-project was known to be working, this was incorporated in the heating section during production. To see whether the piston actuator could be produced and implemented in the system, the Double piston actuator was brought to a workshop, which does precision machining. They concluded that they did not possess the necessary competence required to fabricate a functional piston actuator. Therefore, the Double piston actuator was discarded. The pneumatic piston was connected to a copper coil to investigate whether this could be used instead. Leaks from the connection between the copper coil and piston cylinder proved it was dysfunctional, and a new connection had to be acquired. Due to the need for customised parts, which were hard to get hand of, the work on the piston actuator was put

(a) The heat storage and fill valve container.

(b) The test setup at Makerere. Insulated parts are covered with yellow tape.

(c) The test setup at Makerere seen from behind. In front is the variac and pico logger for the thermocouples.

Figure 5.1: Metal containers and the test setup.

aside. As time was limited, the attention was therefore directed towards making a functional solar cooking system. Consequently, sliding valve 2 was not tested. All the parts, except the fill valve, were left at Makerere for further development and testing.

The system setup was made similar to the one at NTNU. However, as time was of the essence during the stay at Makerere, some changes were made to the solar cooking system. The main difference was changing the design of the heat storage from a rock bed to a rectangular tank not utilising stratification. This made the system simpler, and thus less time-consuming to build.

The heat storage, heating container and fill valve container were built from 1 mm thick steel plates, bought at a local market. All of which were bent into a rectangular shape and welded along the seam on one of the edges, as seen in figure 5.1a. The bottoms were made from rectangular plates, which were welded to the cylinder. A rectangular lid was made for the heat storage, made with a hole in the centre to fit the connecting pipe from the heating container.

A large plastic tank with a tap, measuring approximately 40 litres, was used as the cold oil supply reservoir. A plastic hose, with an inner diameter of 1/2", was connected from the oil supply reservoir to the fill valve container. The fill valve was mounted at the centre of the tank using a threaded rod welded onto one of the sides. The rod had a pipe clamp attached at the end, holding the fill valve in position. Furthermore, the fill valve container was connected to the heating container with an inclined steel pipe. A heating element of 1500 W was submerged in the oil in the heating container from the open top, held in place by a clamp. Ideally, the heating element should have been inserted from the bottom of the heating container, but this type of heating element was hard to get hand of. Consequently, submerging a element from the top was used as an alternative solution. The power supply was controlled by a variac.

A pipe was welded onto the heating container at an inclined position, with an angled end point-

(a) The three different sized cooking pots in stainless steel stacked.

(b) Holes drilled in the medium cooking pot.

(c) Clumpy welding on the cooking application with silicon sealant.

Figure 5.2: The cooking aplication durng production.

ing into the top of the heat storage, through the lid. At the bottom of the heat storage, a short pipe was welded onto the wall providing an outlet. A ball valve was connected to the short outlet pipe. Moreover, a pipe system was made, connecting the cooking application to the rest of the system. Threaded pipe bends were used to connect the pipes. The cooking application was mounted to the pipe system at its bottom centre. The height difference from the outlet of the heat storage and the inlet of the cooking application was approximately 60 cm, providing a hydrostatic pressure force to the oil. Pictures of the system is given in figure 5.1. More pictures, measurements and materials are listed in Appendix D.

The cooking application was made, based on the Three-pot cooker design described in chapter 4. Three cooking pots made of stainless steel, as seen in figure 5.2a, were bought at a local supermarket. The handles were cut off the small and medium pots to have them fit inside each other. 12 holes, measuring 8 mm in diameter, were drilled in the medium cooking pot, 50 mm from the bottom, as seen in figure 5.2b. A 1" hole was drilled in the bottom of the medium and large pot to fit an inlet pipe for oil. A same sized hole was drilled in the side of the large pot, making an outlet for the used oil. A steel pipe was fitted inside the bottom hole and welded onto the medium cooking pot. Later, the medium pot, with the steel pipe attached, was placed inside the large cooking pot. The steel pipe was then welded to the large pot, attaching the pots together in addition to making a seal. A pipe was also welded onto the side hole of the large pot, providing an outlet to the residual tank. A picture of the welding is shown in figure 5.2c.

The heat storage, pipes from the heat storage to the cooking application and the cooking application were insulated using FyreWrap LT AL matte of thickness 50 mm, which was brought from NTNU at an earlier time. The insulated surfaces are seen covered in yellow tape in figure 5.1b. For more information about the insulation, see Appendix B. The oil used throughout the experiments was sunflower oil bought at a local supermarket, which were assumed to have the same thermodynamic properties as the oil used at NTNU.

5.2.1 Production challenges

Leaks caused a substantial problem throughout the production of the system and its components. This was mainly due to poor welding. All the containers made from the thin metal plates were leaking in the welding seams along the bottom and sides. In addition, leaks formed around all the welds of the pipe outlets/inlets and in the cooking application. The leaks were sealed by applying significant amounts of silicon sealant.

Another source of leaks were the pipe joints, as the threads on the pipes did not match the threads inside the joints. Consequently, some of the joints were flexible even after they were tightened. Thus, silicone sealant was applied around all the joints as well.

Poor welding did not only cause problems in the form of leaks. The welds were big and clumpy, resulting in large gaps between the pots in the cooking application. The gaps allowed oil to be left between the medium and large pots, absorbing heat. This may result in a lower heat transfer to the cooking goods. Ideally, to make the pots fit better, the inlet pipe to the cooking application should have been mounted using a pipe fitting. However, this was not done due to the lack of time and parts. In addition, the bottoms of the cooking pots were made with an aluminium core, the same way as the pots used at NTNU, which induced clumpy welding. More pictures of the components and the production challenges are presented in Appendix D.

5.3 Testing

The heating element provided problems while heating the oil. As the heating element contained some parts made of plastic, this melted due to hot gases emerging from the hot oil. Despite this, the fill valve had been calibrated and tested successfully in time before the heating element melted. Thus, a proof of concept for the heating section had been achieved. For more details, see the co-project report, as this is a part of the scope of that thesis.

At the time the fill valve was tested, the cooking application was not finished. Hence, a complete system was never tested. However, the cooking application was tested separately, unaffected by the faulty heating element. A large cooking pot containing 15 litres of sunflower oil was heated on a hot plate while monitoring the temperature using a thermocouple. When the oil reached a temperature of $220°C$, the oil was carefully poured into the heat storage.

During cooking, the small pot in the cooking application contained 2 litres of water and a thermocouple to monitor the water temperature. The lid was kept on throughout the testing and was only removed during short periods of inspections. Thermocouples were also put in the outlet of the heat storage, the inlet, and outlet of the cooking application. The ball valve from the heat storage was opened, allowing oil to flow through the cooking application. The volume flow was adjusted by changing the valve position. After approximately ten minutes it was noticed that the valve position did not affect the volume flow as much as it did initially. Hence, it was concluded the valve was faulty, possibly due to a small rubber gasket inside the valve which was assumed to have melted. The valve was set at a closed position, reducing the volume flow as much as possible.

5.4 Results

Results from the calibration of the fill valve and the accuracy of the temperature delivered to the heat storage will not be presented in this section. This may be reviewed in the report from the co-project. It should also be noted that the boiling temperature is $96{,}8°C$, as the the tests have been conducted in Kampala, which has an altitude of 1190 meters above sea level.

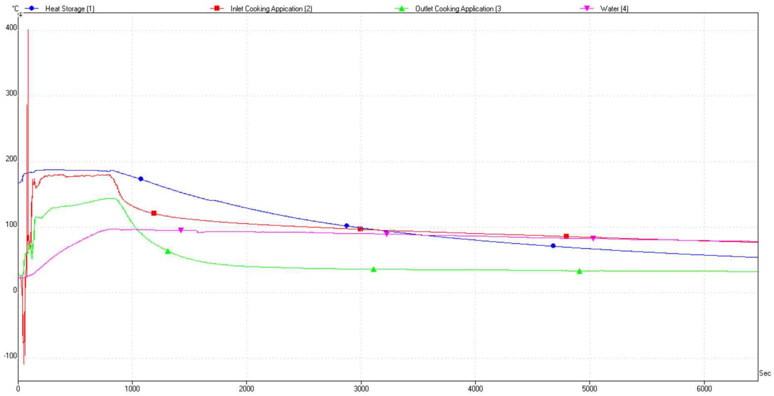

Figure 5.3: Test results for the cooking application made at Makerere. The disturbances in the start is due to a change in the thermocouple connection to the pico logger.

From the plot in figure 5.3, there are some disturbances at the beginning, which can be disregarded. This was caused by a thermocouple, which was not connected properly to the pico logger but did not influence the rest of the experiment. Otherwise, it can be observed that the temperature of the inlet and the outlet of the cooking application were almost the same as the first 800 seconds, meaning a high mass flow. After 800 seconds, the problem regarding the ball valve was discovered, and the valve was fully closed to minimise the mass flow. The heat storage supplied oil for approximately 20 more minutes, before the storage tank was empty. Hot oil was still in the system and in the cooking application. This provided heat to the water until the water and surrounding oil reached the same temperature at t = 5500 seconds.

The water started to boil at the same time as the mass flow of the hot oil was reduced, t = 800 seconds. It maintained a boiling temperature for almost 20 more minutes, before gradually decreasing towards $80°C$ during the next 75 minutes. A comparison of the overall heat transfer coefficient times area, UA, could be made with the value obtained from the tests at NTNU. By using equation 4.2, the temperature of the water at the time the flow of oil ended, $93°C$, and the temperature of the water at t = 6000 seconds,$79°C$, the calculated average heat loss rate was 25,75 W. Having the ambient temperature to be $23°C$, the LMTD was equal to 62,7$°C$, according to equation 4.4. By applying equation 4.3, the UA was calculated to be 0,41 $\frac{W}{K}$.

5.5 Discussion

A solar cooking system was successfully made at Makerere. Even though the complete system was not tested as one unit, two separate tests proved the concept, which formed the basis for a full system. Production demonstrated the importance of local knowledge. Buying parts and materials were limited for foreigners, whereas local knowledge provided solutions to whereabouts, prices and what to buy. Despite this, the quality promised by the supplier did not always reflect the quality of the product. The valve did not tolerate high temperatures, even though a guarantee was given from the supplier. The difference in production facilities provoked alternative solutions, which influenced the design of the system. Some shortcuts had to be made due to limited time, others due to lack of parts and material.

The goal of boiling water was achieved, and to a relative good extent. 2 litres were boiled in roughly 13 minutes, and maintained a temperature above $90^{\circ}C$ for 50 more minutes. This implied that a lot of the heat was being stored in the system. This were promising results, as a lot of the food that was being cooked in this area, is food that does not necessarily needs a boiling temperature, but needs high temperature over a longer period of time. As the ball valve malfunctioned, a better valve should be installed, which may result in an even longer period of cooking. On the other hand, the pots used in the cooking application for this test were expensive compared to the other parts, and would not be applicable for later production. In addition, the insulation used was far better than the locally available insulation. This raises the question of how well the concept would work if it is made using cheaper materials.

Chapter 6

Discussion

Some of the components tested proved to be more complicated producing than anticipated. The machining accuracy required to make a functional piston actuator was not achieved at NTNU. The combination of a piston moving smooth while still giving a complete seal was challenging. During production, getting one of these criteria met was achieved. Satisfying both were not achieved. However, during tests of the pistons made at NTNU leaks were assumed to be caused at the pistons, even though not being visible. From the tests, the pistons did not retract to their initial position during cooling. However, as the pistons could be pushed into their initial position after retraction, this proved there had to be air inside the copper coil. This could have been caused by air being inside the coil from the start of the test due to insufficient filling, or due to air being sucked in during retraction of the piston. Since the pistons did not extract to the same extent during reheating, it was concluded some oil had leaked out of the copper coil. Except for a small leak at the inlet of the copper pipe to the Double piston actuator cylinder, which was sealed using plumber tape, no leaks were visible while testing the two first piston actuators. However, when the pneumatic pistons were tested, leaks were discovered in one of the pipe connectors. Consequently, this raises the question whether this had been the cause of leaks for all the pistons, but was not noticed. Despite this, the machining of the pistons brings an uncertainty whether the pistons create a sufficient seal or not, and may therefore not be an adequate solution after all.

A functional sliding valve was achieved using circular holes. A better opening response of the valve could be achieved using rectangular holes, but this design was not produced without having leaks. The sealing surface between the slider and the inlet chamber was not sufficient while having rectangular holes, even after several surface treatments using various tools. Making the valve from prefabricated metal profiles saved both time and money in production and was definitely in line with the idea of an affordable and simple solar cooking system. The production did not require any special tools or machines, and should be manageable reproducing locally in Africa.

During tests of the heating container, a large temperature gradient inside was observed. Thus, the response of the piston actuator was difficult to predict as the temperature of the surrounding oil was not uniform. Having a larger tank with a slow heating of the oil could help achieving a more uniform temperature in the surrounding oil. Hence, a better correlation between the temperature in the heating container and the copper coil. The copper coil should be positioned near the inlet of cold oil, giving a faster cooling of the coil, and hence a faster and more accurate response of the piston actuator. None of the features discussed introduce complicated design challenges. Therefore, this component should also be manageable reproducing locally as well.

Due to limited time, tests of a complete mechanical temperature controller made with pneumatic pistons was not tested. Therefore, a full solar cooking system using the sliding valve and the piston actuator was never tested. However, a fully functional system was tested using the fill valve produced in the co-project. As mentioned, this solution does not provide the same flexibility for different heating sources, and implementation of oil circulation, as the mechanical temperature controller tested in this project. Nevertheless, a functional system has successfully been produced and tested.

A test rig with sliding valve 3 and the pneumatic pistons was made at NTNU for the purpose of further testing at a later point. This will decide whether the concept of the mechanical temperature controller truly works or not. From preliminary tests the pneumatic pistons proved to extract and retract in a satisfying manner, even though there were leaks from one of the copper pipe connectors. The sliding valve in the new test rig is known to have small leaks, which need to be taken into account during testing. If the results are satisfying, a new system setup should be made in order to make a more user-friendly system. Leaks have been an issue throughout this project, being present in all components including the copper pipe connections. The copper pipe system was not addressed as one of the biggest challenges while making the test setup. Nonetheless, more attention should have been directed towards this at an early stage.

The solar cooking system made at Makerere yielded promising results for cooking. However, from the test data, the average heat loss rate for the cooking application made at Makerere was greater than the one made at NTNU. Several factors affects this, including the size of the cooking application, insulation and thermal mass. Despite having the pipe system at Makerere made of steel, which offers a lower thermal conductivity, and the insulation applied more carefully, the overall U-value was greater than for the cooking application made at NTNU. This was most likely because the Three pot solution from NTNU was insulated by professionals, using a better material. If a new system will be made, choosing the right insulation and material, while reducing the thermal mass by having a more streamlined design, should be prioritised. This would also make the system more user-friendly.

Adjusting the mass flow through the cooking application affects the total efficiency of the cooking system. While all the tests conducted had oil flowing through the cooker continuously, a different approach should have been made. Large amounts of used oil exiting the cooker had a high temperature compared to the water, especially in the start phase. Instead of having a continuous mass flow, stopping some of the flow inside the cooking application would have utilised more of the available energy. As long as the oil inside the cooking application has a higher temperature than the water, it should be kept inside the cooker. When the temperature of the oil approaches the water temperature, the cooled oil should be replaced by new hot oil. In that way, more of the available energy will be utilised, increasing the system efficiency. In addition, the residual oil holds a high temperature and should be considered for further use with a different purpose.

Data sampled throughout the tests conducted could have been done more accurately, paying more attention to the positioning of the thermocouples. More thermocouples are usually better, giving more details and insight of what is monitored. While measuring the effectiveness of the cooking application and heat losses in the pipes, an extra thermocouple should have been used in the inlet of the cooking application. This way, losses and the effectiveness of the cooking application could have been addressed with more accuracy. More thermocouples should also have been used in the heating container, giving the temperature distribution instead of only having a point measure.

As mentioned in the introduction, Schwarzer and da Silva were able to boil 5 litres of water in 10-12 minutes using an indirect solar cooker [41]. The system made at Makerere did not give the same amount of energy output, but managed to boil 2 litres of water in roughly 13 minutes. This represents a good potential for the simple system. In order to have an energy output in the same order of magnitude, an improved and upscaled version of the system should be made. If the intended production volume of systems is high, the production cost is assumed to decrease, making higher quality components, such as better insulation, more applicable.

Chapter 7

Conclusion

The objective of this project was to design a full solar cooking system, consisting of a mechanical temperature controller and a cooking application. The components were divided into separate parts, so that the production, testing and troubleshooting were made easier. Work was done separately, yet parallel, on each of the parts, to increase the productivity. The goal of the project was to make a solution that is feasible, not only for implementation in rural communities of Africa, but for local production as well. Consequently, the complexity of the components and the production methods, in addition to the price and accessibility of materials, were aspects to keep in mind throughout the project.

Three different designs were made for the piston actuator, whereas the solution consisting of prefabricated pneumatic pistons was the most promising. The other two piston actuators, made from basic parts in the workshop at NTNU, had issues regarding the response of the pistons' displacement length. No leaks were visible, but seemingly present. It was concluded that the effort needed for the surface treatment was too demanding, given the facilities available. Thus, the designs were not suitable for local production in Africa. Three different designs were also made for the sliding valve. The size of the holes between the chambers and the size of the holes in the slider seemed to be the decisive factor for success. Sliding valve 1 was made with rectangular holes, valve 2 was made with circular holes and valve 3 was made as a hybrid. The only functional valve was design 2. However, it was less temperature responsive in regard to the displacement length of the piston actuator. It was concluded that combining a temperature sensitive piston actuator made of prefabricated pistons and a sliding valve having circular holes was the best solution for further development. On the other hand, using a fill valve may after all be the best solution, as this thermostat has a simple design and yields an accurate oil temperature output. However, the fill valve has a drawback when it comes to flexibility. If a circulating system, containing a pump, is desired, the fill valve cannot be applied, and the mechanical temperature controller made in this project may be an appropriate substitute.

Producing a full solar cooking system with the mechanical temperature controller also prompted the need for a new heating container. A solution was made, and successfully tested when assembled with the piston actuator. However, improvements should be done, especially with respect to geometry and dimensions, as the small size resulted in a less temperature sensitive controller due to delay in the system.

Although each part has been tested separately and offered promising results, it is still indecisive whether the system will work as a functional temperature controller. The piston actuator, the sliding valve and the heating container were never assembled all together, and tested as one unit. Thus, a full test is necessary to measure the actual temperature of the oil exiting the thermostat, before a conclusion can be made.

Two cooking applications were designed, whereas only one was produced and tested. The goal of boiling water was achieved, both by the solutions made at NTNU and at Makerere University. The Three pot solution was concluded to be a fully functional cooking application. However, due to difficulties when welding certain types of material, expensive pots had to be acquired for making the cooking application in Uganda. In addition, expensive insulation was used to prevent heat loss. These are costs that need to be avoided if the solution should be applicable in rural communities.

Under these conditions, the described solar cooking system has a very good chance for large-scale use in various applications.

Chapter 8

Further work

8.1 Mechanical temperature valve testing

As mentioned, a test of the mechanical temperature valve in its full set up is needed. This includes the piston actuator, the sliding valve and the heating container assembled together, and mounted inside the full test rig. By the time this report was written, the Pneumatic piston actuator and sliding valve 3 had been assembled together on a rack, but not yet tested. The rack may be seen in figure 8.1. This rack will be mounted near the rock bed in the test rig, where the sliding valve will be connected to the heating container, while the piston actuator will be connected to the copper coil within the heating container. Although all parts have been tested with promising results, this does not guarantee that the complete system will work properly. For instance, sliding valve 3 is known to have small leaks. However, as the Pneumatic piston actuator is being used, which is regarded to have a high temperature sensitivity, sliding valve 2 may be reproduced and used instead of sliding valve 3, as this was ascertained to be working fine. Moreover, if no additional leaks are present, and oil is heated and directed towards the rock bed, the question to which extent it will deliver the oil at a desired and stable temperature arises.

8.2 New system setup

So far, the full solar cooking system has been installed in an test rig with the size of approximately 1x2x2 m, which barely fits all the components. However, a more effective structure is required if this is going to be installed in homes, at schools, or in other similar locations. Especially if the system is being upscaled. A design where the components are arranged closer together, and possibly aligned in a vertical direction, rather than in a horizontal direction, should be made. This does not only make the system easier to implement in the institutions, but also enhances user-friendliness. In addition, this will reduce material consumption, as the piping system will be shortened. Consequently, the heat loss may be reduced, and thus, the efficiency of the system will be improved. Also, by streamlining the setup, more space will be available for implementing a solution for utilising the residual heat in the oil exiting the cooking application. As of now, no thoughts have been offered the development of a design that will extract the excessive energy. Since most of the oil that leaves the cooking application contains a temperature above $100^{\circ}C$, a substantial amount of energy is still left in this oil. This has a great potential for further use, and should be addressed.

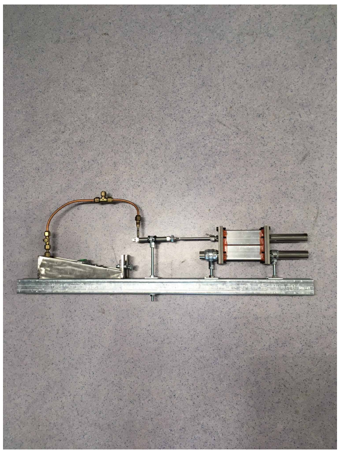

(a) The big piston to the left, was connected to the small piston with a 1/4" copper pipe. The small piston was assembled in the middle, pushing the sliding valve on the right hand side.

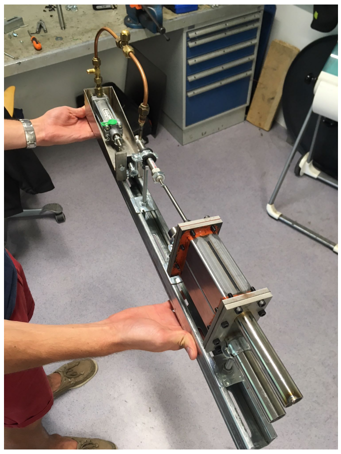

(b) A stopper was placed in the big piston displacement length direction, to instigate the movement of the small piston. The heating container will be attached to the tee.

Figure 8.1: The mechanical temperature valve, consisting of the Pneumatic piston actuator and sliding valve 3. The heating container with the copper coil has not yet been attached.

8.3 Upscaling

The objective of the project was to investigate whether the system could provide enough energy for cooking purposes. During testing at NTNU, 1 litre of water was boiling for 20 minutes. However, to provide enough energy for preparing food, the system needs to be upscaled, so more energy can be stored. First off, the user group has to be addressed to figure out the energy consumption and thus the energy supply needed. Whether the system is intended for a family or intended for a school may result in two completely different sizes of the system. When scaling the solar cooker, it is not only the size of the TES that needs to change. It is also the size of the cooking application, and the dimensions of the pipes for the whole system. More tests should be conducted, as the flow rate through the cooking application should be optimised, and to investigate the amount of energy provided. This way, the size of the system versus the amount of food that may be prepared can be determined.

8.4 Switch controller

The TES system is intended for receiving the excessive energy after a battery has been charged by the PV-panels. A controller must therefore be designed to switch the direction of the current from the battery, as soon as it is fully charged, to the heating element in the heating container, to reduce the energy waste.

8.5 Safety

If a failure occurs in the oil supply, piston actuator or the sliding valve, the temperature in the heating container may exceed a critical value. This may lead to hazardous situations. In addition, when the TES is fully charged, and the supply of hot oil is not stopped, the excessive oil may inflict damage to other parts of the system. Therefore a safety mechanism must be designed to cut the power supply to the heating element preventing such situations.

Bibliography

[1] J. Tabuti, S. Dhillion, and K. Lye, "Firewood use in bulamogi county, uganda: Species selection, harvesting and consumption patterns," *Biomass and Bioenergy*, vol. 25, no. 6, pp. 581–596, 2003.

[2] Ministry of energy and mineral development Uganda, "National biomass energy demand strategy 2001-2010," Ministry of Energy and Mineral Development Uganda, Tech. Rep., Jun. 2001.

[3] H. J. Geist and E. F. Lambin, "Proximate causes and underlying driving forces of tropical deforestation: Tropical forests are disappearing as the result of many pressures, both local and regional, acting in various combinations in different geographical locations," *BioScience*, vol. 52, no. 2, pp. 143–150, 2002.

[4] P. T. Heteu, "Uanda's sustainable energy for all initiative - action agenda," Ministry of Energy and Mineral Development Uganda, Tech. Rep., Jun. 2015.

[5] E. Kebede, J. Kagochi, and C. M. Jolly, "Energy consumption and economic development in sub-sahara africa," *Energy economics*, vol. 32, no. 3, pp. 532–537, 2010.

[6] J. Mubiru, K. Karume, M. Majaliwa, E. Banda, and T. Otiti, "Interpolating methods for solar radiation in uganda," *Theoretical and applied climatology*, vol. 88, no. 3, pp. 259–263, 2007.

[7] A. Shibeshi, "Education for rural people in africa," Food and Agriculture Organization of the United Nations, Tech. Rep., 2016.

[8] O. J. Nydal, "Small scale concenctrating solar energy system with heat storage," Norwegian University of Science and Technology, Trondheim, Norway, Technical report, Tech. Rep., 2014.

[9] A. B. Steen and O. S. Sjøgren, "Solar heat storage in oil based rock bed," Dept. Energy and Process Engineering, Norwegian University of Science and Technology, Tech. Rep., 2017, Project work 9th semester.

[10] C. Bogsnes and E. E. Hansen, "Passive temperature control of heat based storage," Dept. Energy and Process Engineering, Norwegian University of Science and Technology, Tech. Rep., 2017, Project work 9th semester.

[11] E. Cuce and P. M. Cuce, "A comprehensive review on solar cookers," *Applied Energy*, vol. 102, pp. 1399–1421, 2013.

[12] *Types of solar coockers*, `https://lifetheexperience.wordpress.com/2016/01/21/solar-cookers/`, retrieved 14.11.17 11:26, Jan. 2016.

[13] K. Ashok, "Review of solar cooker designs," *TIDE*, vol. 8, no. 1, pp. 1–37, 1998.

[14] C. Kimambo, “Development and performance testing of solar cookers,” *Journal of energy in Southern Africa*, vol. 18, no. 3, pp. 41–51, 2017.

[15] A. Saxena, S. Pandey, G. Srivastav, *et al.*, “A thermodynamic review on solar box type cookers,” *Renewable and Sustainable Energy Reviews*, vol. 15, no. 6, pp. 3301–3318, 2011.

[16] M. Telkes, “Solar cooking ovens,” *Solar Energy*, vol. 3, no. 1, pp. 1–11, 1959.

[17] S. Pohekar and M. Ramachandran, “Utility assessment of parabolic solar cooker as a domestic cooking device in india,” *Renewable energy*, vol. 31, no. 11, pp. 1827–1838, 2006.

[18] S. Hasnain, “Review on sustainable thermal energy storage technologies, part i: Heat storage materials and techniques,” *Energy conversion and management*, vol. 39, no. 11, pp. 1127–1138, 1998.

[19] H.-J. Kilger, *Heat transfer media*, `http://www.thermopedia.com/content/842/`, retrieved 11.11.17 14:55, Feb. 2014.

[20] B. A. Garg H.P. Mullick S.C., *Sensible Heat Storage. In: Solar Thermal Energy Storage.* Springer, Dordrecht, 1985.

[21] A. Sharma, V. V. Tyagi, C. Chen, and D. Buddhi, “Review on thermal energy storage with phase change materials and applications,” *Renewable and Sustainable energy reviews*, vol. 13, no. 2, pp. 318–345, 2009.

[22] *Temperature vs thermal energy*, `http://www.energyville.be/en/sheet/latent-heat-storage-phase-changing-materials`, retrieved 14.11.17 11:44.

[23] P. Pardo, A. Deydier, Z. Anxionnaz-Minvielle, S. Rougé, M. Cabassud, and P. Cognet, “A review on high temperature thermochemical heat energy storage,” *Renewable and Sustainable Energy Reviews*, vol. 32, pp. 591–610, 2014.

[24] D. Aydin, S. P. Casey, and S. Riffat, “The latest advancements on thermochemical heat storage systems,” *Renewable and Sustainable Energy Reviews*, vol. 41, pp. 356–367, 2015.

[25] P. de Dianous, F. Pincemin, G. Boulet, P. Jeandel, “Modelling and experimental evaluation of thermal insulation properties of mineral wool products at high temperature thermal insulation materials: Testing and applications,” *ASTM STP*, 1997.

[26] R. Spur, D. Fiala, D. Nevrala, and D. Probert, “Performances of modern domestic hot-water stores,” *Applied energy*, vol. 83, no. 8, pp. 893–910, 2006.

[27] R. Cole and F. Bellinger, “Thermally stratified tanks,” Argonne National Lab., IL (USA), Tech. Rep., 1982.

[28] L. Nkhonjera, T. Bello-Ochende, G. John, and C. K. King’ondu, “A review of thermal energy storage designs, heat storage materials and cooking performance of solar cookers with heat storage,” *Renewable and Sustainable Energy Reviews*, vol. 75, pp. 157–167, 2017.

[29] Y. H. Zurigat, P. R. Liche, and A. J. Ghajar, “Influence of inlet geometry on mixing in thermocline thermal energy storage,” *International Journal of Heat and Mass Transfer*, vol. 34, no. 1, pp. 115–125, 1991.

[30] A. J. Ghajar and Y. H. Zurigat, “Numerical study of the effect of inlet geometry on stratification in thermal energy storage,” *Numerical Heat Transfer*, vol. 19, no. 1, pp. 65–83, 1991.

[31] S. Ievers and W. Lin, “Numerical simulation of three-dimensional flow dynamics in a hot water storage tank,” *Applied Energy*, vol. 86, no. 12, pp. 2604–2614, 2009.

[32] A. Castell, M. Medrano, C. Solé, and L. F. Cabeza, "Dimensionless numbers used to characterize stratification in water tanks for discharging at low flow rates," *Renewable Energy*, vol. 35, no. 10, pp. 2192–2199, 2010.

[33] A. Mawire, M. McPherson, and R. Van den Heetkamp, "Simulated energy and exergy analyses of the charging of an oil–pebble bed thermal energy storage system for a solar cooker," *Solar Energy Materials and Solar Cells*, vol. 92, no. 12, pp. 1668–1676, 2008.

[34] R.-J. Shyu, J.-Y. Lin, and L.-J. Fang, "Thermal analysis of stratified storage tanks," *Journal of solar energy engineering*, vol. 111, no. 1, pp. 54–61, 1989.

[35] A. Mawire, M. McPherson, and R. Van den Heetkamp, "Discharging simulations of a thermal energy storage (tes) system for an indirect solar cooker," *Solar Energy Materials and Solar Cells*, vol. 94, no. 6, pp. 1100–1106, 2010.

[36] Z. Lavan and J. Thompson, "Experimental study of thermally stratified hot water storage tanks," *Solar Energy*, vol. 19, no. 5, pp. 519–524, 1977.

[37] S. Zavattoni, M. Barbato, A. Pedretti, G. Zanganeh, and A. Steinfeld, "High temperature rock-bed tes system suitable for industrial-scale csp plant–cfd analysis under charge/discharge cyclic conditions," *Energy Procedia*, vol. 46, pp. 124–133, 2014.

[38] M. Rady, "Thermal performance of packed bed thermal energy storage units using multiple granular phase change composites," *Applied energy*, vol. 86, no. 12, pp. 2704–2720, 2009.

[39] Z. Erregueragui, N. Boutammachte, A. Bouatem, O. Merroun, and E. M. Zemmouri, "Packed-bed thermal energy storage analysis: Quartzite and palm-oil performance," *Energy Procedia*, vol. 99, pp. 370–379, 2016.

[40] S. Duley and R. Skahjem, "Oil based solar concentrator with heat storage," Master's thesis, NTNU, Jun. 2016.

[41] K. Schwarzer and M. E. V. Da Silva, "Solar cooking system with or without heat storage for families and institutions," *Solar Energy*, vol. 75, no. 1, pp. 35–41, 2003.

[42] S. B. Joshi and A. Jani, "Design, development and testing of a small scale hybrid solar cooker," *Solar Energy*, vol. 122, pp. 148–155, 2015.

[43] *Mechanical thermostat valve*, `http://www.spiraxsarco.com/Resources/Pages/Steam-Engineering-Tutorials/control-hardware-sa-actuation/self-acting-temperature-controls.aspx`, retrieved 01.05.18 09:26.

[44] O. J. Nydal, *Empirical data - discussed orally*, Sep. 2017.

[45] *Water properties*, `https://www.engineeringtoolbox.com/water-density-specific-weight-d_595.html`, retrieved 11.05.18 09:30, 2017.

[46] D. K. De, M. Nathaniel, N. Nath De, and M. Ajaeroh Ikechukwu, "Cooking rice with minimum energy," *Journal of Renewable and Sustainable Energy*, vol. 6, no. 1, p. 013 138, 2014.

[47] O. Fasina and Z. Colley, "Viscosity and specific heat of vegetable oils as a function of temperature: 35 c to 180 c," *International Journal of Food Properties*, vol. 11, no. 4, pp. 738–746, 2008.

[48] B. Esteban, J.-R. Riba, G. Baquero, A. Rius, and R. Puig, "Temperature dependence of density and viscosity of vegetable oils," *Biomass and bioenergy*, vol. 42, pp. 164–171, 2012.

[49] J.-F. Hoffmann, J.-F. Henry, G. Vaitilingom, R. Olivès, M. Chirtoc, D. Caron, and X. Py, "Temperature dependence of thermal conductivity of vegetable oils for use in concentrated solar power plants, measured by 3omega hot wire method," *International Journal of Thermal Sciences*, vol. 107, pp. 105–110, 2016.

[50] F. P. Incropera, *Fundamentals of Heat and Mass Transfer*. USA: John Wiley & Sons, Inc., 2006, ISBN: 0470088400.

[51] E. Næss, *Assumptions in calculating heat propagation in metals - discussed orally*, Feb. 2018.

[52] C. Bogsnes and E. E. Hansen, “Self-regulating oil based heat storage,” Master’s thesis, NTNU, Jun. 2018.

Appendices

Appendix A

Machine drawings of the sliding valves

Sliding valve 1

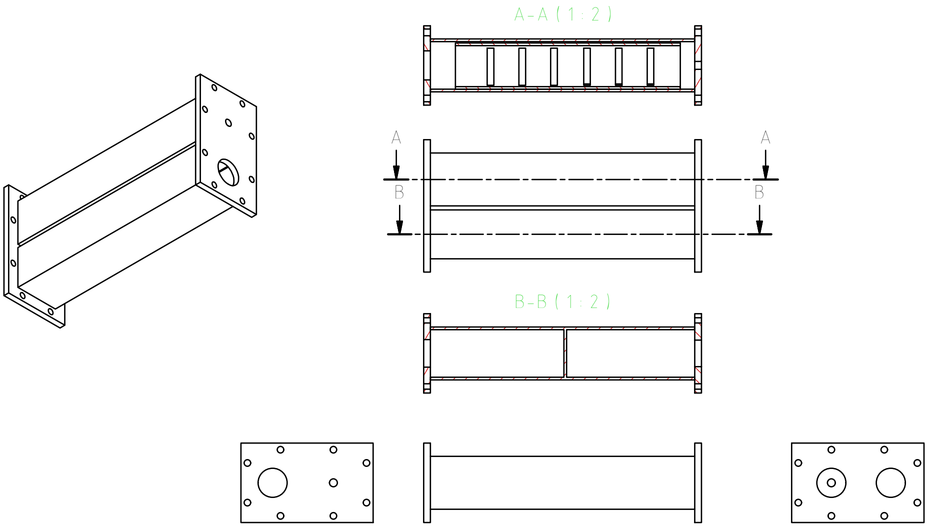

Figure A.1: Sliding valve 1 assembly.

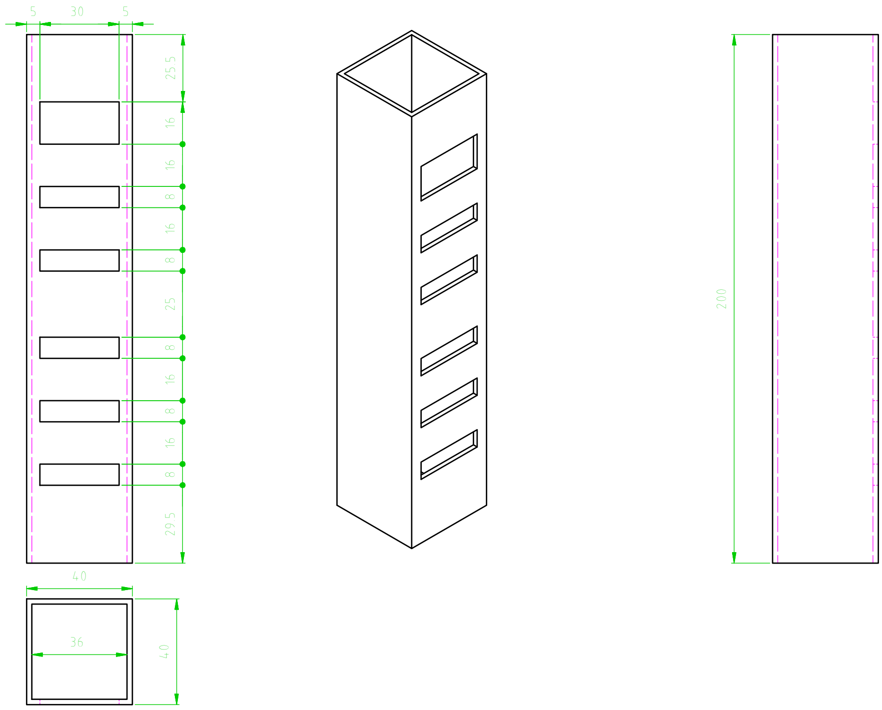

Figure A.2: Sliding valve 1 inlet chamber.

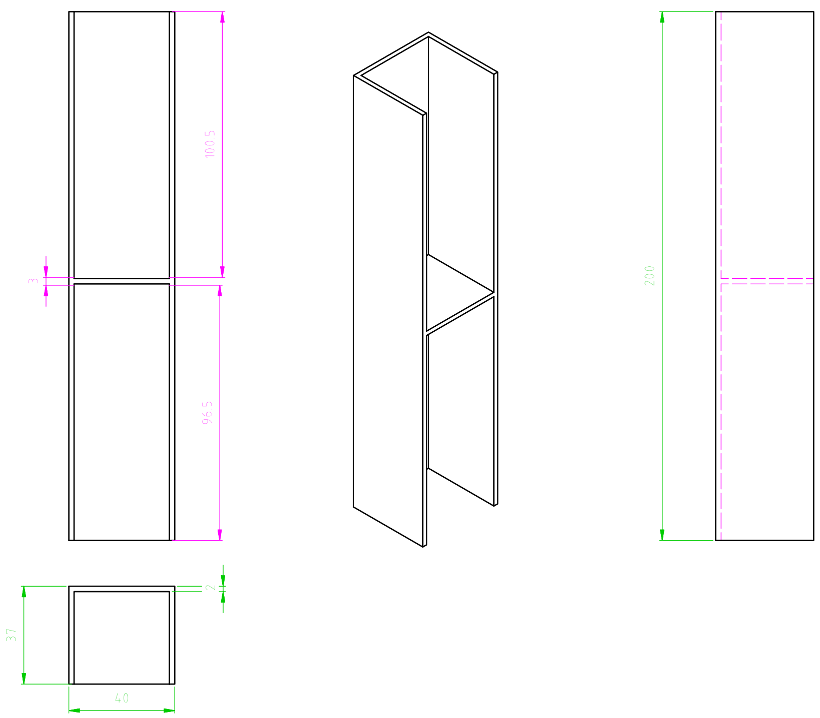

Figure A.3: Sliding valve 1 outlet chamber.

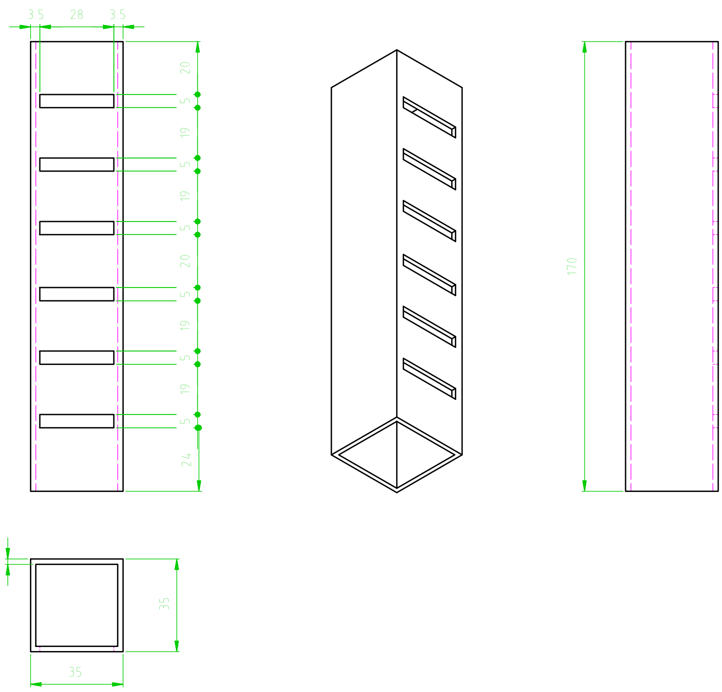

Figure A.4: Sliding valve 1 slider.

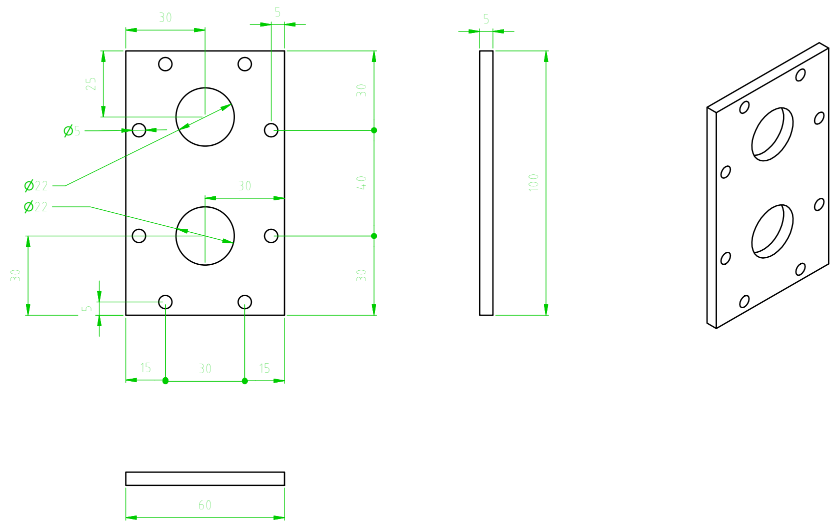

Figure A.5: Sliding valve 1 flange 1.

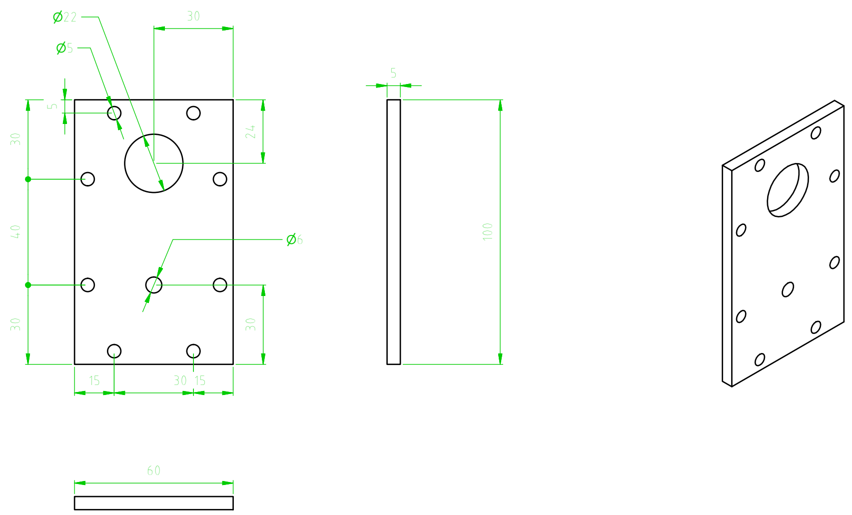

Figure A.6: Sliding valve 1 flange 2.

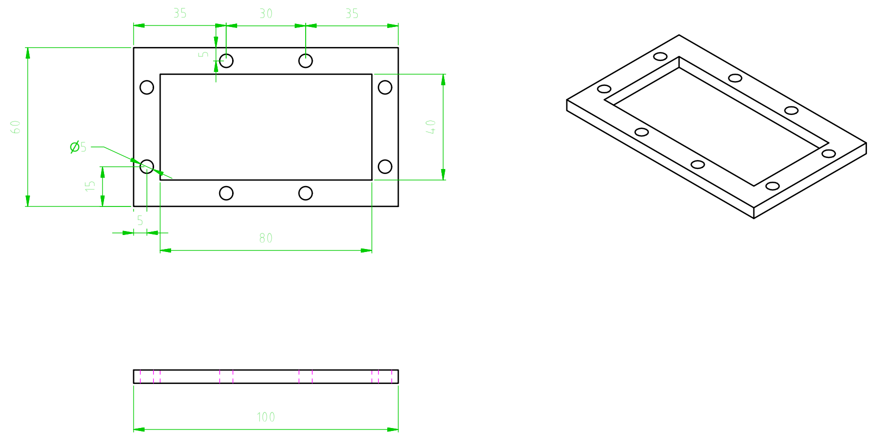

Figure A.7: Sliding valve 1 flange 3.

Sliding valve 2

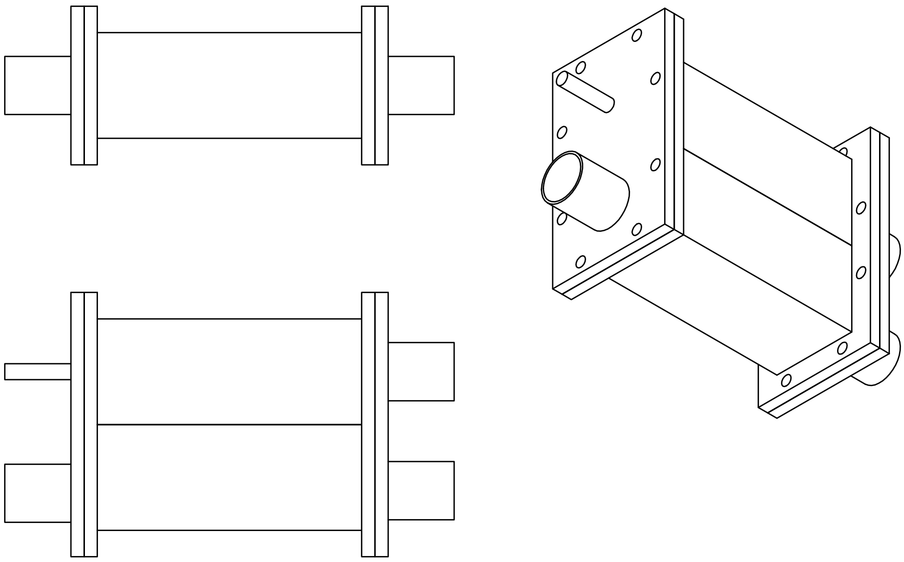

Figure A.8: Sliding valve 2 assembly.

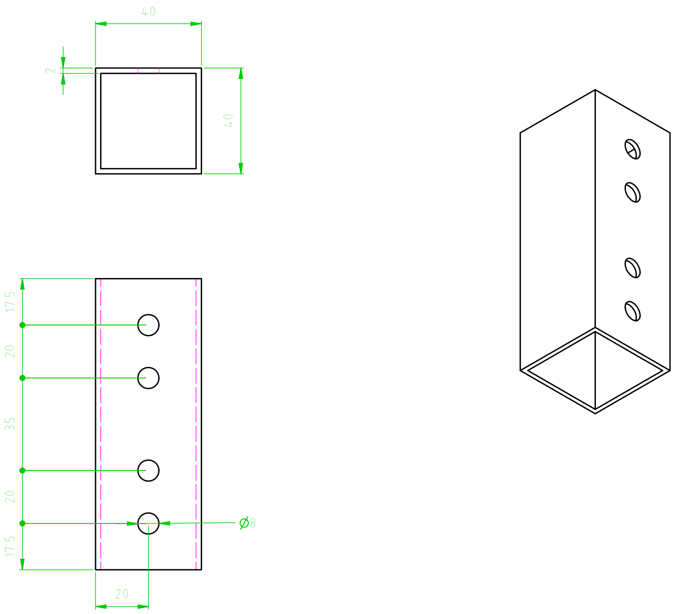

Figure A.9: Sliding valve 2 inlet and outlet chamber.

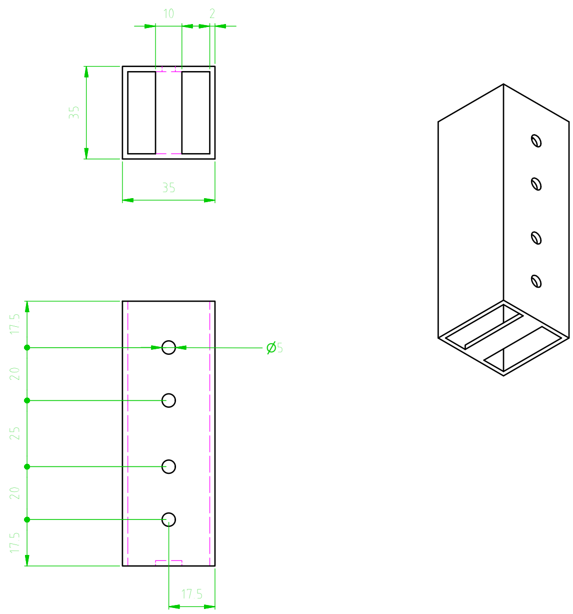

Figure A.10: Sliding valve 2 slider.

Sliding valve 3

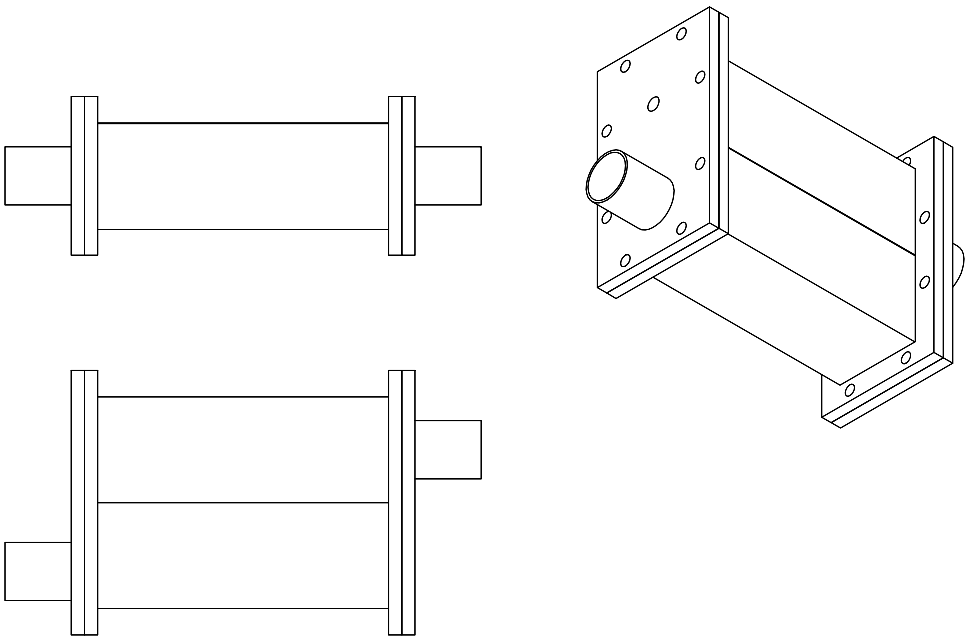

Figure A.11: Sliding valve 3 assembly.

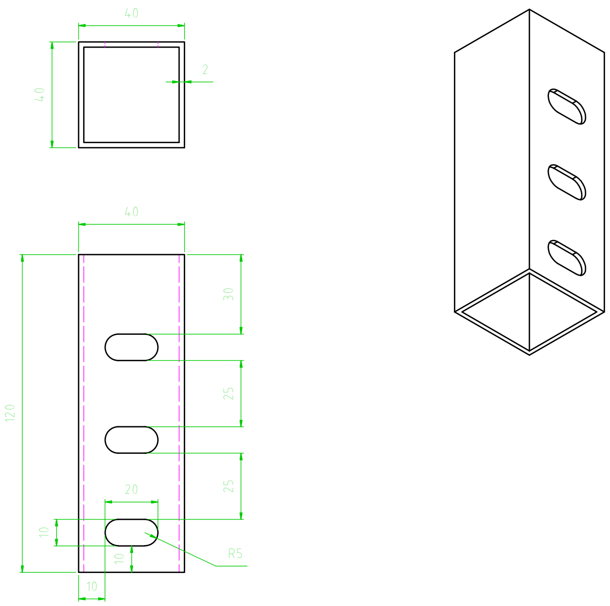

Figure A.12: Sliding valve 3 inlet and outlet chamber.

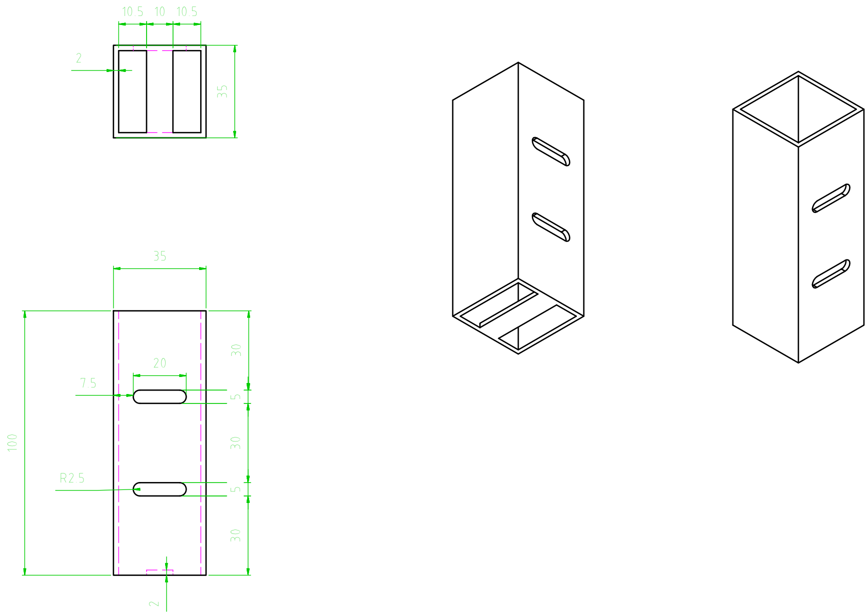

Figure A.13: Sliding valve 3 slider.

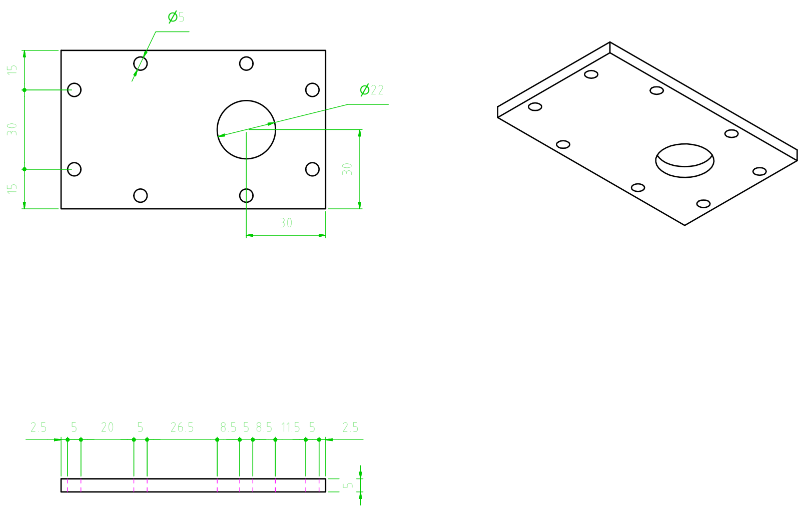

Figure A.14: Sliding valve 3 flange.

Appendix B

Insulation: Technical Specifications

FyreWrap® LT Blanket

DESCRIPTION

FyreWrap® LT Blanket from Unifrax is a new lightweight, & flexible high temperature insulation blanket manufactured from Insulfrax low bio-persistence fibres & is specifically designed for passive fire protection applications.

With its enhanced fibre properties, FyreWrap LT Blanket offers significant weight savings when compared with both traditional AES wool blankets and more particularly mineral wool based products. The modified fibre characteristics also give FyreWrap LT Blankets improved handling characteristics.

Thin, lightweight systems, combined with a flexible and easy to install form result in lower installation costs and significant weight savings. The fibres are totally inorganic and FyreWrap LT Blanket contains no binder no smoke or fumes are generated when exposed heat.

FIRE PROTECTION PROPERTIES

- Non Combustible to IMO FTP Code Part 1
- Classified A1 to EN 13501-1

0062

TYPICAL APPLICATIONS

Unifrax FyreWrap LT Blanket is suitable for use in a wide variety of passive fire protection applications including:

- Marine deck and bulkhead insulation in all types of craft
- Hydrocarbon and jet fire protection of vessels and pipes
- Bulkhead & deck insulation for offshore oil platforms & FPSO's
- Cable tray fire protection
- Ductwork fire protection
- Infill of fire doors and lightweight cladding panels

Any new and/or special use of these products, whether or not in an application listed in our literature, must be submitted to our technical department for their prior written approval.

When Fire Protection Matters Most
Contact your local distributor.

Unifrax Ltd.
T:+44 (0)1744 88 7600 F: +44 (0)1744 88 9916
www.unifrax.com

FyreWrap® LT Blanket

TYPICAL PRODUCT PARAMETERS

Thermal Characteristics

Ambient Insulation Performance

Blanket Thickness (mm)	R Value	U Value
25	0.78	1.28
40	1.25	0.80
45	1.41	0.71
50	1.56	0.64
55	1.72	0.58

Based on thermal conductivity of FyreWrap LT Blanket 64 kg/m³ density measured to BS EN 12667 at 10°C of 0.0320 W/mK. For blanket densities above 64kg/m³ the same values may be used.

Thermal Conductivity (W/mK)

Mean Temp. (°C)	64kg/m³	96kg/m³	128kg/m³
200	0.06	0.06	0.05
400	0.11	0.09	0.08
600	0.17	0.14	0.12
800	0.26	0.20	0.18
1000	0.38	0.29	0.25

Thermal Conductivity measured in accordance with ASTM C-201.

Acoustic Characteristics

Sound Absorption

Frequency (Hz)	50mm x 70kg/m³	50mm x 96kg/m³
125	0.47	0.26
250	1.05	0.94
500	1.09	1.03
1000	1.09	1.03
2000	1.12	1.09
4000	1.12	1.14
5000	1.18	1.09
NRC	**1.10**	**1.00**

Test method BS EN ISO 354:2003. Foil facing will reduce the sound absorption characteristics.

Blanket Facings

FyreWrap LT Blanket can be supplied faced with choice of facing. The following grades are available :

FyreWrap LTF Blanket with 30µm foil on one face.

FyreWrap LTFR Blanket with 30µm foil & glass fibre mesh reinforcement on one face.

FyreWrap LTG Blanket with glass fibre cloth on one face.

FyreWrap LTF, LTFR & LTG blankets are available with the covering on both top and bottom surfaces of the blanket and are designated LTF2, LTFR2, and LTG2 respectively.

AVAILABILITY

Standard Roll Sizes

Thickness (mm)	Roll Length (m)	Density (kg/m³)
25	7.32	64,96,128
35	5.0	70
38	5.0	96, 128
40	5.0	70
45	5.0	64
50	3.66	70, 96,128
55	3.66	64

Non-standard combinations may be available upon request subject to minimum quantity orders.

HANDLING INFORMATION

A Material Safety Data Sheet has been issued describing the health, safety and environmental properties of this product, identifying the potential hazards and giving advice on handling precautions and emergency procedures. This must be consulted and fully understood before handling, storage or use.

Supplied by:

COLD to HOT
We've Got You Covered

aspen aerogels®

DATA SHEET

Pyrogel® XT-E

FLEXIBLE INDUSTRIAL INSULATION FOR HIGH-TEMPERATURE APPLICATIONS

Pyrogel® XT-E is a high-temperature insulation blanket that is formed of silica aerogel – which possesses the lowest thermal conductivity of any known solid – and reinforced with a non-woven, glass-fiber batting.

Pyrogel® XT-E is our easiest product ever to handle, store, and install. It offers the same industry-leading thermal performance as Pyrogel® XT, with standard roll sizes and a product form that dramatically reduces handling dust and simplifies installation and clean-up.

Ideal for insulating piping, vessels, tanks, and equipment, Pyrogel® XT-E is an essential material for those seeking the ultimate in thermal efficiency.

Physical Properties

Thicknesses*	0.20 in (5 mm)	0.40 in (10 mm)
Material Form*	1,500 ft² rolls	850 ft² rolls
Max. Use Temp.	1200°F (650°C)	
Color	Maroon	
Density*	12.5 lb/ft³ (0.20 g/cc)	
Hydrophobic	Yes	

* Nominal values. Thicknesses measured using a method derived from ASTM C 518 and another proprietary method to provide resolutions an order of magnitude smaller than ASTM C 167.

Advantages

Superior Thermal Performance
Up to five times better thermal performance than competing insulation products

Reduced Thickness and Profile
Equal thermal resistance at a fraction of the thickness

Less Time and Labor to Install
Easily cut and conformed to complex shapes, tight curvatures, and spaces with restricted access

Physically Robust
Soft and flexible but with excellent springback, Pyrogel® XT-E recovers its thermal performance even after compression events as high as 100 psi

Shipping and Warehousing Savings
Reduced material volume, high packing density, consistent roll sizes, and low scrap rates can reduce logistics costs by a factor of five or more compared to rigid, pre-formed insulations

Simplified Inventory
Unlike rigid pre-forms such as pipe cover or board, the same Pyrogel® XT-E blanket can be cut to fit any piece of piping or equipment

Hydrophobic Yet Breathable
Pyrogel® XT-E repels liquid water but allows vapor to pass through, helping to prevent corrosion under insulation

Environmentally Safe
Landfill disposable, shot-free, minimal dust with no respirable fiber content

Thermal Conductivity†

ASTM C 177 Results

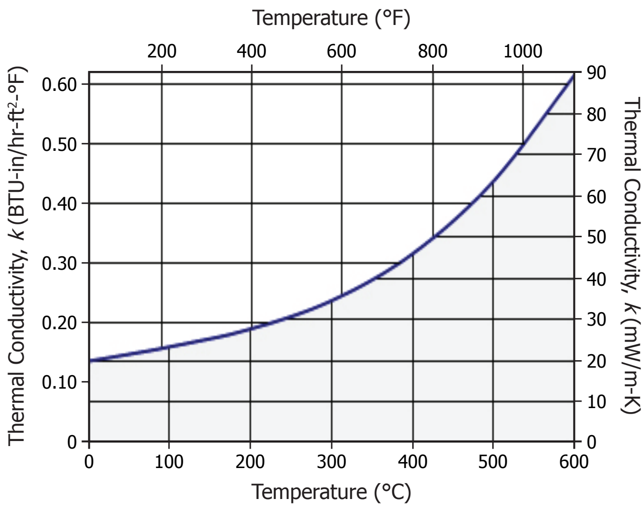

Mean Temp.	°C	0	100	200	300	400	500	600
	°F	32	212	392	572	752	932	1112
k	mW/m-K	20	23	28	35	46	64	89
	BTU-in/hr-ft²-°F	0.14	0.16	0.19	0.24	0.32	0.44	0.62

† Thermal conductivity measurements taken at a compressive load of 2 psi and standard atmospheric pressure.

COLD to HOT
We've Got You Covered

aspen aerogels®

Pyrogel® XT-E

Thicknesses Required for Personnel Protection*

Assumed design conditions:

Ambient temperature = 86°F (30°C)
Wind speed = 2.2 mph (1 m/s)
Surface emissivity = 0.15
Max. touch temp = 140°F (60°C)

* These data are provided as an example only. Actual performance should be determined using the parameters relevant to the particular application.

Pyrogel® XT-E Thickness (mm) vs. Process Temperature and Nominal Pipe Size

NPS **in** (mm)	**100°C** (210°F)	**150°C** (300°F)	**200°C** (390°F)	**250°C** (480°F)	**300°C** (570°F)	**350°C** (660°F)	**400°C** (750°F)	**450°C** (840°F)	**500°C** (930°F)	**550°C** (1020°F)	**600°C** (1110°F)	**650°C** (1200°F)	
0.5 (15)	5	5	5	10	10	15	15	20	20	25	30	40	5 mm product
0.75 (20)	5	5	5	10	10	15	15	20	25	30	35	45	
1 (25)	5	5	10	10	15	15	20	25	30	35	40	50	
1.5 (40)	5	5	10	10	15	20	20	25	30	40	45	55	
2 (50)	5	5	10	15	15	20	25	30	35	40	50	60	
3 (80)	5	10	10	15	20	25	30	35	40	50	60	70	
4 (100)	5	10	10	15	20	25	30	35	45	55	65	75	
6 (150)	5	10	15	20	25	30	35	45	50	60	75	85	
8 (200)	5	10	15	20	25	30	40	45	55	70	80	95	5 mm and/or 10 mm product
10 (250)	5	10	15	20	25	35	40	50	60	75	85	105	
12 (300)	5	10	15	20	30	35	45	55	65	75	90	110	
14 (350)	5	10	15	25	30	35	45	55	65	80	95	110	
16 (400)	5	10	15	25	30	40	45	55	70	80	100	115	
18 (450)	5	10	20	25	30	40	50	60	70	85	100	120	
20 (500)	5	10	20	25	30	40	50	60	75	90	105	125	
24 (600)	5	15	20	25	35	40	50	65	75	90	110	130	
28 (700)	5	15	20	25	35	45	55	65	80	95	115	135	
30 (750)	5	15	20	25	35	45	55	65	80	95	115	140	
36 (900)	5	15	20	30	35	45	55	70	85	100	120	145	
48 (1200)	10	15	20	30	40	50	60	75	90	105	130	150	
Flat	10	15	20	35	45	50	65	80	100	125	150	175	

Product Performance Data

Test Procedure	Property	Results
ASTM C 1728, Type III, Grade 1A	Standard Specification for Flexible Aerogel Insulation	Complies
ASTM C 165	Compressive Strength	Stress at 10% strain = 11.4 psi (78.3 kPa) Stress at 25% strain = 37.0 psi (255.2 kPa)
ASTM C 356	Linear Shrinkage Under Soaking Heat	<2% @ 1200°F (650°C)
ASTM C 411	Hot Surface Performance	Passed
ASTM C 447	Estimation of Maximum Use Temperature	1200°F (650°C)
ASTM C 795	Insulation for Use Over Austenitic Stainless Steel	Passed
ASTM C 1101	Classifying the Flexibility of Mineral Fiber Blankets	Class: Resilient Flexible
ASTM C 1104	Water Vapor Sorption	<5% (by weight)
ASTM C 1338	Fungal Resistance of Insulation Materials	Passed
ASTM C 1511	Liquid Water Retention After Submersion	<5% (after heat treatment)
ASTM E 84	Surface Burning Characteristics	Flame Spread Index = 0 Smoke Developed Index = 0

Characteristics

Pyrogel® XT-E can be cut using conventional cutting tools including scissors, tin snips, and razor knives. It is recommended gloves, safety glasses, and dust mask be worn when handling material. See MSDS for complete health and safety information.

aspen aerogels®

Aspen Aerogels, Inc.
30 Forbes Road, Building B
Northborough, MA 01532
USA

Phone: 508.691.1111
Fax: 508.691.1200
E-Mail: info@aerogel.com
Web: www.aerogel.com

REV 1.0

Appendix C

Pictures of components made at NTNU

Figure C.1: Three pots of different sizes, acquired for the Three-pot cooker made at NTNU.

(a) The inlet pipe going through the large and medium pot, seen form inside the medium pot.

(b) Seen from above, with the small cooking pot inside.

(c) Seen from below, with the inlet pipe entering at the bottom.

Figure C.2: Pictures of the finished cooking application with its insulation and casing, inlet and outlet pipe.

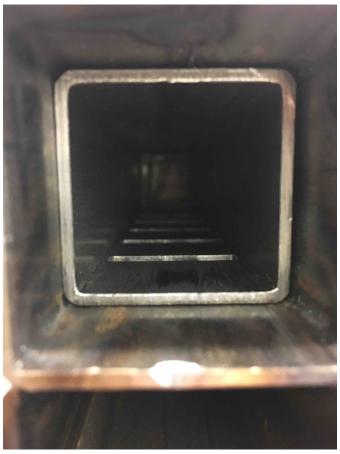

(a) A small gap between the slider and the surface providing leaks through the inlet and outlet chamber.

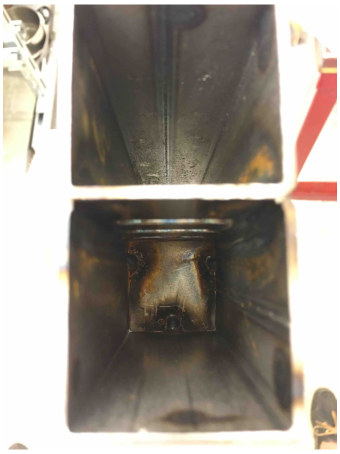

(b) Leaks formed around the separation plate in the outlet chamber.

Figure C.3: Pictures of where leaks occurred in sliding valve 1.

Figure C.4: The test rig made at NTNU. The cooking application is located low at the right hand side. The rock bed is located in the middle. The fill valve from the co-project is located above the cooking application.

Appendix D

Pictures and measures of components made at Makerere University

Table D.1: Measures of components used at Makerere University.

Measures of the components			
Component	**Height x Width x Depth**	**Total volume**	**Material**
Oil supply tank	-	40,0 [L]	Plastic
Floating valve container	55 x 20 x 20 [cm]	22,0 [L]	Steel
Heating container	50 x 5 x 10 [cm]	2,5 [L]	Steel
Heat storage	40 x 20 x 20 [cm]	16,0 [L]	Steel
Component	**Diameter**	**Total length / Total Volume**	**Material**
Pipes	1 [inch]	2,6 [m]	Steel
Residual tank	-	25 [L]	Aluminium
Cooking pot, small	-	3 [L]	Steel
Cooking pot, medium	-	5 [L]	Steel
Cooking pot, large	-	7 [L]	Steel

(a) The oil supply tank connected to the floating valve via a plastic hose.

(b) Floating valve mounting with a hose clamp on the end of a threaded rod.

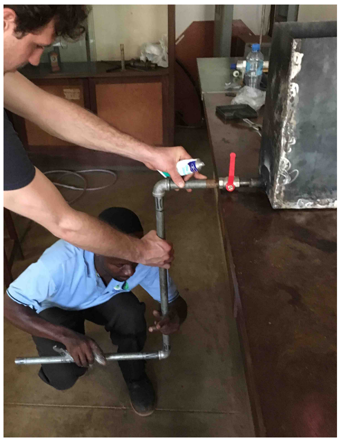

(c) The piping system, with a bullet valve, from the heat storage to the cooking application.

(d) Silicon sealant used where leaks were discovered.

(e) Gap between the medium and large cooking pot due to clumpy welding.

Figure D.1: Components of the system built at Makerere University.

(a) The metal containers during production. From left to right: fill valve container, heating container and thermal heat storage. The heating element is held in front of the containers.

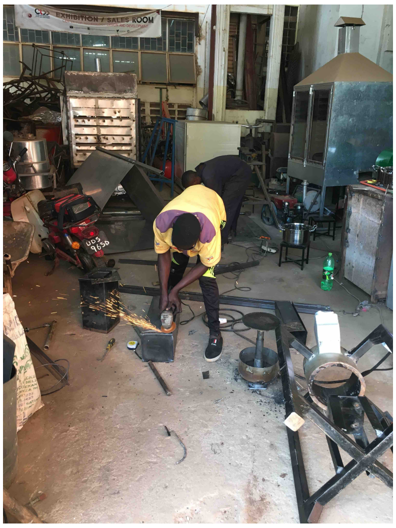

(b) The workshop at Makerere University where the system was produced.

Figure D.2: The solar cooking system during production and the workshop at Makerere University

Appendix E

Calculations for the cooking application

b/a	$C_{fP}Re$	K_∞	c
	Pipe or Concentric Annulus		
0.0	16.00	1.25	0.000212
0.05	21.57	0.830	0.000050
0.10	22.34	0.784	0.000043
0.50	23.81	0.688	0.000032
0.75	23.97	0.678	0.000030
1.00	24.00	0.674	0.000029
	Rectangular Duct		
1.00	14.23	1.43	0.00029
0.50	15.55	1.28	0.00021
0.20	19.07	0.931	0.000076
0.00	24.00	0.674	0.000029
	Equilateral Triangle		
—	13.33	1.69	0.00053

Annulus: Rectangular duct: Triangular duct:

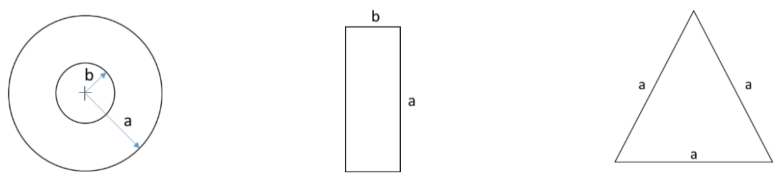

$D_h = 2\cdot(a-b)$ $D_h = 2\cdot\frac{a\cdot b}{a+b}$ $D_h = \frac{\sqrt{3}}{4}\cdot a^2$

Figure E.1: Coefficients for different geometries used in calculating the pressure loss for laminar flow in conducts. Equation 4.8.

Appendix F

Risk assessment

NTNU SINTEF

Risk Assessment Report

Oil based Heat Storage Rig

Prosjektnavn	Solar heat storage in oil based rock bed
Apparatur	Oil based heat storage rig
Enhet	NTNU
Apparaturansvarlig	Ole Jørgen Nydal
Prosjektleder	Ole Jørgen Nydal
HMS-koordinator	Morten Grønli
HMS-ansvarlig (linjeleder)	Therese Løvås
Plassering	EPT-TermiskLab
Romnummer	C082
Risikovurdering utført av	Oskar Stadaas Sjøgren

Approval:

Apparatur kort (UNIT CARD) valid for:	12 months
Forsøk pågår kort (EXPERIMENT IN PROGRESS) valid for:	12 months

Rolle	Navn	Dato	Signatur
Prosjektleder	Ole Jørgen Nydal	5/12/2017	Ole Jørgen Nydal
HMS koordinator	Morten Grønli	23/10-2017	M Grønli
HMS ansvarlig (linjeleder)	Therese Løvås	25/10-2017	Therese Løvås

NTNU SINTEF

TABLE OF CONTENTS

1 INTRODUCTION

The setup consists of a small pipe system, including a heating element, connected to a heat storage. The heat storage is composed of a large aluminium cylinder filled with rocks. The heating element is insulated and out inside an aluminium cylinder. There is hot oil flowing from a cold reservoir into the heating component. From there it is directed into the rock bed, which is initially filled with cold oil. The cold oil is forced out by the added hot oil and is directed into a cold reservoir. The maximum temperature for the experiment will be around 220°C. The flow in this system is driven by gravitational forces. There is a valve between the rock bed and the cold reservoir to ensure atmospheric pressure.

The purpose of the experiment is to test the stratification of hot oil and see if the gravitational forces can be used as a driving force for this system.

The experimental rig is located at the cellar floor, room C082, in Varmeteknisk Lab.

2 ORGANISATION

Rolle	
Prosjektleder	Ole Jørgen Nydal
Apparaturansvarlig	Ole Jørgen Nydal
Romansvarlig	Paul Svendsen
HMS koordinator	Morten Grønli
HMS ansvarlig (linjeleder):	Therese Løvås

3 RISK MANAGEMENT IN THE PROJECT

Hovedaktiviteter risikostyring	Nødvendige tiltak, dokumentasjon	DATE
Prosjekt initiering	Prosjekt initiering mal	21.08.2017
Veiledningsmøte Guidance Meeting	Skjema for Veiledningsmøte med pre-risikovurdering	28.08.2017
Innledende risikovurdering Initial Assessment	Fareidentifikasjon – HAZID Skjema grovanalyse	
Vurdering av teknisk sikkerhet Evaluation of technical security	Prosess-HAZOP Tekniske dokumentasjoner	
Vurdering av operasjonell sikkerhet Evaluation of operational safety	Prosedyre-HAZOP Opplæringsplan for operatører	
Sluttvurdering, kvalitetssikring Final assessment, quality assurance	Uavhengig kontroll Utstedelse av apparaturkort Utstedelse av forsøk pågår kort	

4 DESCRIPTIONS OF EXPERIMENTAL SETUP

The rig consists of the following components (see figure below):

1. Cold oil reservoirs
2. Float ball
3. Heating tube
4. Heating element
5. Output valve for hot oil when system is reversed
6. Rock bed (heat storage)
7. Draining valve
8. Pressure valve
9. Thermocouple wires connected to a Piko Logger

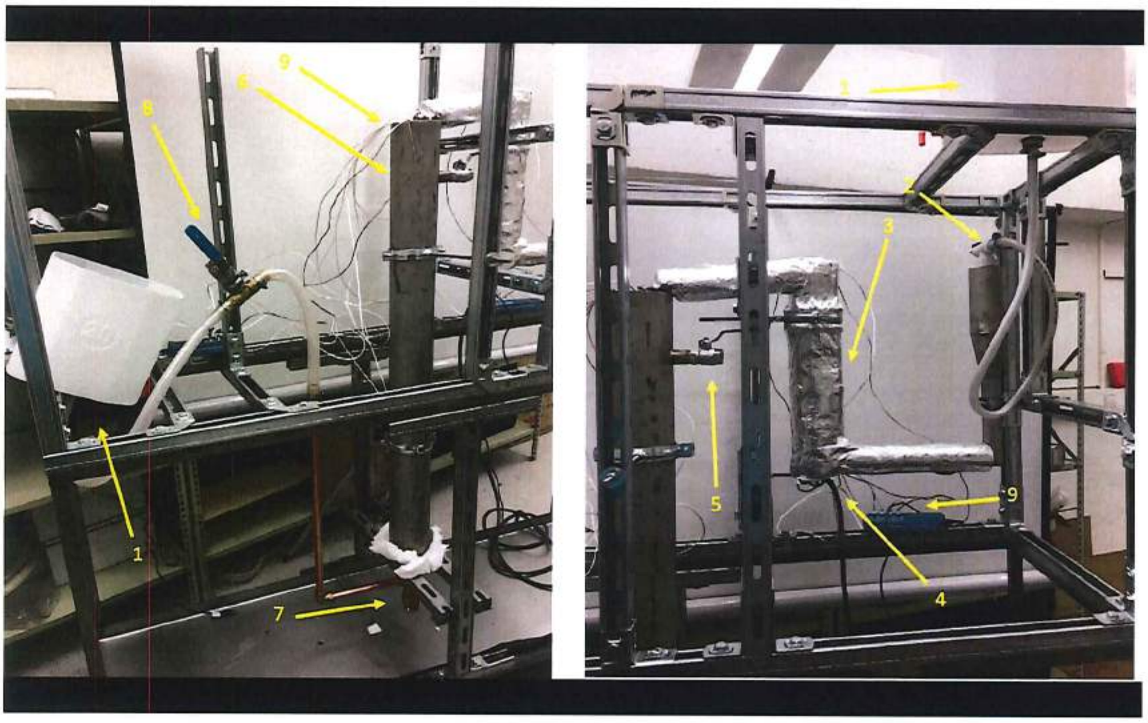

The shutdown of the system is simple and is done by unplugging the power supply to the heating element in the heat tube. If required, the oil can be drained from the system by using the valve below the rock bed. The hot oil shall never exceed the bottom of the rock bed.

5 EVACUATION FROM THE EXPERIMENTAL AREA

Evacuate at signal from the alarm system or local gas alarms with its own local alert with sound and light outside the room in question, see 6.2

Evacuation from the rigging area takes place through the marked emergency exits to the assembly point, (corner of Old Chemistry Kjelhuset or parking 1a-b.)

Action on rig before evacuation:
Turn off the power supply of the electrical heater by unplugging it.

6 WARNING

6.1 Before experiments

Send an e-mail with information about the planned experiment to:
iept-experiments@ivt.ntnu.no

The e-mail must include the following information:

- Name of responsible person:
- Experimental setup/rig:
- Start Experiments: (date and time)
- Stop Experiments: (date and time)

You must get the approval back from the laboratory management before start up. All running experiments are notified in the activity calendar for the lab to be sure they are coordinated with other activity.

6.2 Non-conformance

FIRE

If you are NOT able to extinguish the fire, activate the nearest fire alarm and evacuate area. Be then available for fire brigade and building caretaker to detect fire place.
If possible, notify:

NTNU	SINTEF
Morten Grønli, Mob: 918 97 515	Linda Helander, Mob: +47 406 48 621
Terese Løvås: Mob: 918 97 209	Petter Røkke, Mob: 901 20 221
NTNU – SINTEF Beredskapstelefon	800 80 388

GAS ALARM

If a gas alarm occurs, close gas bottles immediately and ventilate the area. If the level of the gas concentration does not decrease within a reasonable time, activate the fire alarm and evacuate the lab. Designated personnel or fire department checks the leak to determine whether it is possible to seal the leak and ventilate the area in a responsible manner.

PERSONAL INJURY

- First aid kit in the fire / first aid stations
- Shout for help
- Start life-saving first aid
- **CALL 113** if there is any doubt whether there is a serious injury

OTHER NON-CONFORMANCE (AVVIK)

NTNU:

You will find the reporting form for non-conformance on:
https://innsida.ntnu.no/wiki/-/wiki/Norsk/Melde+avvik

SINTEF:

Synergi

7 ASSESSMENT OF TECHNICAL SAFETY

7.1 HAZOP

The experiment set up is divided into the following nodes:

Node 1	Testing the oil stratification in the storage

Attachments, Form: Hazop_mal
Conclusion: No real dangers. Avoid touching potential hot surfaces (storage, pipes, heat tube).

7.2 Flammable, reactive and pressurized substances and gas

Are any flammable, reactive and pressurized substances and gases in use?

NO	

Attachments: EX zones?
Conclusion: No real dangers.

7.3 Pressurized equipment

Is any pressurized equipment in use?

NO	

Attachments: Certificate for pressurized equipment (see Attachment to Risk Assessment)
Conclusion: No real dangers. No attachment necessary

7.4 Effects on the environment (emissions, noise, temperature, vibration, smell)

NO	

Attachments: No attachment necessary.
Conclusion: The experiment shall not generate emission of smoke, gas, odour, etc when operated properly. Still, there should be used a ventilation channel over the rock bed "just in case". The oil should be stored safe in an own container and considered as special waste when the experiments are done.

7.5 Radiation

See Chapter 13 "Guide to the report template".

NO	

Attachments: No attachment necessary
Conclusion: No real dangers. No attachment necessary.

7.6 Chemicals

YES	Duratherm 630 heat oil

Attachments: MSDS

Conclusion: The oil used is a high heat transfer oil but it is not dangerous for health, you can smell it and touch it like the common oil we use in our houses. Of course, you must not use it like an edible product.

7.7 Electricity safety (deviations from the norms/standards)

NO	

Attachments: No attachment necessary.
Conclusion: No real dangers.

8 ASSESSMENT OF OPERATIONAL SAFETY

Ensure that the procedures cover all identified risk factors that must be taken care of. Ensure that the operators and technical performance have sufficient expertise.

8.1 Procedure HAZOP

The method is a procedure to identify causes and sources of danger to operational problems.
Procedure:

1) Put a board in the bottom of the structure to avoid spills of hot oil.
2) Tested all the system connections using water to check for leaks.
3) Ensure the heater is working and we can control it using the thermostat.
4) Insulated some of the pipes where necessary.
5) Use thermal camera in addition to thermocouples to see if we get a thermal front in the rock bed.

Attachments:: HAZOP_MAL_Prosedyre
Conclusion: The procedure is safe, only needs avoid the contact with the hot elements during the heating of the oil.

8.2 Operation procedure and emergency shutdown procedure

The operating procedure is a checklist that must be filled out for each experiment.
Emergency procedure should attempt to set the experiment set up in a harmless state by unforeseen events.

Attachments: Procedure for running experiments
Emergency shutdown procedure: Pull out the plug connected to the heat element box (no power means no heat)

8.3 Training of operators

A Document showing training plan for operators

- *What are the requirements for the training of operators?*
- *What it takes to be an independent operator*
- *Job Description for operators*

Attachments*:* Training program for operators

8.4 Technical modifications

No technical modifications needed during the experiment that produce risk. Only possible addition of rock-bed to the main storage, that means full the storage with little rocks, this does not become in a dangerous situation.

Conclusion: No dangerous/important modifications during the experiment.

8.5 Personal protective equipment

Eye protection should be used in the rig zone. Gloves should be used when handling the tubes as some of them can be hot.

Conclusion: Plastic glasses and gloves is the only special equipment needed to protect.

8.6 General Safety

Warning signs must be close the hot elements.
An operator must be controlling the rig.

Conclusion*:* Signs and monitoring by operator.

8.7 Safety equipment

No need for any special safety equipment except warning signs, gloves and plastic glasses.

8.8 Special predations

One operator must be in the rig zone during tests to make sure the temperature is within safe range and there is no major leaks.

9 QUANTIFYING OF RISK - RISK MATRIX

See Chapter 13 "Guide to the report template".
The risk matrix will provide visualization and an overview of activity risks so that management and users get the most complete picture of risk factors.

IDnr	Aktivitet-hendelse	Frekv-Sans	Kons	RV
1	*People getting burned on heat element*	2	C	C2
3	*Oil leakage*	1	B	B1

Conclusion: We consider the risk to people, environment and economic very small. The aim of the risk assessment is to achieve avoid all the risk related with the possible burns.

CONSEQUENSES						
	Catastrophic	E1	E2	E3	E4	E5
	Major	D1	D2	D3	D4	D5
	Moderate	C1	C2	C3	C4	C5
	Minor	B1	B2	B3	B4	B5
	Insignificant	A1	A2	A3	A4	A5
		Rare	Unlikely	Possible	Likely	Almost
		PROBABILITY				

Table 8. Risk's Matrix

Table 9. The principle of the acceptance criterion. Explanation of the colors used in the matrix

COLOUR		DESCRIPTION
Red		Unacceptable risk Action has to be taken to reduce risk
Yellow		Assessment area. Actions has to be considered
Green		Acceptable risk. Action can be taken based on other criteria

10 REGULATIONS AND GUIDELINES

Se http://www.arbeidstilsynet.no/regelverk/index.html

- Lov om tilsyn med elektriske anlegg og elektrisk utstyr (1929)
- Arbeidsmiljøloven
- Forskrift om systematisk helse-, miljø- og sikkerhetsarbeid (HMS Internkontrollforskrift)
- Forskrift om sikkerhet ved arbeid og drift av elektriske anlegg (FSE 2006)
- Forskrift om elektriske forsyningsanlegg (FEF 2006)
- Forskrift om utstyr og sikkerhetssystem til bruk i eksplosjonsfarlig område NEK 420
- Forskrift om håndtering av brannfarlig, reaksjonsfarlig og trykksatt stoff samt utstyr og anlegg som benyttes ved håndteringen
- Forskrift om Håndtering av eksplosjonsfarlig stoff
- Forskrift om bruk av arbeidsutstyr.
- Forskrift om Arbeidsplasser og arbeidslokaler
- Forskrift om Bruk av personlig verneutstyr på arbeidsplassen
- Forskrift om Helse og sikkerhet i eksplosjonsfarlige atmosfærer
- Forskrift om Høytrykksspyling
- Forskrift om Maskiner
- Forskrift om Sikkerhetsskilting og signalgivning på arbeidsplassen
- Forskrift om Stillaser, stiger og arbeid på tak m.m.
- Forskrift om Sveising, termisk skjæring, termisk sprøyting, kullbuemeisling, lodding og sliping (varmt arbeid)
- Forskrift om Tekniske innretninger
- Forskrift om Tungt og ensformig arbeid
- Forskrift om Vern mot eksponering for kjemikalier på arbeidsplassen (Kjemikalieforskriften)
- Forskrift om Vern mot kunstig optisk stråling på arbeidsplassen
- Forskrift om Vern mot mekaniske vibrasjoner
- Forskrift om Vern mot støy på arbeidsplassen

Veiledninger fra arbeidstilsynet
se: http://www.arbeidstilsynet.no/regelverk/veiledninger.html

11 DOCUMENTATION

- Tegninger, foto, beskrivelser av forsøksoppsetningen
- Hazop_mal
- Sertifikat for trykkpåkjent utstyr
- Håndtering avfall i NTNU
- Sikker bruk av LASERE, retningslinje
- HAZOP_MAL_Prosedyre
- Forsøksprosedyre
- Opplæringsplan for operatører
- Skjema for sikker jobb analyse, (SJA)
- Apparaturkortet
- Forsøk pågår kort

NTNU SINTEF

Attachment to Risk Assessment report

Oil based Heat Storage Rig

Prosjektnavn	Solar heat storage in oil based rock bed
Apparatur	Oil based heat storage rig
Enhet	NTNU
Apparaturansvarlig	Ole Jørgen Nydal
Prosjektleder	Ole Jørgen Nydal
HMS-koordinator	Morten Grønli
HMS-ansvarlig (linjeleder)	Therese Løvås
Plassering	EPT-TermiskLab
Romnummer	C082
Risikovurdering utført av	Oskar Stadaas Sjøgren

TABLE OF CONTENTS

ATTACHMENT A: PROCESS AND INSTRUMENTATION DIAGRAM

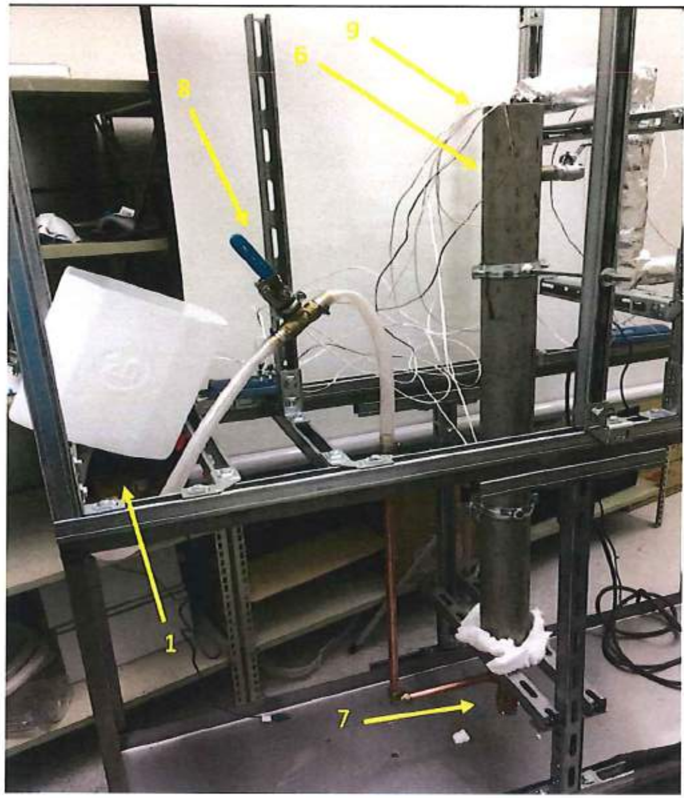

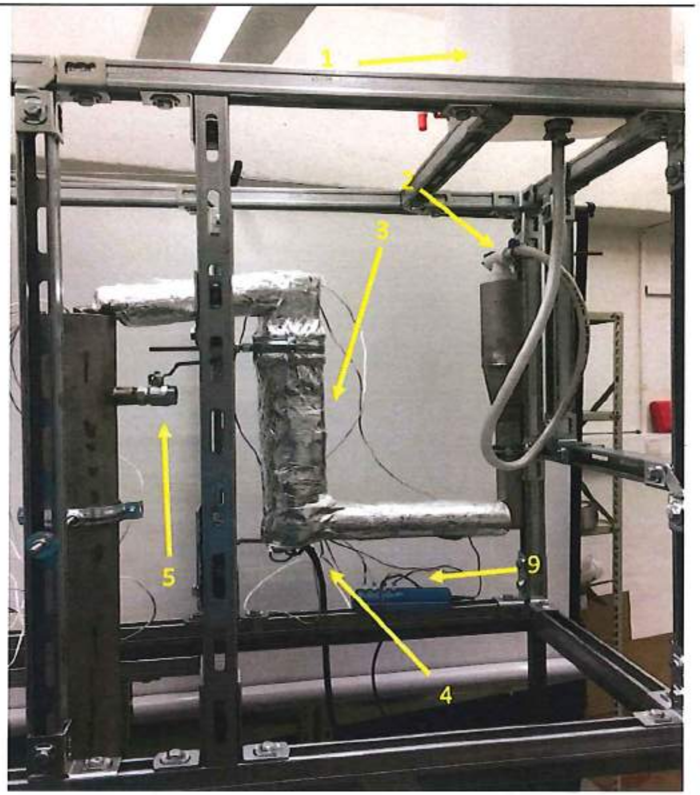

The rig consists of the following components (see figure below):

1. Cold oil reservoirs
2. Float ball
3. Heating tube
4. Heating element
5. Output valve for hot oil when system is reversed
6. Rock bed (heat storage)
7. Draining valve
8. Pressure valve
9. Thermocouple wires connected to a Piko Logger

NTNU SINTEF

ATTACHMENT B: HAZOP TEMPLATE

Project: Node: 1						Page	
Ref	Guideword	Causes	Consequences	Safeguards	Recommendations	Action	Date/Sign
	No flow						
	Reverse flow						
	More flow						
	Less flow						
	More level						
	Less level						
	More pressure						
	Less pressure						
	More temperature						
	Less temperature						
	More viscosity						
	Less viscosity						
	Composition Change						
	Contamination						
	Relief						
	Instrumentation						
	Sampling						
	Corrosion/erosion						
	Service failure						
	Abnormal Operation						

NTNU SINTEF

Project: Node: 1						Page	
Ref	**Guideword**	**Causes**	**Consequences**	**Safeguards**	**Recommendations**	**Action**	**Date/Sign**
	Maintenance						
	Ignition						
	Spare equipment						
	Safety						

ATTACHMENT C: TEST CERTIFICATE FOR LOCAL PRESSURE TESTING

Trykkpåkjent utstyr:	
Benyttes i rigg:	
Design trykk for utstyr (bara):	
Maksimum tillatt trykk (bara): (i.e. burst pressure om kjent)	
Maksimum driftstrykk i denne rigg:	

Prøvetrykket skal fastlegges i følge standarden og med hensyn til maksimum tillatt trykk.

Prøvetrykk (bara):			
X maksimum driftstrykk: I følge standard			
Test medium:			
Temperatur (°C)			
Start tid:		Trykk (bara):	
Slutt tid:		Trykk (bara):	
Maksimum driftstrykk i denne rigg:			

Eventuelle repetisjoner fra atm. trykk til maksimum prøvetrykk:................

Test trykket, dato for testing og maksimum tillatt driftstrykk skal markers på (skilt eller innslått)

______________________ ______________________

Sted og dato Signatur

ATTACHMENT D: HAZOP PROCEDURE (TEMPLATE)

Project: Node: 1						Page	
Ref#	**Guideword**	**Causes**	**Consequences**	**Safeguards**	**Recommendations**	**Action**	**Date/Sign**
	Not clear procedure	Procedure is to ambitious, or confusingly					
	Step in the wrong place	The procedure can lead to actions done in the wrong pattern or sequence					
	Wrong actions	Procedure improperly specified					
	Incorrect information	Information provided in advance of the specified action is wrong					
	Step missing	Missing step, or step requires too much of operator					
	Step unsucessful	Step has a high probability of failure					
	Influence and effects from other	Procedure's performance can be affected by other sources					

NTNU SINTEF

ATTACHMENT E: PROCEDURE FOR RUNNING EXPERIMENTS

Prosjekt Solar heat storage in oil based rock bed	**Dato**	**Signatur**
Apparatur Oil based heat storage rig		
Prosjektleder Ole Jørgen Nydal	23/10/17	Ole Jørgen Nydal

	Conditions for the experiment:	**Completed**
	Experiments should be run in normal working hours, 08:00-16:00 during winter time and 08.00-15.00 during summer time.	
	One person must always be present while running experiments, and should be approved as an experimental leader.	
	Be sure that everyone taking part of the experiment is wearing the necessary protecting equipment and is aware of the shut down procedure and escape routes.	
	Preparations	**Carried out**
	Post the "Experiment in progress" sign.	
	Be sure that the ventilation in the room is working	
	Start of Experiment	**Carried out**
	Plug wire from heating element into electrical output	
	During the experiment	
	Control of temperature	
	End of experiment	
	Unplug wire from heating element	
	Remove all obstructions/barriers/signs around the experiment.	
	Tidy up and return all tools and equipment.	
	Tidy and cleanup work areas.	
	Return equipment and systems back to their normal operation settings (fire alarm)	
	To reflect on before the next experiment and experience useful for others	
	Was the experiment completed as planned and on scheduled in professional terms?	
	Was the competence which was needed for security and completion of the experiment available to you?	
	Do you have any information/ knowledge from the experiment that you should document and share with fellow colleagues?	

NTNU SINTEF

Operator(s):

Navn	Dato	Signatur
Christian Bogsnes	23/10 -17	Christian Bogsnes
Even Ersdal Hansen	23/10 -17	Even E. Hansen
Alexander Bjåen Steen	23/10 -17	Alexander B. Steen
Oskar Stadaas Sjøgren	23/10 - 17	Oskar St. Sjøgren

NTNU SINTEF

ATTACHMENT F: TRAINING OF OPERATORS

Prosjekt Solar heat storage in oil based rock bed	**Dato**	**Signatur**
Apparatur Oil based heat storage rig		
Prosjektleder Ole Jørgen Nydal	23/10/17	[signature]

	Knowledge about EPT LAB in general	
	Lab • Access • routines and rules • working hour	
	Knowledge about the evacuation procedures.	
	Activity calendar for the Lab	
	Early warning, **iept-experiments@ivt.ntnu.no**	
	Knowledge about the experiments	
	Procedures for the experiments	
	Emergency shutdown.	
	Nearest fire and first aid station.	

I hereby declare that I have read and understood the regulatory requirements has received appropriate training to run this experiment and are aware of my personal responsibility by working in EPT laboratories.

Operator(s):

Navn	Dato	Signatur
Christian Bogsnes	23/10-17	Christian Bogsnes
Even Ersdal Hansen	23/10-17	Even E. Hansen
Alexander Bjåen Steen	23/10-17	Alexander B. Steen
Oskar Stadaas Sjøgren	23/10-17	Oskar St. Sjøgren

NTNU SINTEF

APPARATURKORT / UNITCARD

Dette kortet SKAL henges godt synlig på apparaturen!
This card MUST be posted on a visible place on the unit!

Apparatur (Unit) Oil based heat storage rig	
Prosjektleder (Project Leader) Ole Jørgen Nydal	**Telefon mobil/privat** (Phone no. mobile/private) +47 97715994
Apparaturansvarlig (Unit Responsible) Ole Jørgen Nydal	**Telefon mobil/privat** (Phone no. mobile/private) +47 97715994
Sikkerhetsrisikoer (Safety hazards) Hot surfaces Heated oil	
Sikkerhetsregler (Safety rules) Use safety gloves and googles Do not touch the rig without approval of the opperator	
Nødstopp prosedyre (Emergency shutdown) Unplug the heating element.	

Her finner du (Here you will find):

Prosedyrer (Procedures)	HSE handbook
Bruksanvisning (Users manual)	HSE handbook

Nærmeste (Nearest)

Brannslukningsapparat (fire extinguisher)	
Førstehjelpsskap (first aid cabinet)	

NTNU
Institutt for energi og prosessteknikk

Dato

Signert

SINTEF Energi
Avdeling energiprosesser

Dato

Signert

NTNU SINTEF

FORSØK PÅGÅR /EXPERIMENT IN PROGRESS

Dette kortet SKAL henges opp før forsøk kan starte!
This card MUST be posted on the unit before the experiment startup!

Apparatur (Unit) Oil based heat storage rig	
Prosjektleder (Project Leader) Ole Jørgen Nydal	**Telefon mobil/privat** (Phone no. mobile/private) +47 97715994
Apparaturansvarlig (Unit Responsible) Ole Jørgen Nydal	**Telefon mobil/privat** (Phone no. mobile/private) +47 97715994
Godkjente operatører (Approved Operators) Paul Svendsen Even Ersdal Hansen Christian Bogsnes Alexander Bjåen Steen Oskar Stadaas Sjøgren	**Telefon mobil/privat** (Phone no. mobile/private) +47 91897987 +47 91574645 +47 91790717 +47 99301245 +47 92653327
Prosjekt (Project) Solar heat storage in oil based rock bed	
Forsøkstid / Experimental time (start - stop)	
Kort beskrivelse av forsøket og relaterte farer (Short description of the experiment and related hazards) • Hot circulating oil (through insulated pipes and heat storage). • Do not touch the surfaces to avoid scald risk. • Be careful with the electric cable from the heating element and thermocouples.	

NTNU
Institutt for energi og prosessteknikk

Dato

____

Signert

____

SINTEF Energi
Avdeling energiprosesser

Dato

____

Signert

____